Medium-induced gluon branching

Jean-Paul Blaizot, Fabio Dominguez, Edmond Iancu and Yacine Mehtar-Tani

Institut de Physique Théorique, CEA Saclay,
F-91191 Gif-sur-Yvette, France

E-mail: jean-paul.blaizot@cea.fr, fabio.dominguez@cea.fr,
edmond.iancu@cea.fr, yacine.mehtar-tani@cea.fr

ABSTRACT: We study the evolution of an energetic jet which radiates gluons while propagating through a dense QCD medium modeled as a random distribution of color sources. Motivated by the heavy ion experimental program at the LHC, we focus on the medium-induced radiation of (relatively) soft gluons, which are abundantly emitted at large angles and thus can transport a small fraction of the jet energy far away from the jet axis. We perform a complete calculation of the medium-induced gluon branching in the regime where the gluons that take part in the branching undergo multiple soft scattering with the medium. We extend the BDMPSZ theory of radiative energy loss by including the transverse momentum dependence in the kernel that describes the branching and by analyzing the correlations between the two offspring gluons. We demonstrate that these gluons lose color coherence with respect to each other over a time scale that is comparable to the duration of the branching. It follows that interference effects between successive emissions are suppressed, a necessary ingredient for a description of multiple emission of soft gluons by a probabilistic, branching process.

JHEP01(2013)143

Contents

1 Introduction

The LHC heavy ion program has produced a wealth of remarkable results [1–4] that motivate new theoretical efforts in the study of jet propagation in matter. For one thing, these results confirm those obtained at RHIC [5–7], indicating that matter formed in the collisions strongly suppresses the yield of high-p_T hadrons as compared to the yield that one deduces from proton-proton collisions after proper scaling by the number of binary collisions in the nucleus-nucleus collision. This suppression of high-p_T hadrons, referred to as "jet-quenching", is usually attributed to the energy loss of the leading partons caused by the radiation of soft gluons induced by their collisions with the matter constituents. The theory of radiative parton energy loss has been developed in late 90's. It is commonly referred to as BDMPSZ theory, from the names of the original authors [8–12]. Further developments are presented in [13–20]. In this theory, the energy loss is characterized by a single parameter, a transport coefficient called $\hat{q}$ (the 'jet quenching parameter'), which

measures how much transverse momentum $\Delta k_\perp$ a given parton acquires through multiple scattering as it travels through the medium over a distance Δl: $\Delta k_\perp^2 = \hat{q}\Delta l$.

However, the LHC experiments provide much more detailed information about what is going on as the jet propagates through the medium, beyond the mere evidence for energy loss. There is in particular clear evidence that the jet shape is affected with a large number of soft particles being emitted at larger angles, i.e., outside the jet cone, and carrying a small (some ten percent or so) of the total energy [2–4]. While these soft particles do not contribute much to the energy loss, they carry important information, as we shall see, on the basic microscopic mechanisms at work. In order to fully exploit this new available information, a more complete description of exclusive jet observables (such as jet-shapes, particle correlations, etc) is called for. This paper presents the first step towards such a more complete theory of jet propagation in matter, which is valid in a specific regime that we shall specify shortly.

In order to put our work into perspective, we need first to recall a few basic features of the BDMPSZ theory [8–12]. When propagating through a medium in which it undergoes multiple scattering, a high energy parton can radiate a gluon over a typical time scale ("formation time") $\tau_{\rm f}$ given by

$$\frac{1}{\tau_{\rm f}} \sim \frac{k_\perp^2}{2\omega}, \tag{1.1}$$

where ω and $k_\perp$ are respectively the energy of the radiated gluon and its transverse momentum (with respect to the parent gluon). The quantity $1/\tau_{\rm f}$, which, as suggested by eq. (1.1) may be read as a non relativistic energy, with ω playing the role of a mass (the relevance of this analogy will be clarified in the main text) is essentially the amount of energy that is required to put the gluon on-shell. In the medium, such an energy is obtained from multiple scattering with the plasma constituents, each collision providing the colliding hard partons some transverse momentum. As mentioned earlier, the rate at which transverse momentum is accumulated by a parton along its trajectory is given by $\hat{q}$, that is $\Delta k_\perp^2 = \hat{q}\Delta t$. One sees therefore that emission of a gluon of a given energy ω can take place if the transverse momentum acquired during $\tau_{\rm f}$ matches $2\omega/\tau_{\rm f}$, that is if $1/\tau_{\rm f} \sim (\hat{q}\tau_{\rm f}/\omega)$. This provides a self-consistency condition that determines, as a function of ω, the time scale for in-medium splitting, that we shall denote by $\tau_{\rm br}$:

$$\tau_{\rm br}(\omega) \sim \sqrt{\frac{2\omega}{\hat{q}}}. \tag{1.2}$$

Related to $\tau_{\rm br}$, it is also convenient to define $k_{\rm br}$, the typical transverse momentum acquired during the time $\tau_{\rm br}$: $k_{\rm br}^2 = \hat{q}\tau_{\rm br}$, or $k_{\rm br}(\omega) \sim (2\omega\hat{q})^{1/4}$. Note that the time scale of the branching process is larger for harder gluons, because it requires more collisions to put a hard radiated gluon on-shell than a soft one ($k_{\rm br}$ is as slowly growing function of ω). Note also that the radiation is emitted with a characteristic angle $\theta_{\rm br} \sim k_{\rm br}/\omega \sim (\hat{q}/\omega^3)^{1/4}$. Thus the softer the emission, the larger the emission angle, with all angles such that $\theta \gtrsim \theta_c$, the minimal angle $\theta_c = (\hat{q}L^3)^{-1/2}$ corresponding to $\tau_{\rm br} = L$, the length of the medium.

The BDMPSZ energy spectrum of the radiated gluons is of the form

$$\omega \frac{\mathrm{d}N}{\mathrm{d}\omega} \simeq \frac{\alpha_s N_c}{\pi} \sqrt{\frac{\omega_c}{\omega}} \equiv \bar{\alpha}\sqrt{\frac{\omega_c}{\omega}}, \tag{1.3}$$

for $\omega \lesssim \omega_c$ (and more strongly suppressed for $\omega > \omega_c$). The frequency ω_c is that for which $\tau_{\mathrm{br}}(\omega_c) \sim L$, that is, $\omega_c = \frac{1}{2}\hat{q}L^2$. The first factor in eq. (1.3) is the standard bremsstrahlung spectrum for radiation by the parent gluon. The correction factor, which we can write as $\sqrt{\omega_c/\omega} = L/\tau_{\mathrm{br}}(\omega)$, increases as ω decreases, and the spectrum (1.3) should be cut-off at a minimal frequency ω_{BH}, at which multiple scattering ceases to be important and the radiation is produced by incoherent collisions (Bethe-Heitler spectrum): ω_{BH} is the frequency for which the formation time is of the order of the mean free path ℓ between successive collisions, that is $\tau_{\mathrm{br}}(\omega_{\mathrm{BH}}) \sim \ell$. Thus, $L/\tau_{\mathrm{br}}(\omega)$ is the number of effective scattering centers, which is maximum for $\omega \sim \omega_{\mathrm{BH}}$ and is of order 1 in the vicinity of ω_c. The decrease of $L/\tau_{\mathrm{br}}(\omega)$ as ω increases may be understood as a consequence of the Landau-Pomeranchuk-Migdal (LPM) effect.

This mechanism for gluon production, and the approximations used to calculate it, require the formation time to be much larger than the mean free path ℓ, but smaller than the size L of the medium, that is $\omega_{\mathrm{BH}} \ll \omega \lesssim \omega_c$. For energies within this range, there is a large number of scattering centers, of order $\tau_{\mathrm{br}}(\omega)/\ell \gg 1$, which coherently contribute to the emission process. This can be rephrased in terms of the typical transverse momentum exchanged in one collision. Having in mind a picture of the medium where the typical collisions are induced by a screened one gluon exchange, we call that typical momentum m_D (with m_D the screening mass). Then, from the definition of $\hat{q}$ given earlier, $m_D^2 = \hat{q}\ell$, and the condition $\omega_{\mathrm{BH}} \ll \omega$ translates into $k_{\mathrm{br}}^2(\omega) \gg m_D^2$.

The initial motivation for the BDMPSZ theory was to provide a framework for calculating the energy loss. An estimate of this energy loss can be obtained by integrating the spectrum (1.3):

$$\Delta E = \int_{\omega_0}^{\omega_c} \mathrm{d}\omega\, \omega \frac{\mathrm{d}N}{\mathrm{d}\omega} \sim \bar{\alpha}\omega_c \sim \bar{\alpha}\,\hat{q}L^2. \tag{1.4}$$

This is dominated by the upper limit $\omega = \omega_c$, the maximal energy that can be taken away by a single gluon. Such emissions of hard gluons are rather rare: they occur with a probability of order $\bar{\alpha}$. However, from the spectrum (1.3) one can also compute the average number of gluons emitted with energies larger than a given value ω:

$$\Delta N(\omega) = \int_{\omega}^{\omega_c} \mathrm{d}\omega' \frac{\mathrm{d}N}{\mathrm{d}\omega'} \sim \bar{\alpha}\,\frac{L}{\tau_f(\omega)}. \tag{1.5}$$

As long as $\Delta N(\omega) \lesssim 1$ (that is, as long as $\omega \gtrsim \bar{\alpha}^2\,\omega_c$), it may be identified to the probability to emit one gluon with energy $\omega' \geq \omega$. In such a case, the probability for multiple emissions is small. This is the case of the relatively hard emissions that dominate the energy loss. But for sufficiently soft gluon emissions, such that

$$\omega \lesssim \omega_s \equiv \bar{\alpha}^2\,\omega_c, \tag{1.6}$$

one has $\Delta N(\omega) \gtrsim 1$ and then the multiple emissions are clearly important. Note that these multiple emissions are 'large angle' emissions, with $\theta \sim \bar{\alpha}^{-3/2}\theta_c \gg \theta_c$. Of course this can only occur if the medium is large enough, since the condition $\omega_{\mathrm{BH}} \ll \omega_s$ implies $\ell \ll \bar{\alpha}L$.

To summarize, there is a regime, characterized by gluon energies in the range $\omega_{\mathrm{BH}} \ll \omega \ll \omega_c$, were medium induced radiation dominates, and where multiple emissions are important. This is the regime that we explore in this paper. Note that the conditions on ω and L that characterize this regime are not very restrictive, and in fact they are expected to be well satisfied in the LHC experiments. For a rough orientation, taking $\hat{q} \sim 1\mathrm{GeV}^2/\mathrm{fm}$ and $L \sim 6\,\mathrm{fm}$, one finds $\omega_c \sim 100\,\mathrm{GeV}$, while the typical energy of soft particles is in the GeV range.

When multiple emissions become important, i.e., when $\Delta N(\omega) \gtrsim 1$, the whole calculationnal setting needs to be revised. In technical terms, when $\bar{\alpha}L/\tau_{\mathrm{br}} \sim 1$, the perturbative expansion breaks down, and powers of $\bar{\alpha}L/\tau_{\mathrm{br}}$ have to be resummed. (For instance, the longitudinal phase-space for two independent successive branchings goes like L^2 and the process is of order $(\bar{\alpha}L/\tau_{\mathrm{br}})^2$.) The treatment of multiple emission is a priori complicated by interferences between various high order processes. Various aspects of interference phenomena for medium-induced gluon radiation have been recently studied, but only for the case of a frozen configuration of the emitters (a pair of partons forming a 'colour antenna') [21–25]. However, in the soft regime of interest for us here, these interferences turn out to be negligible. Indeed, as we shall see, color correlations between the offspring gluons disappear on the same time scale τ_{br} at which the splitting occurs. As a consequence, the newly formed gluons propagate independently from each other except for a relatively small period $\tau_{\mathrm{br}} \ll L$. Subsequent emissions from these gluons can interfere with each other only if they occur during that period of order τ_{br} where color coherence is still present. This implies that the longitudinal phase space for interference effects is smaller, by a factor $\tau_{\mathrm{br}}/L \ll 1$, than the corresponding phase space for independent emissions. Note that these features are specific to medium induced radiation.[1] By contrast, in vacuum, color is conserved along the parton shower, which implies coherence of successive parton branchings, that is responsible for angular ordering [26–29].

The argument of the previous paragraph suggests that multiple emissions could be treated as a probabilistic cascade of independent branchings, since this naturally resums the terms with maximal powers of $(\bar{\alpha}L/\tau_{\mathrm{br}})$. There is however a limit to this argument, since successive emissions may overlap with each other when the energies of the produced gluons become too soft. Consider indeed the probability for emitting one gluon with frequency $\omega \geq \omega_0$ during an interval Δt. In the regime where this probability is small, this may be estimated from the BDMPSZ spectrum, eq. (1.3), and is (see eq. (1.5))

$$P(\Delta t; \omega_0) \sim \bar{\alpha}\,\frac{\Delta t}{\tau_{\mathrm{br}}(\omega_0)}. \tag{1.7}$$

---

[1]In fact, the same estimate for the color decoherence time, that is, a time scale of order $\tau_{\mathrm{br}}(\omega)$, would also follow from the previous analyses of a quark-antiquark color antenna in refs. [21, 23] provided in these analyses one identifies the angular opening of the antenna with the formation angle $\theta_{\mathrm{br}} \sim \left(\hat{q}/\omega^3\right)^{1/4}$.

This becomes of order unity when $\Delta t = \tau_{\rm rad}(\omega_0)$ with

$$\tau_{\rm rad}(\omega_0) \,=\, \frac{1}{\bar\alpha}\,\tau_{\rm br}(\omega_0) = \frac{1}{\bar\alpha}\sqrt{\frac{2\omega_0}{\hat q}}\,. \tag{1.8}$$

This quantity $\tau_{\rm rad}(\omega_0)$ may be understood as the typical time interval that a gluon with energy ω can survive without emitting any gluon with energy ω' within the interval $\omega_0 < \omega' < \omega$. Note that it is the emission of the softest allowed gluons which controls the size of this interval. Because of the inverse power of $\bar\alpha$ in eq. (1.8), $\tau_{\rm rad}(\omega_0)$ is parametrically larger than the formation time of the radiated gluon. This property would hold all along the cascade if produced gluons are emitted with comparable frequencies: successive emissions remain well separated, the phase-space for overlapping emissions is small and successive emissions can be treated as independent. This is what is implicitly assumed in the previous paragraph. Under these conditions, the whole branching process reduces to a classical stochastic process obtained by iterating the elementary building block corresponding to one single splitting of a gluon into two gluons. This is the process that will be studied in detail in this paper.

However, one cannot exclude a priori the situation where a very soft gluon is emitted, with $\tau_{\rm rad}(\omega_0)$ comparable to the formation time of the parent gluon (with energy ω). The condition $\tau_{\rm rad}(\omega_0) \gtrsim \tau_{\rm br}(\omega)$ holds if $\omega_0 \gtrsim \bar\alpha^2\omega$. Thus, if ω_0 is parametrically smaller than ω (by two powers of $\bar\alpha$), the interval $\tau_{\rm rad}(\omega_0)$ between two successive emissions becomes of the order of the duration of the branching process that has produced the gluon ω in the previous step, and then the argument of independent emissions breaks down. This particular issue related to the role of very soft emissions in an actual cascade will be discussed in a forthcoming publication.

The assumption of factorization of succesive emissions has already been used in different BDMPSZ inspired phenomenological studies [30–32] and in particular Monte Carlo codes developed in refs. [33–35]. Our conclusion shows how this approach is justified theoretically in the desired kinematical regime where multiple emissions are indeed important.

The calculation to be presented in this paper is technically involved, but conceptually simple. We consider a high energy gluon propagating in a quark-gluon plasma. The medium is modeled by a random color field whose fluctuations account for collisions with plasma constituents and determine $\hat q$. In section 2, we present the general strategy of the calculation by discussing the well known phenomenon of momentum broadening. Then, in section 3 we discuss the general structure of the gluon splitting amplitude and probability. The proof of factorization of the splitting probability requires a special study of a 4-point function, that we shall be able to explicitly compute only in the limit of a large number of colors $N_c \gg 1$. The corresponding analysis is presented in section 4. However, the physical argument for the color decoherence between the offspring gluons is quite general and we expect it to remain valid for any value of N_c. Section 5 is devoted to the calculation of the splitting kernel and the completion of the formula for the splitting probability. In the conclusion we summarize the results and their range of validity. Technical material is gathered in the appendices. Appendix A reviews general features of gluon propagation in a specific background field. Appendix B is devoted to the calculation of specific path

integrals that enter the n-point functions that are studied in the text. Finally appendix C provides details on the color algebra that is needed to calculate the 4-point function.

2   Setting up the calculation with a simple example

We shall set up formalism, and fix the notation, by reviewing the well known phenomenon of momentum broadening of a parton traveling through a quark-gluon plasma. This will also give us the opportunity to present our main results concerning the medium-induced gluon branching, anticipating on the detailed calculations to be done in the forthcoming sections.

We consider an energetic parton propagating through a quark-gluon plasma. For simplicity, we restrict ourselves to the case where this energetic parton is a gluon. The extension to the case where it is a quark is straightforward. The gluon is produced inside the medium, via some hard scattering process, and then it propagates along a distance L until it escapes into the vacuum. During this propagation, the gluon interacts with the medium, and exchanges with it color and transverse momentum.

We assume that the energetic parton propagates at nearly the speed of light along the x^3 axis and we use light-cone coordinates, e.g. $x^\mu = (x^+, x^-, \boldsymbol{x})$, with[2]

$$x^+ = \frac{1}{\sqrt{2}}\left(x^0 + x^3\right), \quad x^- = \frac{1}{\sqrt{2}}\left(x^0 - x^3\right), \quad \boldsymbol{x} = (x^1, x^2), \tag{2.1}$$

together with the light-cone gauge $A_a^+ = 0$. We describe the medium as a random color field with correlation function

$$\langle \mathcal{A}_a^-(x^+, x^-, \boldsymbol{x}) \mathcal{A}_b^-(y^+, x^-, \boldsymbol{y}) \rangle = \delta_{ab}\delta(x^+ - y^+)\gamma(\boldsymbol{x} - \boldsymbol{y}), \tag{2.2}$$

where the angular brackets denote the medium average. More general situations may be considered, e.g. we may allow γ to depend on x^+, but we shall not consider such straightforward extensions here.

In writing eq. (2.2), we have made implicitly several simplifications. The coupling of the energetic gluon with the medium is described in the eikonal approximation, i.e., we assume that it couples only to the component A^- of the gauge field. Furthermore, this field is probed only at small values of x^- (closed to the trajectory of the gluon $x^- \simeq 0$), and we can ignore its dependence on x^-. In other words, we assume that the $+$ component of the gluon momentum is conserved during the propagation through the medium. Furthermore, because of Lorentz time dilation, the hard gluon has a very poor resolution in x^+, and the medium correlations, that have a finite extent in x^+, appear to it as effectively *local*: this is the origin of the δ-function $\delta(x^+ - y^+)$ in the correlator (2.2). By the same token, the field of the medium, which has a finite longitudinal extent L, appears frozen during the time when the hard gluon traverses it. That implies that the average over the medium will be done after squaring the amplitudes. We take this average over the fields to be

---

[2]From now on, we renounce to the subscript $\perp$ on transverse components, that is, we write e.g. $\boldsymbol{x}_\perp \equiv \boldsymbol{x}$ to alleviate notations.

Gaussian, assuming that the corrections to this approximation are of higher order in the coupling strength. Finally, as obvious in eq. (2.2) we assume homogeneity in the transverse plane, i.e., the correlation γ is a function of $\boldsymbol{x} - \boldsymbol{y}$ alone. In summary, the problem that we address is the propagation of an energetic gluon in a random background A^- field that is independent of x^-, with Gaussian correlations. Technical aspects of this problem are studied in detail in appendix A.

Although this will not enter explicitly in our derivations, it is perhaps useful to have in mind a specific model for the medium. We then briefly discuss the case where this medium is a weakly coupled quark-gluon plasma in thermal equilibrium at high enough temperature T. In this case, the medium constituents are quarks and gluons with energies and momenta $p \sim T$. Assuming that the charge carriers are correlated over distances determined by the screening length (inverse Debye mass) m_D^{-1}, one can estimate the correlator of field fluctuations:

$$\gamma(\boldsymbol{x} - \boldsymbol{y}) \,=\, g^2 n \int \frac{\mathrm{d}^2 \boldsymbol{q}}{(2\pi)^2} \, \mathrm{e}^{i\boldsymbol{q} \cdot (\boldsymbol{x} - \boldsymbol{y})} \, \frac{1}{(\boldsymbol{q}^2 + m_D^2)^2}, \tag{2.3}$$

where $n \propto T^3$ is the density of (point-like) color charges (weighted with appropriate color factors), and $1/(\boldsymbol{q}^2 + m_D^2)$ is the screened Coulomb propagator. In fact, the quantity which will enter our analysis is not γ itself, but the difference $\gamma(0) - \gamma(\boldsymbol{r})$,

$$\gamma(0) - \gamma(\boldsymbol{r}) \,=\, g^2 n \int \frac{\mathrm{d}^2 \boldsymbol{q}}{(2\pi)^2} \, \frac{1 - \mathrm{e}^{i\boldsymbol{q} \cdot \boldsymbol{r}}}{(\boldsymbol{q}^2 + m_D^2)^2}. \tag{2.4}$$

The integral over $\boldsymbol{q}$ in eq. (2.4) is dominated by $q \lesssim 1/r$, and in the relevant case where, typically, $1/r \gg m_D$, it is logarithmically sensitive to all the scales within the range $m_D \ll q \ll 1/r$. To leading logarithmic accuracy, it can be evaluated by expanding the complex exponential to second order. One gets

$$\gamma(0) - \gamma(\boldsymbol{r}) \simeq \frac{1}{4} g^2 n \, \boldsymbol{r}^2 \int \frac{\mathrm{d}^2 \boldsymbol{q}}{(2\pi)^2} \, \frac{\boldsymbol{q}^2}{(\boldsymbol{q}^2 + m_D^2)^2} \approx \frac{1}{16\pi} g^2 n \, \boldsymbol{r}^2 \, \ln \frac{1}{r^2 m_D^2}. \tag{2.5}$$

In the context of the present calculation the relevant values of r are typically fixed by transverse momentum broadening. In the regime dominated by multiple scattering, one often uses the *harmonic approximation*, where one ignores the weak dependence on r of the logarithm, and set

$$g^2 N_c \big[\gamma(0) - \gamma(\boldsymbol{r}) \big] \approx \frac{1}{4} \hat{q} \, \boldsymbol{r}^2, \tag{2.6}$$

with the jet quenching parameter $\hat{q}$ (evaluated at the typical scale $1/\bar{r}$) given by

$$\hat{q} \approx 4\pi \alpha_s^2 N_c \, n \, \ln \frac{1}{\bar{r}^2 m_D^2} \,. \tag{2.7}$$

Parametrically, we have, $m_D \sim gT$, $\ell \sim 1/g^2 T$, $\hat{q} \sim g^4 T^3$, and $\omega_{BH} \sim T$.

We now return to our main discussion. We assume that the energetic gluon is created inside the medium at time $x^+ = t_0$ by some local current $\boldsymbol{J}(t_0)$, and then propagates up

to time $x^+ = t_L$, when it escapes the medium. Note that, as mentioned already in the introduction, we ignore in our calculation the 'vacuum radiation' that would be associated with the possible virtuality of the energetic gluon. (In what follows we shall often denote the light-cone time x^+ simply as t, to alleviate the notation. Note that $t_L = \sqrt{2}L$.) The probability amplitude for finding the (on-shell) gluon at t_L, with momentum $k^\mu = (k^- = \boldsymbol{k}^2/2k^+, k^+, \boldsymbol{k})$, colour b, and polarization λ, can be obtained from a standard calculation, as explained in appendix A (see also refs. [21, 23, 36] for previous applications of a similar formalism). One gets

$$\mathcal{M}^b_\lambda(k^+, \boldsymbol{k}) = \mathrm{e}^{i\frac{\boldsymbol{k}^2}{2k^+}t_L} \int \frac{\mathrm{d}^2\boldsymbol{p}_0}{(2\pi)^2} \, (\boldsymbol{k}\, b| \, \mathcal{G}(t_L, t_0) \, |\boldsymbol{p}_0\, a) \, \boldsymbol{\epsilon}^i_\lambda \, (p_0^+ \, \boldsymbol{p}_0 \, a|\boldsymbol{J}^i(t_0)|0), \tag{2.8}$$

with $(p_0^+ \, \boldsymbol{p}_0 \, a|\boldsymbol{J}^i(t_0)|0)$ the matrix element of the current creating the gluon from the vacuum, with momentum $(p_0^+ = k^+, \boldsymbol{p}_0)$ and color a. Summation over repeated discrete indices is implied. Here, $(\boldsymbol{k}| \, \mathcal{G}^{ba}(t_L, t_0) \, |\boldsymbol{p}_0) = (\boldsymbol{k}\, b| \, \mathcal{G}(t_L, t_0) \, |\boldsymbol{p}_0\, a)$ (we use indifferently both notations) is the effective propagator that describes the (non relativistic) motion of the gluon in the transverse plane under the influence of the time dependent background field A^-. This propagation preserves k^+, as already mentioned, and $\mathcal{G}$ depends on k^+, but we shall generally not indicate this dependence explicitly. Note also that the propagator $\mathcal{G}$ do not carry any Lorentz indices. This is because, as shown in appendix A, the propagation in the background field preserves the (transverse) polarization of the gluon.

It is shown explicitly in appendix A that $\mathcal{G}$ is the propagator of a Schrödinger equation in two dimensions (the transverse plane) for a non relativistic particle of mass k^+ moving in a time dependent potential $A^-(x^+, \boldsymbol{x})$, with x^+ playing the role of the time. That is, it satisfies the equation

$$\left[i\mathcal{D}^- + \frac{\nabla^2_\perp}{2k^+}\right]_{ac} (\boldsymbol{x}| \, \mathcal{G}^{cb}(x^+, y^+; k^+) \, |\boldsymbol{y}) = i\delta_{ab}\delta(x^+ - y^+)\delta(\boldsymbol{x} - \boldsymbol{y}), \tag{2.9}$$

with $i\mathcal{D}^- = i\partial^- + gA^-$ and $\partial^- = \partial/\partial x^+$. The solution can be written as a path integral

$$(\boldsymbol{x}| \, \mathcal{G}(x^+, y^+; k^+) \, |\boldsymbol{y}) = \int \mathcal{D}\boldsymbol{r} \, \mathrm{e}^{i\frac{k^+}{2}\int_{y^+}^{x^+} \mathrm{d}t \, \dot{\boldsymbol{r}}^2} \, \tilde{U}(x^+, y^+; \boldsymbol{r}), \tag{2.10}$$

with $\boldsymbol{r}(y^+) = \boldsymbol{y}$, $\boldsymbol{r}(x^+) = \boldsymbol{x}$, and $\tilde{U}$ is a Wilson line evaluated along the path $\boldsymbol{r}(t)$ in the adjoint representation

$$\tilde{U}(x^+, y^+; \boldsymbol{r}) = \mathrm{T} \exp\left\{ig \int_{y^+}^{x^+} \mathrm{d}t \, A^-_a(t, \boldsymbol{r}(t)) \, T^a\right\}. \tag{2.11}$$

Note that we work in a regime dominated by multiple scattering, so that the accumulated phase over a typical interval Δt is large, i.e., $gA^-\Delta t \sim 1$. It follows that the exponential cannot be expanded in general (as done for instance in the opacity expansion [14, 16]).

The probability to find the gluon with momentum $\boldsymbol{k}$ is obtained by taking the modulus squared of the amplitude in eq. (2.8), summing over the final color indices, and then averaging over the color background field. Since the distribution of gauge fields is taken
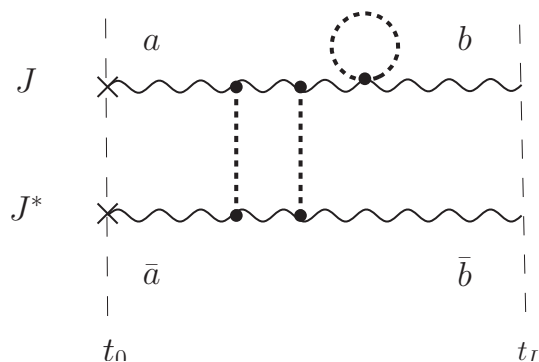
Figure 1. Amplitude (upper part of the diagram) and complex conjugate amplitude (lower part) describing the propagation of a gluon in the medium from time t_0 to time t_L when it leaves the medium. The horizontal wavy lines represent the gluon propagator or its complex conjugate. Note that we use a bar to indicate color indices in the conjugate amplitude. At time $t = t_L$, $b = \bar{b}$. The (Gaussian) medium average generates instantaneous contractions that are depicted as vertical dotted lines, or as dotted circles.

to be Gaussian, cf. eq. (2.2), the medium averaging amounts to contracting pairs of fields from the Wilson lines in the two propagators representing the gluon in the direct and the complex conjugate amplitudes, respectively. These contractions can either connect the two gluon lines, or they can be 'tadpoles' with both endpoints on a same gluon line. It is convenient to represent the amplitude together with its complex conjugate on the same diagram, with time flowing from left to right. (This is somewhat analogous to the close time path technique, although we shall not explicitly use this particular formalism here.) The ensuing diagram, shown in figure 1, displays typical contractions. This representation makes it easier to discuss color and momentum flows.

Let us consider first the color structure. At time t_L, the system formed by the gluons in the amplitude and its complex conjugate is clearly in a color singlet state: both gluons carry the same color index b (i.e., $b = \bar{b}$ in figure 1), which is summed over since we do not observe the color of the final gluon. The field contractions involved in the medium averaging do not change the overall color state of the two gluon system, which remains therefore a color singlet at any intermediate time between t_0 and t_L. This implies that the medium averaged squared amplitude depicted in figure 1 contains a contribution of the form (as we shall see shortly $\bar{\boldsymbol{k}} = \boldsymbol{k}$)

$$\left\langle (\boldsymbol{k}|\mathcal{G}^{ba}(t_L, t_0)|\boldsymbol{p}_0)(\bar{\boldsymbol{p}}_0|\mathcal{G}^{\dagger\,\bar{a}b}(t_0, t_L)|\bar{\boldsymbol{k}}) \right\rangle = \delta^{a\bar{a}}(\boldsymbol{k}; \bar{\boldsymbol{k}}|S^{(2)}(t_L, t_0)|\boldsymbol{p}_0; \bar{\boldsymbol{p}}_0), \qquad (2.12)$$

where the sum over the repeated color index b is implied, and

$$(\boldsymbol{k}; \bar{\boldsymbol{k}}|\, S^{(2)}(t_L, t_0)\, |\boldsymbol{p}_0; \bar{\boldsymbol{p}}_0) = \frac{1}{N_c^2 - 1} \left\langle \mathrm{Tr}\,(\boldsymbol{k}|\,\mathcal{G}(t_L, t_0)\,|\boldsymbol{p}_0)(\bar{\boldsymbol{p}}_0|\,\mathcal{G}^{\dagger}\,(t_0, t_L)|\bar{\boldsymbol{k}}) \right\rangle, \quad (2.13)$$

where the trace Tr concerns color indices. The quantity $S^{(2)}$, referred to as a 2-point function, is the simplest of several n-point functions that we shall have to consider in this

– 9 –

paper, and which are calculated explicitly in appendix B. Note that, in defining $S^{(2)}$, we choose to keep the time ordering given by the propagator in the amplitude, and to put all the momentum variables at the final time in the bra, and the ones at the initial time in the ket. The variables corresponding to the conjugate propagator are denoted by a bar, and are separated from the variables of the propagator by a semicolon. This notation will be used throughout (see also appendix B).

Similarly, since the correlator of the background field is invariant under translations in the transverse plane, the medium does not change the overall transverse momentum of the pair of gluons: whichever momentum is picked up from the medium by the gluon in the amplitude is compensated at the same time by a similar transfer to the gluon in the complex conjugate amplitude. Thus, if one chooses the final momentum to be the same in the amplitude and the complex conjugate amplitude, i.e., $\boldsymbol{k} = \bar{\boldsymbol{k}}$ (as we need to do if we consider the production of a gluon with a given transverse momentum) then, at each instant of time, the momenta remain equal in the amplitude and its complex conjugate. In coordinate space, as shown explicitly in appendix B, this corresponds to the two gluons in the amplitude and its complex conjugate propagating with a fixed separation. The medium average of the Wilson lines in the pair of propagators is then of the form

$$
\begin{aligned}
C_g^{(2)}(t_L - t_0; \boldsymbol{r}) &\equiv \frac{1}{N_c^2 - 1} \left\langle \operatorname{Tr} \tilde{U}(t_L, t_0; \boldsymbol{x}) \tilde{U}^\dagger(t_L, t_0; \bar{\boldsymbol{x}}) \right\rangle, \\
&= \exp\left\{ -g^2 N_c (t_L - t_0) \left[\gamma(0) - \gamma(\boldsymbol{r}) \right] \right\}, \\
&= \exp\left[-\frac{N_c n}{2} (t_L - t_0) \, \sigma(\boldsymbol{r}) \right],
\end{aligned}
\tag{2.14}
$$

where $\boldsymbol{r} \equiv \boldsymbol{x} - \bar{\boldsymbol{x}}$ is the constant distance between the two gluons. This is recognized as the forward scattering amplitude for a color dipole which propagates through the medium. This is of course a fictitious dipole, which is formed with the gluon in the direct amplitude and that in the complex conjugate amplitude, which in the calculation of the probability group together in an overall color singlet state — the 'dipole'. The expression in the third line of the above equation, which features the dipole cross-section $\sigma(\boldsymbol{r})$, will often be used to simplify writing in what follows.

Altogether, the medium averaging of the squared amplitude will therefore generate a 2-point function of the form (see appendix B for details)

$$
(\boldsymbol{k}; \boldsymbol{k} | S^{(2)}(t_L, t_0) | \boldsymbol{p}_0; \bar{\boldsymbol{p}}_0) = (2\pi)^2 \delta^{(2)}(\boldsymbol{p}_0 - \bar{\boldsymbol{p}}_0) \, \mathcal{P}(\boldsymbol{k} - \boldsymbol{p}_0, t_L - t_0),
\tag{2.15}
$$

where

$$
\mathcal{P}(\Delta \boldsymbol{p}, \Delta t) = \int \mathrm{d}^2 \boldsymbol{r} \, \mathrm{e}^{-i\Delta \boldsymbol{p} \cdot \boldsymbol{r}} \, C_g^{(2)}(\Delta t; \boldsymbol{r}),
\tag{2.16}
$$

can be interpreted as the probability that a gluon acquires a transverse momentum $\Delta \boldsymbol{p}$ while traversing the medium during a time Δt. This is best seen by using the harmonic approximation (2.6), where

$$
N_c n \sigma(\boldsymbol{r}) \approx \frac{1}{2} \hat{q} \, \boldsymbol{r}^2.
\tag{2.17}
$$
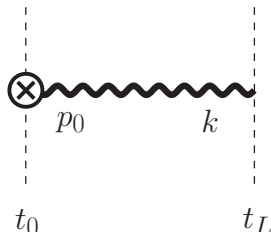
Figure 2. Diagrammatic illustration for the process in which a gluon of momentum $(p_0^+, \boldsymbol{p}_0)$ is produced via a hard process (represented by the circled cross) and acquires transverse momentum $\boldsymbol{k} - \boldsymbol{p}_0$ in its propagation though the medium (the thick wavy line). The $+$ component of the momentum is conserved in this propagation, i.e., $k^+ = p_0^+$.

Then we get

$$C_g^{(2)}(\Delta t; \boldsymbol{r}) = \exp\left(-\frac{\hat{q}\,\Delta t}{4}\,\boldsymbol{r}^2\right), \tag{2.18}$$

and

$$\mathcal{P}(\Delta\boldsymbol{p}, \Delta t) = \int \mathrm{d}^2\boldsymbol{r}\; \mathrm{e}^{i\boldsymbol{r}\cdot\Delta\boldsymbol{p} - \frac{\hat{q}\Delta t}{4}\boldsymbol{r}^2} \;=\; \frac{4\pi}{\hat{q}\Delta t}\; \mathrm{e}^{-\frac{(\Delta\boldsymbol{p})^2}{\hat{q}\Delta t}}. \tag{2.19}$$

This formula confirms the physical interpretation of $\hat{q}$: $\hat{q}\Delta t$ is the transverse momentum squared acquired by a gluon after it has traveled through the medium for a duration Δt. In fact, in the harmonic approximation, $\mathcal{P}(\Delta\boldsymbol{p}, \Delta t)$ solves the diffusion equation with initial condition $\mathcal{P}(\Delta\boldsymbol{p}, \Delta t = 0) = (2\pi)^2\,\delta^{(2)}(\Delta\boldsymbol{p})$, with $\hat{q}$ playing the role of a diffusion coefficient. Note also that this probability is independent of the gluon longitudinal momentum k^+. This is to be expected from the formal analogy of the present problem with the 2-dimensional diffusion of a non relativistic particle with mass k^+.

The exponential factor in eq. (2.18) reflects a general feature of the interaction of color objects with the medium: the propagation of the color dipole (formed by the gluons in the amplitude and its complex conjugate) is not affected by the interaction as long as its size is small enough to be 'viewed' by the medium as a color singlet, but it is strongly damped as soon as the size of the dipole exceeds $2/\sqrt{\hat{q}\Delta t}$.

We are now in a position to calculate the differential cross section to observe a gluon with transverse momentum $\boldsymbol{k}$ and arbitrary color and spin at time t_L, after its production through some hard process at time t_0. This is given by[3]

$$\frac{\mathrm{d}\sigma_0}{\mathrm{d}\Omega_k} \;=\; \int \frac{\mathrm{d}^2\boldsymbol{p}_0}{(2\pi)^2}\; \mathcal{P}(\boldsymbol{k} - \boldsymbol{p}_0, t_L - t_0)\; \frac{\mathrm{d}\sigma_{\text{hard}}}{\mathrm{d}\Omega_{p_0}}, \tag{2.20}$$

where $\mathrm{d}\Omega_k \equiv (2\pi)^{-3}\mathrm{d}^2\boldsymbol{k}\,\mathrm{d}k^+/2k^+$ is the invariant phase-space element, and $\mathrm{d}\sigma_{\text{hard}}/\mathrm{d}\Omega_{p_0} = |\boldsymbol{J}^a(\boldsymbol{p}_0)|^2$ is the 'hard cross section' for producing the gluon (the sum over color a is understood — we also assume that all kinematical factors necessary to build a cross section are

---

[3]The subscript 0 on this cross-section refers to the fact that the process considered here involves no gluon branching. Similarly, the quantity σ_1 in eq. (2.21) below refers to a process which involves one branching.
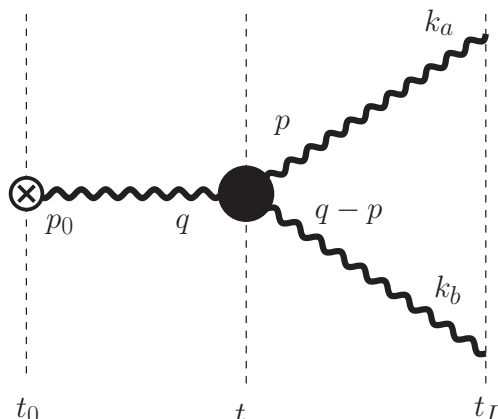
Figure 3. Graphical illustration of the equation (2.21). The thick wavy lines represent the probability $\mathcal{P}$ for transverse momentum broadening, the black dot is the splitting probability $\mathcal{K}$, and the circled cross is the cross section of the hard process producing a gluon of momentum p_0.

included in the current $\boldsymbol{J}$). In deriving this result, we have summed over the polarization vectors with the help of the completeness relation $\sum_\lambda \epsilon^i_\lambda(k)\epsilon^{*j}_\lambda(k) = \delta^{ij}$. This process, depicted in figure 2, has a probabilistic interpretation, with the wavy line representing the probability (2.19).

It will be our main goal in this paper to show that the cross section for the process where one gluon splits into two gluons under the effect of medium interactions can be given an analogous probabilistic interpretation. Our subsequent calculations will lead to the following estimate for producing soft gluons (k^+_a, $k^+_b \ll \omega_c$)

$$
\frac{\mathrm{d}^2\sigma}{\mathrm{d}\Omega_{k_a}\mathrm{d}\Omega_{k_b}} = 2g^2 z(1-z)
$$
$$
\times \int_{t_0}^{t_L} \mathrm{d}t \int_{\boldsymbol{p}_0,\boldsymbol{q},\boldsymbol{p}} \mathcal{P}(\boldsymbol{k}_a - \boldsymbol{p}, t_L - t)\,\mathcal{P}(\boldsymbol{k}_b - \boldsymbol{q} + \boldsymbol{p}, t_L - t)
$$
$$
\times \mathcal{K}(\boldsymbol{p} - z\boldsymbol{q}, z, p^+_0)\,\mathcal{P}(\boldsymbol{q} - \boldsymbol{p}_0, t - t_0)\,\frac{\mathrm{d}\sigma_{hard}}{\mathrm{d}\Omega_{p_0}}\,, \qquad (2.21)
$$

and it is understood that $z = k^+_a/p^+_0$. This result can be interpreted as a classical branching process, illustrated in figure 3: after propagating from t_0 to t, during which it acquires a transverse momentum $\boldsymbol{q}-\boldsymbol{p}_0$, the original gluon splits into gluons a and b with a probability $\sim \alpha_s \mathcal{K}(\boldsymbol{p} - z\boldsymbol{q}, z, q^+)$ that depends upon the longitudinal momentum q^+ of the parent parton, the longitudinal momentum fraction $z = p^+/q^+$ carried by gluon a, and the transverse momentum difference $\boldsymbol{p}-z\boldsymbol{q}$. (The conservation of longitudinal momentum implies of course $p^+_0 = q^+ = k^+_a + k^+_b$ with $k^+_a = p^+ = zq^+$.) After the splitting, the two gluons a and b propagate through the medium from t to t_L, and thus acquire some extra transverse momentum.

Note that, in eq. (2.21), the splitting occurs instantaneously at time t, that is, the effective splitting vertex $\mathcal{K}(\boldsymbol{p} - z\boldsymbol{q}, z, q^+)$ is local in time. Moreover, the transverse momentum is conserved at the splitting, meaning that one neglects the additional momentum

transferred from the medium to the gluons during the branching process. These are of course approximations, which are correct so long as the duration of the branching process, τ_{br}, is much shorter than the medium size[4] L. Previously, in eq. (1.2), we have estimated this time τ_{br} for the case of asymmetric branchings, where one of the daughter gluons is much softer than the other one (say $z \ll 1$). An estimate valid for arbitrary values of z can be obtained by considering ΔE, the change in the light-cone energy (the minus component of the 4-momentum, or equivalently the change in the energy in the equivalent non relativistic 2-dimensional problem), at the splitting vertex:

$$\Delta E = \frac{\boldsymbol{p}^2}{2p^+} + \frac{(\boldsymbol{q} - \boldsymbol{p})^2}{2(q^+ - p^+)} - \frac{\boldsymbol{q}^2}{2q^+} = \frac{(\boldsymbol{p} - z\boldsymbol{q})^2}{2z(1-z)q^+} \,. \tag{2.22}$$

The inverse of this energy is the formation time, which gives access to the duration of the branching process. To get this, all what one needs to do is, as in eq. (1.2), relate $\boldsymbol{p} - z\boldsymbol{q}$ to the transverse momentum acquired by multiple scattering during τ_{br}. That is, $(\boldsymbol{p} - z\boldsymbol{q})^2 \simeq \hat{q}\tau_{\mathrm{br}}$, which together with the above expression for $\Delta E = 1/\tau_{\mathrm{br}}$ provides an estimate for the corresponding branching time:

$$\tau_{\mathrm{br}} = \sqrt{\frac{z(1-z)q^+}{\hat{q}}} \,, \tag{2.23}$$

which generalizes eq. (1.2) by the replacement of $\omega \equiv zp^+$ by $z(1-z)p^+$ (note that the latter quantity can be interpreted as the reduced mass for the effective non-relativistic motion of the two produced gluons in the transverse plane). This makes it clear that eq. (1.2) holds only for asymmetric splitting with $z \ll 1$. A slightly more precise estimate for τ_{br} will be given in section 5 (eq. (5.5)).

## 3 General structure of the in-medium gluon branching

In this section we analyze the main structure of the calculation of the gluon branching, and show how it can be conveniently divided into three main stages: (i) production of the gluon at time t_0 via some local (hard) process, followed by the propagation of the gluon in the medium; (ii) the process where the gluon splits into two gluons; (iii) finally the propagation of the two new gluons until the end of the medium at coordinate $x^+ = t_L \equiv \sqrt{2}L$.

3.1 The amplitude

The amplitude for the branching process is illustrated in figure 4: a gluon is created at time t_0 with color c_0 and momentum $(p_0^+, \boldsymbol{p}_0)$ out of the current $J^{c_0}(p_0^+, \boldsymbol{p}_0) = (\boldsymbol{p}_0 \, c_0 | J(t_0)|0)$; it then propagates in the medium where it acquires a transverse momentum $\boldsymbol{q}_1 - \boldsymbol{p}_0$, changes color form c_0 to c_1, and eventually splits into two gluons at time t_1. The newly produced gluons then propagates through the medium until the time t_L, where they are observed with momenta $\boldsymbol{k}_a, \boldsymbol{k}_b$, colors a, b and polarization λ_a, λ_b. Using the elements described

---

[4]In the presence of multiple emissions, the correct reference scale for τ_{br} is not L, but the typical time interval between two successive emissions. We shall return to this issue in the concluding section.
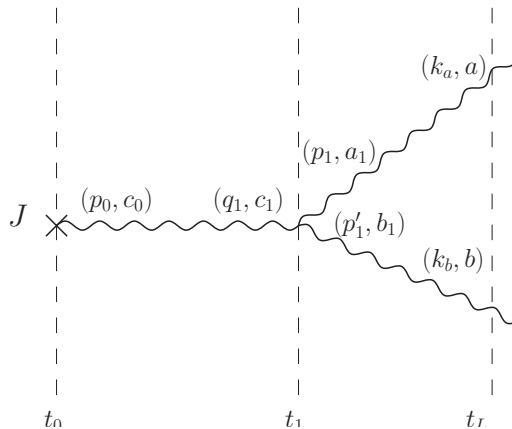
Figure 4. Graphical illustration of the amplitude for one gluon splitting. The initial gluon produced at time t_0 with momentum $\boldsymbol{p}_0$ and color c_0 splits at time t_1 into two gluons with momenta $\boldsymbol{p}_1$ and $\boldsymbol{p}'_1$ $(= \boldsymbol{q}_1 - \boldsymbol{p}_1)$ respectively. Note that the $+$ component of the momenta is conserved both in the propagation and in the splitting, so that $k_a^+ = z p_0^+$, $k_b^+ = (1-z) p_0^+$.

in appendix A, together with compact, matrix, notations similar to those already in the previous section (cf. eq. (2.8)) one easily gets the following expression for this amplitude:

$$
\begin{aligned}
\mathcal{M}_{\lambda_a, \lambda_b}^{ab}(k_a^+ \, \boldsymbol{k}_a, k_b^+ \, \boldsymbol{k}_b) &= \frac{\mathrm{e}^{i(k_a^- + k_b^-) t_L}}{2 p_0^+} \int_{\boldsymbol{p}_0, \boldsymbol{p}_1, \boldsymbol{q}_1, \boldsymbol{p}'_1} \epsilon_{\lambda_b}^j(\boldsymbol{k}_b) \, \epsilon_{\lambda_a}^i(\boldsymbol{k}_a) \\
&\quad \times \int_{t_0}^{t_L} \mathrm{d}t_1 \, (\boldsymbol{k}_a \, a; \boldsymbol{k}_b \, b | \mathcal{G}(t_L, t_1) \mathcal{G}(t_L, t_1) \, | \boldsymbol{p}_1 \, a_1; \boldsymbol{p}'_1 \, b_1) \\
&\quad \times (\boldsymbol{p}_1 \, a_1; \boldsymbol{p}'_1 \, b_1 | \, \Gamma^{ijl} \, | \boldsymbol{q}_1 \, c_1)(\boldsymbol{q}_1 \, c_1 | \, \mathcal{G}(t_1, t_0) | \boldsymbol{p}_0 \, c_0) \, J^{l, c_0}(p_0^+, \boldsymbol{p}_0) \,,
\end{aligned}
$$
(3.1)

with $k_a^- = \boldsymbol{k}_a^2/(2 k_a^+)$, $k_b^- = \boldsymbol{k}_a^2/(2 k_b^+)$ and $z = k_a^+/p_0^+$. A summation over repeated discrete indices is implied. We have defined

$$
\begin{aligned}
(\boldsymbol{k}_a \, a; \boldsymbol{k}_b \, b | \, \mathcal{G}(t_L, t_1) \mathcal{G}(t_L, t_1) \, | \boldsymbol{p}_1 \, a_1; \boldsymbol{p}'_1 \, b_1) &\equiv (\boldsymbol{k}_a | \mathcal{G}^{a a_1}(t_L, t_1) | \boldsymbol{p}_1)(\boldsymbol{k}_b | \, \mathcal{G}^{b b_1}(t_L, t_1) | \boldsymbol{p}'_1) \,, \\
(\boldsymbol{p}_1 \, a_1; \boldsymbol{p}'_1 \, b_1 | \, \Gamma^{ijl} \, | \boldsymbol{q}_1 \, c_1) &\equiv (2\pi)^2 \delta(\boldsymbol{p}_1 + \boldsymbol{p}'_1 - \boldsymbol{q}_1) \, 2g \, f^{a_1 b_1 c_1} \Gamma^{ijl}(\boldsymbol{p}_1 - z \boldsymbol{q}_1, z) \,,
\end{aligned}
$$
(3.2)

and we denote indifferently the matrix elements of the single propagator by $(\boldsymbol{k}_a | \mathcal{G}^{a a_1}(t_L, t_1) | \boldsymbol{p}_1)$ or by $(\boldsymbol{k}_a \, a | \mathcal{G}(t_L, t_1) | \boldsymbol{p}_1 \, a_1)$, and similarly $(\boldsymbol{p}_1 \, a_1; \boldsymbol{p}'_1 \, b_1 | \, \Gamma^{ijl} \, | \boldsymbol{q}_1 \, c_1) = (\boldsymbol{p}_1; \boldsymbol{p}'_1 | \, \Gamma_{a_1 b_1 c_1}^{ijl} \, | \boldsymbol{q}_1)$.

To calculate the cross section, we have to multiply the amplitude by its complex conjugate amplitude. In order to analyze the effect of the medium average, it is convenient to draw the amplitude and the conjugate amplitude in the same diagram, one just below the other as shown in figure 5 (and in figure 1 of the previous section). The upper part of the diagram corresponds to the amplitude and the lower part corresponds to the conjugate amplitude, with time flowing from left to right identically in the amplitude and its complex conjugate. Gluons which are drawn parallel to each other represent the same physical
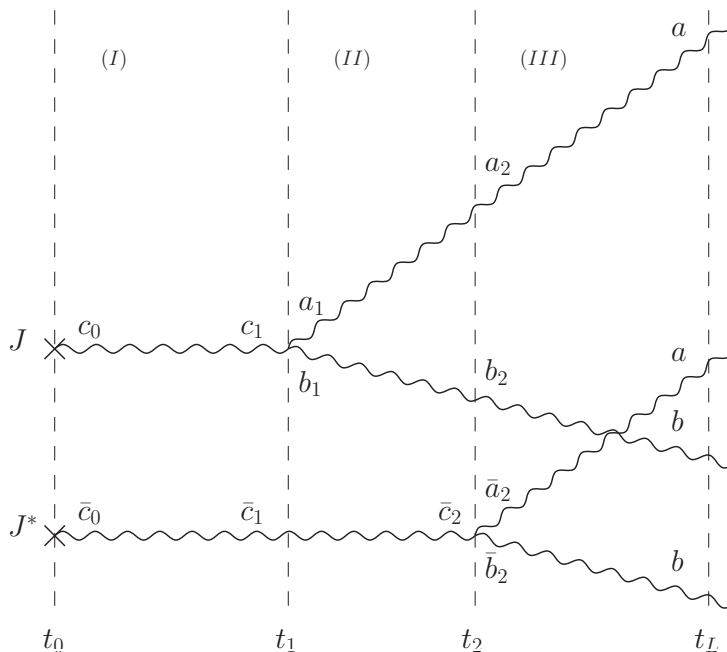
Figure 5. The three regions that are involved in the description of a gluon splitting in a medium. Time flows from left to right and the amplitude (upper part) is drawn together with the complex conjugate amplitude (lower part). The $+$ momentum is conserved in the splitting. The various indices at each ends of the gluon lines (wavy lines) are color indices. The times separating the various regions are light-cone times: t_1 and t_2 are the light-cone times where the gluon splitting occurs in the amplitude and the complex conjugate amplitude, respectively. The indices a, b, c are color indices, with each gluon carrying a given set of color indices that involve the same letter: thus 'gluon a' can be seen in the various colors a, a_1, a_2, etc.

gluon (in the amplitude and conjugate amplitude, respectively), so they have the same momenta and same color at $t = t_L$. For definiteness, we have chosen the splitting to occur first in the amplitude and then in the conjugate amplitude (i.e., $t_1 < t_2$), the inverse ordering can be accounted for by taking 2 times the real part when calculating the cross section (see eq. (3.13) below). One may then identify three distinct time regions that correspond respectively to the propagation between t_0 and t_1 (region I), between t_1 and t_2 (region II), and between t_2 and t_L (region III). To facilitate the grouping of terms in the different regions, we make repeated use of the identity (A.20), writing for instance (in matrix notations) $\mathcal{G}(t_L, t_1) = \mathcal{G}(t_L, t_2)\mathcal{G}(t_2, t_1)$, or $\mathcal{G}^\dagger(t_0, t_2) = \mathcal{G}^\dagger(t_0, t_1)\mathcal{G}^\dagger(t_1, t_2)$. Next, one introduces closure relations at appropriate times, over complete set of states in the transverse plane and in color space. The matrix element in the amplitude can then be

written as (see figures 5 and 7 for pictorial representations)

$$
(\boldsymbol{k}_a; \boldsymbol{k}_b | \mathcal{G}^{aa_2}(t_L, t_2) \mathcal{G}^{a_2 a_1}(t_2, t_1) \, \mathcal{G}^{bb_2}(t_L, t_2) \mathcal{G}^{b_2 b_1}(t_2, t_1) \, \Gamma^{ijl}_{a_1 b_1 c_1} \, \mathcal{G}^{c_1 c_0}(t_1, t_0) | \boldsymbol{p}_0)
$$

$$
= \int_{\boldsymbol{q}_2, \boldsymbol{p}_1, \boldsymbol{p}'_1, \boldsymbol{q}'_2} (\boldsymbol{k}_a | \mathcal{G}^{aa_2}(t_L, t_2) | \boldsymbol{q}_2)(\boldsymbol{q}_2 | \mathcal{G}^{a_2 a_1}(t_2, t_1) | \boldsymbol{p}_1)(\boldsymbol{k}_b | \mathcal{G}^{bb_2}(t_L, t_2) | \boldsymbol{q}'_2)(\boldsymbol{q}'_2 | \mathcal{G}^{b_2 b_1}(t_2, t_1) | \boldsymbol{p}'_1)
$$

$$
\times (\boldsymbol{p}_1; \boldsymbol{p}'_1 | \Gamma^{ijl}_{a_1 b_1 c_1} | \boldsymbol{q}_1)(\boldsymbol{q}_1 | \mathcal{G}^{c_1 c_0}(t_1, t_0) | \boldsymbol{p}_0), \tag{3.3}
$$

and that in the complex conjugate amplitude as

$$
(\bar{\boldsymbol{p}}_0 | \mathcal{G}^{\dagger \bar{c}_0 \bar{c}_1}(t_0, t_1) \mathcal{G}^{\dagger \bar{c}_1 \bar{c}_2}(t_1, t_2) \, \Gamma^{\dagger \, \bar{i}jl}_{\bar{a}_2 \bar{b}_2 \bar{c}_2} \, \mathcal{G}^{\dagger \bar{a}_2 a}(t_2, t_L) \mathcal{G}^{\dagger \bar{b}_2 b}(t_2, t_L) | \boldsymbol{k}_a; \boldsymbol{k}_b)
$$

$$
= \int_{\bar{\boldsymbol{q}}_1, \bar{\boldsymbol{q}}_2, \boldsymbol{p}_2, \boldsymbol{p}'_2} (\bar{\boldsymbol{p}}_0 | \mathcal{G}^{\dagger \bar{c}_0 \bar{c}_1}(t_0, t_1) | \bar{\boldsymbol{q}}_1)(\bar{\boldsymbol{q}}_1 | \mathcal{G}^{\dagger \bar{c}_1 \bar{c}_2}(t_1, t_2) | \bar{\boldsymbol{q}}_2)(\bar{\boldsymbol{q}}_2 | \Gamma^{\dagger \, \bar{i}jl}_{\bar{a}_2 \bar{b}_2 \bar{c}_2} | \boldsymbol{p}_2; \boldsymbol{p}'_2)
$$

$$
\times (\boldsymbol{p}_2 | \mathcal{G}^{\dagger \bar{a}_2 a}(t_2, t_L) | \boldsymbol{k}_a)(\boldsymbol{p}'_2 | \mathcal{G}^{\dagger \bar{b}_2 b}(t_2, t_L) | \boldsymbol{k}_b). \tag{3.4}
$$

One can now multiply the matrix elements of the amplitude and its complex conjugate, and regroup terms in the various regions. One writes the result in the following way

$$
(\boldsymbol{k}_a | \mathcal{G}^{aa_2}(t_L, t_2) | \boldsymbol{q}_2)(\boldsymbol{k}_b | \mathcal{G}^{bb_2}(t_L, t_2) | \boldsymbol{q}'_2)(\boldsymbol{p}_2 | \mathcal{G}^{\dagger \bar{a}_2 a}(t_2, t_L) | \boldsymbol{k}_a)(\boldsymbol{p}'_2 | \mathcal{G}^{\dagger \bar{b}_2 b}(t_2, t_L) | \boldsymbol{k}_b)(\bar{\boldsymbol{q}}_2 | \Gamma^{\dagger \, \bar{i}jl}_{\bar{a}_2 \bar{b}_2 \bar{c}_2} | \boldsymbol{p}_2; \boldsymbol{p}'_2)
$$

$$
\times (\boldsymbol{q}_2 | \mathcal{G}^{a_2 a_1}(t_2, t_1) | \boldsymbol{p}_1)(\boldsymbol{q}'_2 | \mathcal{G}^{b_2 b_1}(t_2, t_1) | \boldsymbol{p}'_1)(\bar{\boldsymbol{q}}_1 | \mathcal{G}^{\dagger \bar{c}_1 \bar{c}_2}(t_1, t_2) | \bar{\boldsymbol{q}}_2)(\boldsymbol{p}_1; \boldsymbol{p}'_1 | \Gamma^{ijl}_{a_1 b_1 c_1} | \boldsymbol{q}_1)
$$

$$
\times (\boldsymbol{q}_1 | \mathcal{G}^{c_1 c_0}(t_1, t_0) | \boldsymbol{p}_0)(\bar{\boldsymbol{p}}_0 | \mathcal{G}^{\dagger \bar{c}_0 \bar{c}_1}(t_0, t_1) | \bar{\boldsymbol{q}}_1),
$$

$$
\tag{3.5}
$$

where the three lines in the expression above correspond to the three regions III, II, I, respectively, from top to bottom. At this point, we are ready to discuss the medium average and identify the simple, factorized, color structure of the three regions.

3.2 Color structure

As already noted in the previous section, the contractions of background fields that are involved in the medium average preserve the overall color of the system, and since all such contractions are instantaneous, the overall color state of the system comprising all gluons in the amplitude and its complex conjugate is conserved at all times. Since, as we shall verify shortly, the overall color state is a color singlet at $t = t_L$, the gluons traversing the medium are in an overall color singlet at any given time. This property allows us to perform the medium averages explicitly by reducing considerably the number of color states to be considered along the calculation: all one needs to do is to find the appropriate singlet state in which the system is at the separation points t_1 and t_2. The resulting color structure is illustrated in figure 6.

That the system of gluons is in a color singlet state at $t = t_L$ is easy to see. Indeed the colors of the gluons are identical in the amplitude and in the complex conjugate amplitude, and since we do not observe the colors of the produced gluons, these colors are summed over, projecting the two pairs of gluons a and b onto color singlets. Since the system remains a color singlet at all times, it is a singlet at time t_0, corresponding to the beginning of region I, with which we start our detailed analysis.
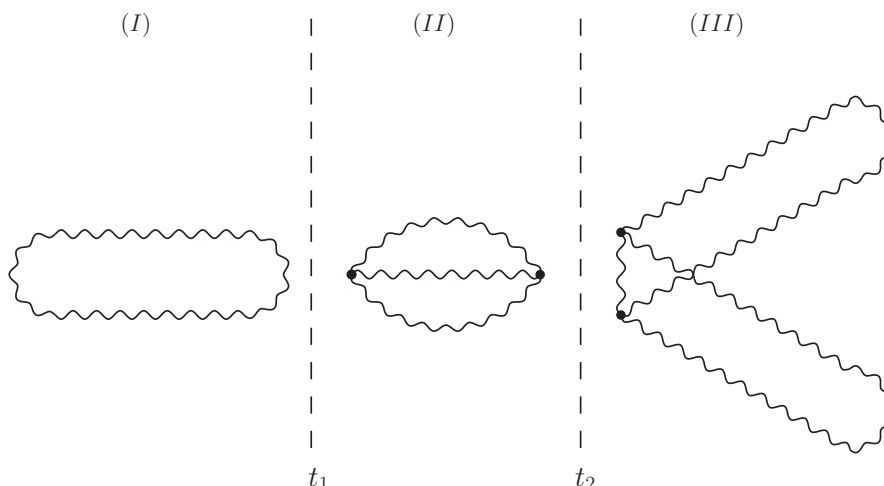
Figure 6. The color connections that are responsible for making the system of gluons a color singlet in each of the three regions. The dotted vertices represents f symbols, f^{abc}, while the 'vertical' connections among them represents Kronecker delta's, δ_{ab}.

Consider then region I, that is, the third line of eq. (3.5). As we have just argued, the gluon system is in a color singlet state. Hence at time t_0, the gluon carries the same color index in the direct and complex conjugate amplitude ($\bar{c}_0 = c_0$), and then the medium averaging yields

$$\delta^{c_0\bar{c}_0}\left\langle(\boldsymbol{q}_1|\mathcal{G}^{c_1 c_0}(t_1,t_0)|\boldsymbol{p}_0)(\bar{\boldsymbol{p}}_0|\mathcal{G}^{\dagger\,\bar{c}_0\bar{c}_1}(t_0,t_1)|\bar{\boldsymbol{q}}_1)\right\rangle = \delta^{c_1\bar{c}_1}(\boldsymbol{q}_1;\bar{\boldsymbol{q}}_1|S^{(2)}(t_1,t_0)|\boldsymbol{p}_0;\bar{\boldsymbol{p}}_0), \quad (3.6)$$

where the quantity $S^{(2)}(t_1,t_0)$ has already been introduced in eq. (2.13) and evaluated in eqs. (2.15)–(2.16). Note that in eq. (3.6) a sum over c_0 is performed. However, this sum is not free since the current also carries the same color index. However, since each term of the sum is eventually independent of c_0, we can correct the result by simply dividing by $N_c^2 - 1$. In summary, the contribution of region I after medium average is

$$\frac{\delta^{c_1\bar{c}_1}}{N_c^2 - 1}(\boldsymbol{q}_1;\bar{\boldsymbol{q}}_1|S^{(2)}(t_1,t_0)|\boldsymbol{p}_0;\bar{\boldsymbol{p}}_0). \quad (3.7)$$

Now we turn our attention to region II, that is the second line of eq. (3.5). We can use the Kronecker delta $\delta^{c_1\bar{c}_1}$ from eq. (3.7) and recall that the color structure of the vertex at t_1 is of the form $f^{a_1 b_1 c_1}$ to realize that the relevant correlator for this region is

$$f^{a_1 b_1 c_1}\left\langle(\boldsymbol{q}_2|\mathcal{G}^{a_2 a_1}(t_2,t_1)|\boldsymbol{p}_1)(\boldsymbol{q}_2'|\mathcal{G}^{b_2 b_1}(t_2,t_1)|\boldsymbol{p}_1')(\bar{\boldsymbol{q}}_1|\mathcal{G}^{\dagger\,c_1\bar{c}_2}(t_1,t_2)|\bar{\boldsymbol{q}}_2)\right\rangle, \quad (3.8)$$

from where it is clear that we have a color singlet state at t_1 by contracting the three initial color indices with an f symbol. This color structure is unchanged by the medium average in this region given that there is no other way to combine these three gluons into a singlet

– 17 –

state. It follows therefore that the color indices at t_2 must also be contracted with an f symbol. More specifically, this means that eq. (3.8) takes the form

$$f^{a_1 b_1 c_1} \left\langle (\boldsymbol{q}_2|\mathcal{G}^{a_2 a_1}(t_2,t_1)|\boldsymbol{p}_1)(\boldsymbol{q}_2'|\mathcal{G}^{b_2 b_1}(t_2,t_1)|\boldsymbol{p}_1')(\bar{\boldsymbol{q}}_1|\mathcal{G}^{\dagger c_1 \bar{c}_2}(t_1,t_2)|\bar{\boldsymbol{q}}_2) \right\rangle$$
$$\equiv f^{a_2 b_2 \bar{c}_2}(\boldsymbol{q}_2 \boldsymbol{q}_2'; \bar{\boldsymbol{q}}_2|S^{(3)}(t_2,t_1)|\boldsymbol{p}_1 \boldsymbol{p}_1'; \bar{\boldsymbol{q}}_1), \tag{3.9}$$

with

$$(\boldsymbol{q}_2 \boldsymbol{q}_2'; \bar{\boldsymbol{q}}_2|S^{(3)}(t_2,t_1)|\boldsymbol{p}_1 \boldsymbol{p}_1'; \bar{\boldsymbol{q}}_1)$$
$$= \frac{1}{N_c(N_c^2-1)} \left\langle (\boldsymbol{q}_2|\mathcal{G}^{a_2' a_1}(t_2,t_1)|\boldsymbol{p}_1)(\boldsymbol{q}_2'|\mathcal{G}^{b_2' b_1}(t_2,t_1)|\boldsymbol{p}_1')(\bar{\boldsymbol{q}}_1|\mathcal{G}^{\dagger c_1 \bar{c}_2'}(t_1,t_2)|\bar{\boldsymbol{q}}_2) \right\rangle f^{a_2' b_2' \bar{c}_2'} f^{a_1 b_1 c_1}. \tag{3.10}$$

Due to the simple color structure of this object, one can calculate explicitly the medium average of the Wilson lines inside the propagators, by resumming the contractions of each pairs of gluons independently. One gets

$$C_g^{(3)} = \frac{1}{N_c(N_c^2-1)} f^{a_1 b_1 c_1} \langle \tilde{U}_{a_2' a_1}(t_2,t_1;\boldsymbol{r}_a) \tilde{U}_{b_2' b_1}(t_2,t_1;\boldsymbol{r}_b) \tilde{U}^\dagger_{c_1 \bar{c}_2'}(t_1,t_2;\boldsymbol{r}_c) \rangle f^{a_2' b_2' \bar{c}_2'}$$
$$= \exp\left\{ -\frac{N_c\, n}{4} \int_{t_1}^{t_2} \mathrm{d}t \, [\sigma(\boldsymbol{r}_b - \boldsymbol{r}_c) + \sigma(\boldsymbol{r}_b - \boldsymbol{r}_a) + \sigma(\boldsymbol{r}_a - \boldsymbol{r}_c)] \right\}. \tag{3.11}$$

The color factor in front of the leading order dipole cross section can be calculated from the appropriate contraction of the color factors in the adjoint representation $f^{abc} f^{cde} f^{efa} = -\frac{N_c}{2} f^{bdf}$. The calculation of the path integral needed to complete the evaluation of $S^{(3)}$ is done in appendix B.2.

Turning our attention to region III, the first line of eq. (3.5), we see that the four gluons form a singlet state through the combination of two f's, one coming from eq. (3.9) and the other from the vertex at t_2 (see eq. (3.5)). As opposed to the previous cases, there are several ways of combining four gluons to form a singlet state. The final color state is given by the identification of two pairs of gluons as the conjugate of each other as explicitly shown by setting the color indices equal for the respective propagators at t_L (as already discussed, $a = \bar{a}$, $b = \bar{b}$). The relevant correlator for region III is therefore

$$f^{a_2 b_2 \bar{c}_2} f^{\bar{a}_2 \bar{b}_2 \bar{c}_2} \langle (\boldsymbol{k}_a|\mathcal{G}^{aa_2}(t_L,t_2)|\boldsymbol{q}_2)(\boldsymbol{k}_b|\mathcal{G}^{bb_2}(t_L,t_2)|\boldsymbol{q}_2')(\boldsymbol{p}_2|\mathcal{G}^{\dagger \bar{a}_2 a}(t_2,t_L)|\boldsymbol{k}_a)(\boldsymbol{p}_2'|\mathcal{G}^{\dagger \bar{b}_2 b}(t_2,t_L)|\boldsymbol{k}_b) \rangle$$
$$\equiv N_c(N_c^2-1)(\boldsymbol{k}_a \boldsymbol{k}_b; \boldsymbol{k}_a \boldsymbol{k}_b|S^{(4)}(t_L,t_2)|\boldsymbol{q}_2 \boldsymbol{q}_2'; \boldsymbol{p}_2 \boldsymbol{p}_2'). \tag{3.12}$$

The fact that there is no unique way to combine the four gluons into color singlets, in contrast to what happened for the 2 and 3-point functions, prevents us to give an explicit expression for the average of the Wilson lines in the propagators analogous to eq. (3.11) for the 3-point function. A more detailed analysis is required, which will be carried out in section 4.

3.3 Momentum structure

The fact that the correlator of the random background field depends only on the difference of the transverse coordinates leads to total transverse momentum conservation. It follows
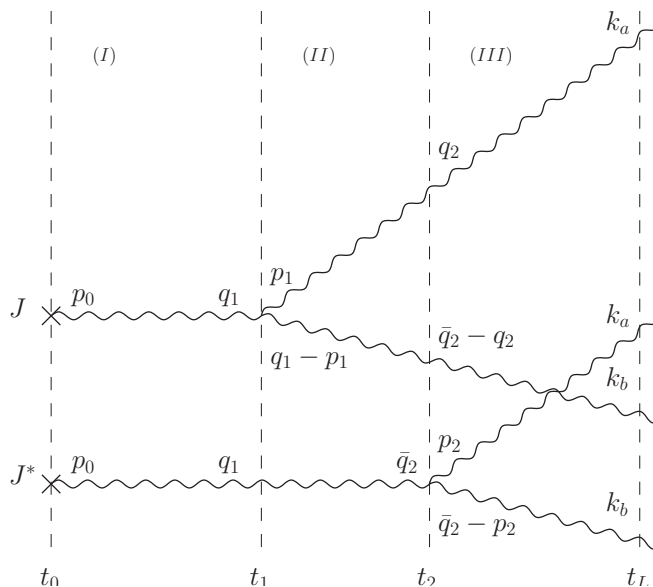
Figure 7. Flow of momenta in the amplitude for one gluon splitting and its complex conjugate. At any given time, the sum of momenta in the amplitude equals the sum of momenta in the complex conjugate amplitude. The + component of the momentum is conserved, $k_a^+ + k_b^+ = p_0^+$, and is not indicated.

that at each instant of time, the sum of momenta in the amplitude equals that of momenta in the complex conjugate amplitude, since this is the case at the final time t_L. As explicitly shown in appendix B, each of the n-point function contains a corresponding δ-function expressing this property. There are also additional δ-functions hidden in the vertices Γ which express the conservation of transverse momentum in the local splitting. Using all these δ-functions, one can then reduce considerably the number of momentum integrations when building the cross section for the branching process. The resulting flow of momenta is displayed in figure 7, which also lists the independent momenta that we use. We denote with a tilde the n-point functions from which the delta function for momentum conservation has been factored out.

There are further simplifications that reduce the number of independent momentum variables. For instance, the 2-point function depends only on the difference of two momenta. Similarly for the 3-point function. Also the vertex depends only on $\boldsymbol{p} - z\boldsymbol{q}$, as visible on eq. (A.23). These extra simplifications will be exploited when needed.

We are now in a position where we can write the cross section for the two gluon production process. After performing the medium average and summing over polarizations, one obtains

$$
\frac{\mathrm{d}^2\sigma}{\mathrm{d}\Omega_{k_a}\mathrm{d}\Omega_{k_b}} = \frac{g^2 N_c}{(2p_0^+)^2} \, 2\Re e \int_{t_0}^{t_L}\mathrm{d}t_2 \int_{t_0}^{t_2}\mathrm{d}t_1 \int_{\boldsymbol{p}_0,\boldsymbol{p}_1\boldsymbol{q}_1\bar{\boldsymbol{q}}_2\boldsymbol{p}_2\boldsymbol{q}_2} \Gamma^{ijl}(\boldsymbol{p}_1 - z\boldsymbol{q}_1, z)\,\Gamma^{\bar{i}jl}(\boldsymbol{p}_2 - z\bar{\boldsymbol{q}}_2, z)
$$
$$
\times(\boldsymbol{k}_a\boldsymbol{k}_b;\boldsymbol{k}_a\boldsymbol{k}_b|\tilde{S}^{(4)}(t_L,t_2)|\boldsymbol{q}_2,\bar{\boldsymbol{q}}_2-\boldsymbol{q}_2;\boldsymbol{p}_2,\bar{\boldsymbol{q}}_2-\boldsymbol{p}_2)(\boldsymbol{q}_2,\bar{\boldsymbol{q}}_2-\boldsymbol{q}_2;\bar{\boldsymbol{q}}_2|\tilde{S}^{(3)}(t_2,t_1)|\boldsymbol{p}_1,\boldsymbol{q}_1-\boldsymbol{p}_1;\boldsymbol{q}_1)
$$
$$
\times(\boldsymbol{q}_1;\boldsymbol{q}_1|\tilde{S}^{(2)}(t_1,t_0)|\boldsymbol{p}_0;\boldsymbol{p}_0)\,J^{i,c_0}(p_0^+,\boldsymbol{p}_0)J^{*\bar{i},c_0}(p_0^+,\boldsymbol{p}_0). \tag{3.13}
$$

In this equation, we used the compact notation $\mathrm{d}\Omega_k \equiv (2\pi)^{-3}\mathrm{d}^2\boldsymbol{k}\,\mathrm{d}k^+/2k^+$ for the element in phase-space and in the r.h.s. it is understood that $p_0^+ = k_a^+ + k_b^+$ and $z = k_a^+/p_0^+$.

3.4 Qualitative comments

Before getting into the details of the evaluation of the various n-point functions that enter the expression above, we find it useful to make a few qualitative observations that will lead us to better appreciate the physical content of the calculations to be performed in subsequent sections.

As we have seen, the n-point functions that appear in the various regions contain a medium average of a product of Wilson lines in an overall color singlet state, inside a path integration. The way to proceed in the explicit average evaluations is to calculate the average of a particular combination of Wilson lines with fixed paths in transverse coordinate space, then perform the integration over these paths. In general, the medium average of the Wilson lines decays exponentially with the distance between particles constituting a color neutral state, typically as $\Delta\boldsymbol{x}^2 \gtrsim 2/(\hat{q}\Delta t)$ (see e.g. eq. (2.18) for the 2-point function). That is, one gets a significant suppression factor whenever the particles are farther apart than the inverse of the typical transverse momentum acquired by multiple collisions. On the other hand, in the path integral, the gluons trajectories diffuse in transverse coordinate space, which typically increases the average distances between the gluons so that $\Delta\boldsymbol{x}^2 \sim \Delta t/\omega$. Combining these two estimates, one gets that in order avoid a large exponential suppression factor the longitudinal extent of the medium average in consideration should be limited to $\Delta t \lesssim \sqrt{2\omega/\hat{q}} = \tau_{\mathrm{br}} \ll L$.

The argument above does not always hold since it assumes that the diffusion in transverse space is independent for all the gluons, so that the mean distance between them is monotonically increasing. However, when two gluons are conjugate to each other their diffusions in transverse coordinate space are correlated, indeed their transverse separation stays constant (see appendix B). This implies that the longitudinal extent of region I is not constrained by the argument above. On the other hand, the three gluons in region II propagate independently. This, combined with the fact that there is only one way to form a color neutral state with three gluons, implies that this region II must be short-lived, i.e., $t_2 - t_1 \lesssim \tau_{\mathrm{br}}$, in order to avoid suppression factors.

In region III we run again into the case where gluons can be paired with their respective conjugates and therefore do not propagate all independently. Moreover, by pairing the gluons this way, two color neutral subsystems are formed, which can propagate independently and be arbitrarily far away from each other without introducing suppression factors. Nevertheless, the general argument concerning the suppression of correlations by medium rescattering still holds within a narrow region bordering region II, where all four gluons are still correlated. We shall find that the longitudinal extent of that intermediate region is of order τ_{br}, for the same basic reasons as for region II. Accordingly, we shall conclude that the four-point correlator obtained for the medium average in region III is factorizable into two two-point correlators except for a parametrically small ($\sim \tau_{\mathrm{br}}/L$) region right after the second splitting.

4 Factorization of two-gluon propagation

We turn now to the detailed analysis of region III. As already anticipated in the previous section, the main goal here is to show that the propagation of the two resulting gluons can be considered as independent and correlations among them are a subleading effect. In that case, all the effects of the splitting can be included inside the splitting kernel of region II, which will be calculated in detail in the next section.

We need to calculate explicitly the 4-point function $S^{(4)}(t_L, t_2)$. Since the definition of the scalar propagators entering the average in (3.12) take a simpler form in coordinate space, it is convenient to calculate first the medium average of the four propagators in coordinate space with arbitrary endpoints, perform the Fourier transform, and then impose the necessary constraints in the momentum variables.

The coordinate space 4-point function under consideration takes the explicit form

$$
\begin{aligned}
&(\boldsymbol{y}_a \boldsymbol{y}_b; \bar{\boldsymbol{y}}_a \bar{\boldsymbol{y}}_b | S^{(4)}(t_L, t_2) | \boldsymbol{x}_a \boldsymbol{x}_b; \bar{\boldsymbol{x}}_a, \bar{\boldsymbol{x}}_b) \\
&= \int \mathcal{D} \boldsymbol{r}_a \mathcal{D} \boldsymbol{r}_b \mathcal{D} \bar{\boldsymbol{r}}_a \mathcal{D} \bar{\boldsymbol{r}}_b \exp\left\{ \frac{i}{2} \int_{t_2}^{t_L} \mathrm{d}t \left(k_a^+ \dot{\boldsymbol{r}}_a^2 + k_b^+ \dot{\boldsymbol{r}}_b^2 - k_a^+ \dot{\bar{\boldsymbol{r}}}_a^2 - k_b^+ \dot{\bar{\boldsymbol{r}}}_b^2 \right) \right\} \\
&\quad \times f^{a_2 b_2 \bar{c}_2} f^{\bar{a}_2 \bar{b}_2 \bar{c}_2} \langle \tilde{U}_{a a_2}(t_L, t_2; \boldsymbol{r}_a) \tilde{U}_{b b_2}(t_L, t_2; \boldsymbol{r}_b) \tilde{U}_{\bar{a}_2 a}^{\dagger}(t_2, t_L; \bar{\boldsymbol{r}}_a) \tilde{U}_{\bar{b}_2 b}^{\dagger}(t_2, t_L; \bar{\boldsymbol{r}}_b) \rangle, \quad (4.1)
\end{aligned}
$$

where $\boldsymbol{r}_{a,b}(t_2) = \boldsymbol{x}_{a,b}, \boldsymbol{r}_{a,b}(t_L) = \boldsymbol{y}_{a,b}$ and similarly for the bar coordinates.

We start by first calculating the medium average of the Wilson lines before attempting to perform the path integrations. Since for the moment we are only concerned with what occurs in region III and all the propagators have the same longitudinal extent, longitudinal coordinates will be dropped from the Wilson lines, and only the transverse trajectories will be kept explicit.

The calculation of the correlator in the last line of eq. (4.1) turns out to be extremely complex even for our simple, Gaussian, model for the random background field. So, before we start the calculation, it is useful to make some remarks about its general structure and the strategy that will be employed for the rest of the section. Since our goal in this section is to show that, to the level of desired accuracy, one can factorize this correlator into the propagation of two independent gluons, it will be convenient to split the evaluation into a 'factorizable' piece and a 'non-factorizable' piece where,

$$
S^{(4)}(t_L, t_2) = S_{\mathrm{fac}}^{(4)}(t_L, t_2) + S_{\mathrm{nfac}}^{(4)}(t_L, t_2), \quad (4.2)
$$

with

$$
\begin{aligned}
&(\boldsymbol{y}_a \boldsymbol{y}_b; \bar{\boldsymbol{y}}_a \bar{\boldsymbol{y}}_b | S_{\mathrm{fac}}^{(4)}(t_L, t_2) | \boldsymbol{x}_a \boldsymbol{x}_b; \bar{\boldsymbol{x}}_a, \bar{\boldsymbol{x}}_b) \\
&= (\boldsymbol{y}_a; \bar{\boldsymbol{y}}_a | S^{(2)}(t_L, t_2) | \boldsymbol{x}_a; \bar{\boldsymbol{x}}_a)(\boldsymbol{y}_b; \bar{\boldsymbol{y}}_b | S^{(2)}(t_L, t_2) | \boldsymbol{x}_b; \bar{\boldsymbol{x}}_b), \quad (4.3)
\end{aligned}
$$

or, in terms of the momentum representation entering the expression for the cross section,

$$
\begin{aligned}
&(\boldsymbol{k}_a \boldsymbol{k}_b; \boldsymbol{k}_a \boldsymbol{k}_b | \tilde{S}_{\mathrm{fac}}^{(4)}(t_L, t_2) | \boldsymbol{q}_2, \bar{\boldsymbol{q}}_2 - \boldsymbol{q}_2; \boldsymbol{p}_2, \bar{\boldsymbol{q}}_2 - \boldsymbol{p}_2) \\
&= (2\pi)^2 \delta^{(2)}(\boldsymbol{p}_2 - \boldsymbol{q}_2) \mathcal{P}(\boldsymbol{k}_a - \boldsymbol{q}_2, t_L - t_2) \mathcal{P}(\boldsymbol{k}_b - \bar{\boldsymbol{q}}_2 + \boldsymbol{q}_2, t_L - t_2). \quad (4.4)
\end{aligned}
$$
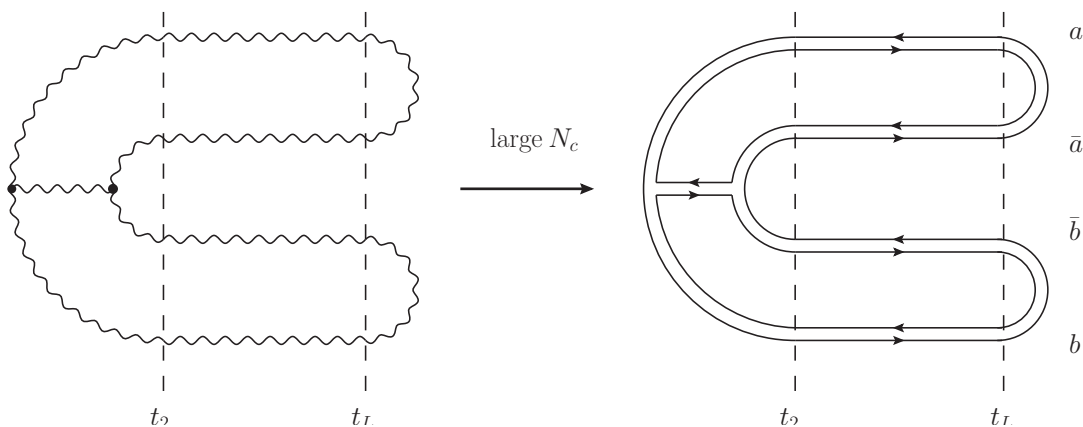
Figure 8. Graphical representation of the correlator (4.6) and its large-N_c version (4.7). The horizontal lines in between the vertical dashed lines represent the Wilson lines either in the adjoint (gluon lines) or fundamental (quark lines) representation. Lines in the right and left ends of the diagrams indicate color connections only, with gluon lines identifying adjoint color indices, quark lines identifying fundamental color indices, and three gluon vertices representing f symbols.

The analysis below is therefore aimed to show explicitly that the non-factorizable pieces are suppressed with respect to the factorizable pieces and therefore it is only the expression in (4.4) which enters the result for the cross section of the two-gluon production process.

The complete evaluation of the correlator in (4.1) is complicated because of the many singlet states that can be constructed with four gluons, but by transforming this expression into one with only Wilson lines in the fundamental representation it is possible to gain some insight about the transitions between the different color states. In order to do that, one makes use of the following identity relating Wilson lines in the adjoint representation with Wilson lines in the fundamental representation,

$$\tilde{U}_{ab}(\boldsymbol{r}) = 2\mathrm{Tr}\left[U^\dagger(\boldsymbol{r})t^a U(\boldsymbol{r})t^b\right]. \tag{4.5}$$

After repeated use of this identity, one can perform the color algebra and eliminate all the explicit color factors (see details in appendix C), arriving at

$$
f^{a_2 b_2 \bar{c}_2} f^{\bar{a}_2 \bar{b}_2 \bar{c}_2} \langle \tilde{U}_{aa_2}(\boldsymbol{r}_a)\tilde{U}_{bb_2}(\boldsymbol{r}_b)\tilde{U}^\dagger_{\bar{a}_2 a}(\bar{\boldsymbol{r}}_a)\tilde{U}^\dagger_{\bar{b}_2 b}(\bar{\boldsymbol{r}}_b)\rangle
$$
$$
= \frac{1}{2}\Big\langle \mathrm{Tr}\left[U(\boldsymbol{r}_a)U^\dagger(\bar{\boldsymbol{r}}_a)\right]\mathrm{Tr}\left[U(\bar{\boldsymbol{r}}_b)U^\dagger(\boldsymbol{r}_b)\right]\mathrm{Tr}\left[U^\dagger(\boldsymbol{r}_a)U(\boldsymbol{r}_b)U^\dagger(\bar{\boldsymbol{r}}_b)U(\bar{\boldsymbol{r}}_a)\right]
$$
$$
-\mathrm{Tr}\left[U(\boldsymbol{r}_a)U^\dagger(\bar{\boldsymbol{r}}_a)U(\boldsymbol{r}_b)U^\dagger(\bar{\boldsymbol{r}}_b)U(\bar{\boldsymbol{r}}_a)U^\dagger(\boldsymbol{r}_a)U(\bar{\boldsymbol{r}}_b)U^\dagger(\boldsymbol{r}_b)\right] + \mathrm{h.c.}\Big\rangle. \tag{4.6}
$$

This may not look like a real improvement: the number of Wilson lines has doubled and now we have several nontrivial terms to deal with! The advantage of this approach is that it greatly simplifies when one considers the large-N_c limit, a common approach used to simplify the calculations while capturing the essential physical behavior. In the fundamental representation, each color trace is proportional to N_c, from where it becomes clear that the first term will dominate over the second in the large-N_c limit. Still in this limit, one can factorize the average of a product of traces as the product of the

independent averages of each individual trace. Indeed, correlations between fields entering different traces are suppressed by inverse powers of N_c. By also using the fact that all the considered correlators are real (at least, in our Gaussian model for the medium averages), we finally get the following expression for the dominant contribution at large N_c:

$$
f^{a_2 b_2 \bar{c}_2} f^{\bar{a}_2 \bar{b}_2 \bar{c}_2} \langle \tilde{U}_{a a_2}(\boldsymbol{r}_a) \tilde{U}_{b b_2}(\boldsymbol{r}_b) \tilde{U}^{\dagger}_{\bar{a}_2 a}(\bar{\boldsymbol{r}}_a) \tilde{U}^{\dagger}_{\bar{b}_2 b}(\bar{\boldsymbol{r}}_b) \rangle
$$
$$
= \left\langle \mathrm{Tr}\left[U(\boldsymbol{r}_a) U^{\dagger}(\bar{\boldsymbol{r}}_a) \right] \right\rangle \left\langle \mathrm{Tr}\left[U(\bar{\boldsymbol{r}}_b) U^{\dagger}(\boldsymbol{r}_b) \right] \right\rangle \left\langle \mathrm{Tr}\left[U^{\dagger}(\boldsymbol{r}_a) U(\boldsymbol{r}_b) U^{\dagger}(\bar{\boldsymbol{r}}_b) U(\bar{\boldsymbol{r}}_a) \right] \right\rangle . \text{(4.7)}
$$

This relation can be easily seen graphically by replacing the gluons with quark-antiquark pairs as shown in figure 8, where only the planar part was kept. Each of the loops corresponds to one of the traces in (4.7) and connections among them are suppressed.

The three factors in (4.7) can then be evaluated independently. Two of them are quark dipoles which take the by now standard form (compare with eq. (2.14))

$$
C_q^{(2)}(t_L, t_2; \boldsymbol{r}, \bar{\boldsymbol{r}}) \equiv \frac{1}{N_c} \left\langle \mathrm{Tr}\left[U(\boldsymbol{r}) U^{\dagger}(\bar{\boldsymbol{r}}) \right] \right\rangle = \exp\left[-\frac{C_F n}{2} \int_{t_2}^{t_L} \mathrm{d}t\, \sigma(\boldsymbol{r} - \bar{\boldsymbol{r}}) \right] . \quad \text{(4.8)}
$$

The third factor in (4.7) has the form of a quadrupole amplitude. This kind of correlator has been studied in the literature, always for Wilson lines with fixed transverse coordinates while here we need to be able to evaluate it for arbitrary trajectories. A straightforward generalization, as it was possible in the case of the dipole amplitude, is so far not available. On the other hand, the use of the large-N_c limit helps greatly to further simplify the calculation and allows us to gain some insight into which terms are the important ones for the situation at hand.

There are only two independent singlet states that can be formed with two quark-antiquark pairs corresponding to the two possible ways of pairing quarks with antiquarks. Considering the way the color indices are contracted for the quadrupole amplitude, one can consider this quadrupole amplitude as the probability of switching from one singlet state to the other one, after undergoing multiple scatterings with the medium. For the case at hand, it is clear that the natural causal way to consider the process is such that the two singlet states are made with the pairs of lines a, b and respectively $\bar{a}, \bar{b}$ in the initial state, and with the pairs $a, \bar{a}$ and $b, \bar{b}$ in the final state.

The two aforementioned singlet states are not orthogonal and therefore one can isolate a contribution where the system was initially in the final color state and all the interactions with the medium preserve this color state. In that case, one can consider the four-particle system as two separate quark dipoles, which do not see each other, yielding a product of two already familiar dipole amplitudes $C_q^{(2)}$. This type of contribution has the exact same structure as what was referred at the beginning of the section as the factorizable piece and the calculation below will show explicitly how one arrives at eq. (4.3).

The non-factorizable piece consists of all the possible cases not accounted for in the factorizable piece, which are those where transitions between the color states are allowed during the interaction. In general one can have an arbitrary number of such transitions, but in the large-N_c limit those are suppressed by inverse powers of N_c. In that case, one must take into account only contributions where there is only one transition between the two
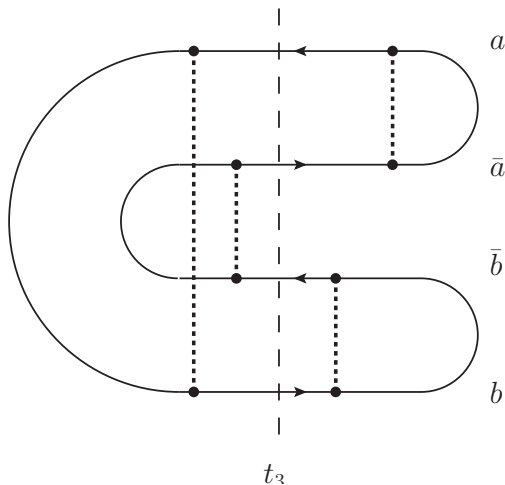
Figure 9. Sample of the kind of interactions allowed at each end of the quadrupole amplitude. The dashed line in the middle represents the transition point in between the two regions where a different kind of contraction is allowed.

possible singlet states. All the diagrams which are not suppressed by inverse powers of N_c have the general form depicted in figure 9: on the left side of the diagram only contractions between lines a and b, or between lines $\bar{a}$ and $\bar{b}$ are allowed, while on the right side of the diagram only contractions between the lines a and $\bar{a}$, or between lines b and $\bar{b}$ are allowed. These two regions are separated by just one contraction performing the transition, which can connect either lines a and $\bar{b}$, or lines $\bar{a}$ and b. It is easy to show that those are the only planar diagrams present in this calculation.

In order to find a closed expression for the sum of all these diagrams one has to choose an orientation to perform the resummation. For our purpose, it is convenient to read the diagrams from right to left. In that case, one starts with the dipole formed by lines $a, \bar{a}$ and $b, \bar{b}$ up to t_3 at which point the transition contraction occurs. Specifically, at t_3, a transition occurs to the singlet state where the two dipoles are formed by the pairs a, b and $\bar{a}, \bar{b}$. All the contractions on both sides of the interactions can be resummed into dipole amplitudes over the corresponding longitudinal extent. This procedure assumes that there is a transition, and therefore ignores all the diagrams with no transition, i.e., the diagrams where all the contractions respect the singlet structure in the right side of the diagram. In order to properly account for those diagrams one must include the factorizable contribution, given by the product of two dipole amplitudes for the respective dipoles in the right hand side of the diagram. The total result is then the following:

$$
\begin{aligned}
Q(t_L, t_2; \boldsymbol{r}_a, \boldsymbol{r}_b, \bar{\boldsymbol{r}}_a, \bar{\boldsymbol{r}}_b) &\equiv \frac{1}{N_c} \left\langle \mathrm{Tr} \left[U^\dagger(\boldsymbol{r}_a) U(\boldsymbol{r}_b) U^\dagger(\bar{\boldsymbol{r}}_b) U(\bar{\boldsymbol{r}}_a) \right] \right\rangle \\
&= C_q^{(2)}(t_L, t_2; \boldsymbol{r}_a, \bar{\boldsymbol{r}}_a) C_q^{(2)}(t_L, t_2; \boldsymbol{r}_b, \bar{\boldsymbol{r}}_b) \\
&\quad + \int_{t_2}^{t_L} \mathrm{d}t_3 \, C_q^{(2)}(t_L, t_3; \boldsymbol{r}_a, \bar{\boldsymbol{r}}_a) C_q^{(2)}(t_L, t_3; \boldsymbol{r}_b, \bar{\boldsymbol{r}}_b) T(t_3) \\
&\quad \times C_q^{(2)}(t_3, t_2; \boldsymbol{r}_a, \boldsymbol{r}_b) C_q^{(2)}(t_3, t_2; \bar{\boldsymbol{r}}_a, \bar{\boldsymbol{r}}_b),
\end{aligned}
\tag{4.9}
$$
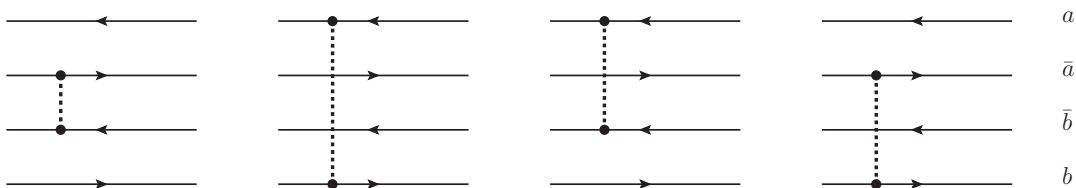
Figure 10. Contractions contributing to the transition amplitude between the two singlet states.

where $T(t_3)$ denotes the transition between the two states. It receives contributions from the diagrams in figure 10 and is explicitly given by

$$T(t_3) = C_F n \left[\sigma(\boldsymbol{r}_a - \boldsymbol{r}_b) + \sigma(\bar{\boldsymbol{r}}_a - \bar{\boldsymbol{r}}_b) - \sigma(\boldsymbol{r}_a - \bar{\boldsymbol{r}}_b) - \sigma(\bar{\boldsymbol{r}}_a - \boldsymbol{r}_b) \right]_{t_3}, \qquad (4.10)$$

where all coordinates are evaluated at t_3. The separation between the factorizable piece and the non-factorizable one is manifest in formula (4.9). It is important to note that the same analysis can be performed by reading the diagrams from left to right. One obtains a formula which is the same as above except that the labels b and $\bar{a}$ are interchanged. In that case the transition amplitude includes $a, \bar{a}$ and $b, \bar{b}$ contractions instead of the first two diagrams of figure 10. It is easy to show that the two expressions are equivalent by noticing that if one substracts the two different ways of writing the non-factorizable term one can perform the t_3 integral explicitly and show that the resulting contribution vanishes.

Now we are in a position to insert the medium average of the Wilson lines into the 4-point function (4.7). Consider first the term corresponding to the factorizable piece of the quadrupole, one gets

$$(\boldsymbol{y}_a \boldsymbol{y}_b; \bar{\boldsymbol{y}}_a \bar{\boldsymbol{y}}_b | S_{\text{fac}}^{(4)}(t_L, t_2) | \boldsymbol{x}_a \boldsymbol{x}_b; \bar{\boldsymbol{x}}_a, \bar{\boldsymbol{x}}_b)$$
$$= \int \mathcal{D}\boldsymbol{r}_a \mathcal{D}\boldsymbol{r}_b \mathcal{D}\bar{\boldsymbol{r}}_a \mathcal{D}\bar{\boldsymbol{r}}_b \exp\left[\frac{i}{2} \int_{t_2}^{t_L} \mathrm{d}t \, \left(k_a^+ \dot{\boldsymbol{r}}_a^2 + k_b^+ \dot{\boldsymbol{r}}_b^2 - k_a^+ \dot{\bar{\boldsymbol{r}}}_a^2 - k_b^+ \dot{\bar{\boldsymbol{r}}}_b^2 \right) \right]$$
$$\times \left[C_q^{(2)}(t_L, t_2; \boldsymbol{r}_a, \bar{\boldsymbol{r}}_a) C_q^{(2)}(t_L, t_2; \boldsymbol{r}_b, \bar{\boldsymbol{r}}_b) \right]^2 . \qquad (4.11)$$

In the large-N_c limit the square of a quark dipole amplitude is equivalent to a gluon dipole amplitude, therefore this factorizable piece can be rewritten as

$$(\boldsymbol{y}_a \boldsymbol{y}_b; \bar{\boldsymbol{y}}_a \bar{\boldsymbol{y}}_b | S_{\text{fac}}^{(4)}(t_L, t_2) | \boldsymbol{x}_a \boldsymbol{x}_b; \bar{\boldsymbol{x}}_a, \bar{\boldsymbol{x}}_b)$$
$$= \int \mathcal{D}\boldsymbol{r}_a \mathcal{D}\bar{\boldsymbol{r}}_a \exp\left\{ \frac{ik_a^+}{2} \int_{t_2}^{t_L} \mathrm{d}t \, \left(\dot{\boldsymbol{r}}_a^2 - \dot{\bar{\boldsymbol{r}}}_a^2 \right) \right\} C_g^{(2)}(t_L, t_2; \boldsymbol{r}_a, \bar{\boldsymbol{r}}_a)$$
$$\times \int \mathcal{D}\boldsymbol{r}_b \mathcal{D}\bar{\boldsymbol{r}}_b \exp\left\{ \frac{ik_b^+}{2} \int_{t_2}^{t_L} \mathrm{d}t \, \left(\dot{\boldsymbol{r}}_b^2 - \dot{\bar{\boldsymbol{r}}}_b^2 \right) \right\} C_g^{(2)}(t_L, t_2; \boldsymbol{r}_b, \bar{\boldsymbol{r}}_b),$$
$$= (\boldsymbol{y}_a; \bar{\boldsymbol{y}}_a | S^{(2)}(t_L, t_2) | \boldsymbol{x}_a; \bar{\boldsymbol{x}}_a)(\boldsymbol{y}_b; \bar{\boldsymbol{y}}_b | S^{(2)}(t_L, t_2) | \boldsymbol{x}_b; \bar{\boldsymbol{x}}_b), \qquad (4.12)$$

where we have identified the path-integral representations of the 2-point function $S^{(2)}(t_L, t_2)$ according to eq. (B.4). We thus find the factorized structure anticipated in eq. (4.3), at least within the large-N_c approximation.

Now let us focus on the non-factorizable piece. The last line on (4.9) has the same structure as the factorizable piece except for the fact that its starting longitudinal coordinate is at t_3. One can still recombine this piece with the remaining dipole amplitudes in (4.7) since those amplitudes can be split in two in the following way:

$$C^{(2)}(t_L, t_2; \boldsymbol{r}, \bar{\boldsymbol{r}}) = C^{(2)}(t_L, t_3; \boldsymbol{r}, \bar{\boldsymbol{r}})C^{(2)}(t_3, t_2; \boldsymbol{r}, \bar{\boldsymbol{r}}), \tag{4.13}$$

yielding to two independent gluon dipoles for the region with longitudinal coordinate greater than t_3.

$$\begin{aligned}
&(\boldsymbol{y}_a \boldsymbol{y}_b; \bar{\boldsymbol{y}}_a \bar{\boldsymbol{y}}_b | S_{\text{nfac}}^{(4)}(t_L, t_2) | \boldsymbol{x}_a \boldsymbol{x}_b; \bar{\boldsymbol{x}}_a, \bar{\boldsymbol{x}}_b) \\
&= \int \mathcal{D}\boldsymbol{r}_a \mathcal{D}\boldsymbol{r}_b \mathcal{D}\bar{\boldsymbol{r}}_a \mathcal{D}\bar{\boldsymbol{r}}_b \exp\left\{\frac{i}{2} \int_{t_2}^{t_L} dt\, (k_a^+ \dot{\boldsymbol{r}}_a^2 + k_b^+ \dot{\boldsymbol{r}}_b^2 - k_a^+ \dot{\bar{\boldsymbol{r}}}_a^2 - k_b^+ \dot{\bar{\boldsymbol{r}}}_b^2)\right\} \\
&\quad \times \int_{t_2}^{t_L} dt_3 \left[C_q^{(2)}(t_L, t_3; \boldsymbol{r}_a, \bar{\boldsymbol{r}}_a)C_q^{(2)}(t_L, t_3; \boldsymbol{r}_b, \bar{\boldsymbol{r}}_b)\right]^2 T(t_3) \\
&\quad \times C_q^{(2)}(t_3, t_2; \boldsymbol{r}_a, \boldsymbol{r}_b)C_q^{(2)}(t_3, t_2; \bar{\boldsymbol{r}}_a, \bar{\boldsymbol{r}}_b)C_q^{(2)}(t_3, t_2; \boldsymbol{r}_a, \boldsymbol{r}_b)C_q^{(2)}(t_3, t_2; \bar{\boldsymbol{r}}_a, \bar{\boldsymbol{r}}_b). \tag{4.14}
\end{aligned}$$

Moreover, in the same way that the scalar propagators follow the convolution relation (A.20), one can also split the longitudinal extent of the path integrals at t_3 and explicitly perform the integration in the region where the system factorizes into two independent gluons. One gets,

$$\begin{aligned}
&(\boldsymbol{y}_a \boldsymbol{y}_b; \bar{\boldsymbol{y}}_a \bar{\boldsymbol{y}}_b | S_{\text{nfac}}^{(4)}(t_L, t_2) | \boldsymbol{x}_a \boldsymbol{x}_b; \bar{\boldsymbol{x}}_a, \bar{\boldsymbol{x}}_b) \\
&= \int_{t_2}^{t_L} dt_3 \int_{\boldsymbol{z}_a \bar{\boldsymbol{z}}_a \boldsymbol{z}_b \bar{\boldsymbol{z}}_b} (\boldsymbol{y}_a; \bar{\boldsymbol{y}}_a | S^{(2)}(t_L, t_3) | \boldsymbol{z}_a; \bar{\boldsymbol{z}}_a)(\boldsymbol{y}_b; \bar{\boldsymbol{y}}_b | S^{(2)}(t_L, t_3) | \boldsymbol{z}_b; \bar{\boldsymbol{z}}_b) T(Z) \\
&\quad \times \int_{t_2}^{t_3} \mathcal{D}\boldsymbol{r}_a \mathcal{D}\boldsymbol{r}_b \mathcal{D}\bar{\boldsymbol{r}}_a \mathcal{D}\bar{\boldsymbol{r}}_b \exp\left\{\frac{i}{2} \int_{t_2}^{t_3} dt\, (k_a^+ \dot{\boldsymbol{r}}_a^2 + k_b^+ \dot{\boldsymbol{r}}_b^2 - k_a^+ \dot{\bar{\boldsymbol{r}}}_a^2 - k_b^+ \dot{\bar{\boldsymbol{r}}}_b^2)\right\} \\
&\quad \times C_q^{(2)}(t_3, t_2; \boldsymbol{r}_a, \boldsymbol{r}_b)C_q^{(2)}(t_3, t_2; \bar{\boldsymbol{r}}_a, \bar{\boldsymbol{r}}_b)C_q^{(2)}(t_3, t_2; \boldsymbol{r}_a, \boldsymbol{r}_b)C_q^{(2)}(t_3, t_2; \bar{\boldsymbol{r}}_a, \bar{\boldsymbol{r}}_b), \tag{4.15}
\end{aligned}$$

with $\boldsymbol{r}_{a,b}(t_3) = \boldsymbol{z}_{a,b}$ and similarly for the bar coordinates.

The transition amplitude T depends explicitly on the new intermediate coordinates. One can easily see that in the harmonic approximation it takes the simple form

$$T(Z) = -\frac{\hat{q}}{2}(\boldsymbol{z}_a - \bar{\boldsymbol{z}}_a) \cdot (\boldsymbol{z}_b - \bar{\boldsymbol{z}}_b). \tag{4.16}$$

When switching to momentum space, these coordinate differences can be expressed in terms of derivatives of the two-point functions going from t_3 to t_L.

After performing the Fourier transform, the non-factorizable piece can be written as

$$\begin{aligned}
&(\boldsymbol{k}_a \boldsymbol{k}_b; \boldsymbol{k}_a \boldsymbol{k}_b | \tilde{S}_{\text{nfac}}^{(4)}(t_L, t_2) | \boldsymbol{q}_2, \bar{\boldsymbol{q}}_2 - \boldsymbol{q}_2; \boldsymbol{p}_2, \bar{\boldsymbol{q}}_2 - \boldsymbol{p}_2) \\
&= \int_{t_2}^{L} dt_3 \int_{\boldsymbol{q}_{3a}\boldsymbol{q}_{3b}} \frac{\hat{q}}{2} \boldsymbol{\nabla}\mathcal{P}(\boldsymbol{k}_a - \boldsymbol{q}_{3a}, t_L - t_3) \cdot \boldsymbol{\nabla}\mathcal{P}(\boldsymbol{k}_b - \boldsymbol{q}_{3b}, t_L - t_3) \tilde{\mathcal{I}}(Q_{3a}, Q_{3b}, Q_2, \bar{Q}_2, P_2),
\end{aligned}$$
$$\tag{4.17}$$

where $\boldsymbol{\nabla}$ denotes the gradient with respect to the transverse momentum variables, and $\tilde{\mathcal{I}}$ is the Fourier transform of the path integral in (4.15) after removing the overall momentum conserving δ-function,

$$
\begin{aligned}
(2\pi)^2 &\delta^{(2)}(\boldsymbol{q}'_2 - \bar{\boldsymbol{q}}_2 + \boldsymbol{q}_2)\tilde{\mathcal{I}}(Q_{3a}, Q_{3b}, Q_2, \bar{Q}_2, P_2) \\
&= \int_{\{\boldsymbol{x},\boldsymbol{z}\}} e^{-i[\boldsymbol{q}_{3a}\cdot(\boldsymbol{z}_a - \bar{\boldsymbol{z}}_a) + \boldsymbol{q}_{3b}\cdot(\boldsymbol{z}_b - \bar{\boldsymbol{z}}_b) - \boldsymbol{q}_2\cdot\boldsymbol{x}_a - \boldsymbol{q}'_2\cdot\boldsymbol{x}_b + \boldsymbol{p}_2\cdot\bar{\boldsymbol{x}}_a + (\bar{\boldsymbol{q}}_2 - \boldsymbol{p}_2)\cdot\bar{\boldsymbol{x}}_b]} \\
&\times \int_{t_2}^{t_3} \mathcal{D}\boldsymbol{r}_a \mathcal{D}\boldsymbol{r}_b \mathcal{D}\bar{\boldsymbol{r}}_a \mathcal{D}\bar{\boldsymbol{r}}_b \exp\left\{\frac{i}{2}\int_{t_2}^{t_3} \mathrm{d}t \, \left(k_a^+ \dot{\boldsymbol{r}}_a^2 + k_b^+ \dot{\boldsymbol{r}}_b^2 - k_a^+ \dot{\bar{\boldsymbol{r}}}_a^2 - k_b^+ \dot{\bar{\boldsymbol{r}}}_b^2\right)\right\} \\
&\times C_q^{(2)}(t_3, t_2; \boldsymbol{r}_a, \boldsymbol{r}_b) C_q^{(2)}(t_3, t_2; \bar{\boldsymbol{r}}_a, \bar{\boldsymbol{r}}_b) C_q^{(2)}(t_3, t_2; \boldsymbol{r}_a, \boldsymbol{r}_b) C_q^{(2)}(t_3, t_2; \bar{\boldsymbol{r}}_a, \bar{\boldsymbol{r}}_b). \quad (4.18)
\end{aligned}
$$

This object is explicitly calculated in appendix B.3. The main result of that calculation is that the result of the path integration is not exponentially suppressed only if its longitudinal extend is small, of order of the formation time. In terms of our result for the non-factorizable piece of the 4-point function it means that we can restrict the integration over t_3 to only the interval between t_2 and $t_2 + t_f$, leading to the the fact that the region after t_3 is of the order of the length of the medium while the region between t_2 and t_3 is of the order of the formation time.

Using the explicit expression for the $\mathcal{P}$'s in eq. (2.19), one can easily see that the derivatives in (4.17) give a factor of

$$
\frac{(\boldsymbol{k}_a - \boldsymbol{q}_{3a}) \cdot (\boldsymbol{k}_b - \boldsymbol{q}_{3b})}{\hat{q}^2(t_L - t_3)^2} \sim \frac{1}{\hat{q}L} \ . \quad (4.19)
$$

This additional factor of L in the denominator can not be compensated in any way since the integration in t_3 was shown to have support over a small region and therefore does not depend on L. Therefore, the non-factorizable piece of $S^{(4)}$ is parametrically smaller than the factorizable piece by a factor of τ_{br}/L and can be safely discarded for the kinematical regime under study.

5 The splitting kernel and the gluon-splitting cross section

In this section we shall complete the calculation of the cross-section for medium-induced gluon branching, establish the formula (2.21), and give an explicit expression for the splitting kernel $\mathcal{K}$.

We return to eq. (3.13), and make a first simplification that exploits the main result of section 4, namely the factorization of the 4-point function. Thus, we replace in eq. (3.13), $S^{(4)}(t_L, t_2)$ by $S_{\mathrm{fac}}^{(4)}(t_L, t_2)$ given by eq. (4.4). We obtain then

$$
\begin{aligned}
\frac{\mathrm{d}^2\sigma}{\mathrm{d}\Omega_{k_a}\mathrm{d}\Omega_{k_b}} = \frac{g^2 N_c}{(2p_0^+)^2} 2\Re e &\int_{t_0}^{t_L} \mathrm{d}t_1 \int_{t_0}^{t_1} \mathrm{d}t_2 \int_{\boldsymbol{p}_0,\boldsymbol{p}_1,\boldsymbol{p}_2,\boldsymbol{q}_1,\boldsymbol{q}_2\bar{\boldsymbol{q}}_2} (2\pi)^2\delta^{(2)}(\boldsymbol{p}_2 - \boldsymbol{q}_2) \\
&\times \Gamma^{ijl}(\boldsymbol{p}_1 - z\boldsymbol{q}_1, z)\,\Gamma^{\bar{i}jl}(\boldsymbol{p}_2 - z\bar{\boldsymbol{q}}_2, z) \\
&\times \mathcal{P}(\boldsymbol{k}_a - \boldsymbol{q}_2, t_L - t_2)\mathcal{P}(\boldsymbol{k}_b - \bar{\boldsymbol{q}}_2 + \boldsymbol{q}_2, t_L - t_2) \\
&\times (\boldsymbol{p}_2, \bar{\boldsymbol{q}}_2 - \boldsymbol{q}_2; \bar{\boldsymbol{q}}_2|\tilde{S}^{(3)}(t_2, t_1)|\boldsymbol{p}_1, \boldsymbol{q}_1 - \boldsymbol{p}_1; \boldsymbol{q}_1) \\
&\times \mathcal{P}(\boldsymbol{q}_1 - \boldsymbol{p}_0, t_1 - t_0)J^{i,c_0}(p_0^+, \boldsymbol{p}_0)J^{*\bar{i},c_0}(p_0^+, \boldsymbol{p}_0), \quad (5.1)
\end{aligned}
$$

where $p_0^+ = k_a^+ + k_b^+$, $z = k_a^+/p_0^+$. (In order to follow the flow of momenta it may be useful to refer to figure 7.) At this point we recognize in eq. (5.1) the three 'classical propagators' $\mathcal{P}$ expressing the transverse momentum broadening of the gluons before and after the branching. These are almost the same as in eq. (2.21), except that the momenta are those appropriate to regions I and III, while in eq. (2.21) the finite extent of region II is neglected. We shall return to this question shortly, and identify now the splitting kernel $\mathcal{K}$ by combining the 3-point function $\tilde{S}^{(3)}(t_2, t_1)$ with the vertex factors that are explicit in eq. (5.1).

Consider first the two vertex functions. They combine to yield

$$\frac{1}{4} \Gamma^{ijl}(\hat{\boldsymbol{P}}_1, z) \, \Gamma^{\bar{i}jl}(\hat{\boldsymbol{P}}_2, z) = \left[\frac{1}{z^2} + \frac{1}{(1-z)^2} \right] \hat{\boldsymbol{P}}_1 \cdot \hat{\boldsymbol{P}}_2 \, \delta^{i\bar{i}} + 2 \, \hat{\boldsymbol{P}}_1^i \, \hat{\boldsymbol{P}}_2^{\bar{i}}, \qquad (5.2)$$

where we have set $\hat{\boldsymbol{P}}_1 = \boldsymbol{p}_1 - z\boldsymbol{q}_1$, $\hat{\boldsymbol{P}}_2 = \boldsymbol{p}_2 - z\bar{\boldsymbol{q}}_2$. For simplicity, we consider here only inclusive cross sections that are averaged over azimuthal angles. Under this assumption one can then replace $2 \, \hat{\boldsymbol{P}}_1^i \, \hat{\boldsymbol{P}}_2^{\bar{i}}$ by $(\hat{\boldsymbol{P}}_1 \cdot \hat{\boldsymbol{P}}_2) \, \delta^{i\bar{i}}$, and get

$$N_c \, \Gamma^{ijl}(\hat{\boldsymbol{P}}_1, z) \Gamma^{\bar{i}jl}(\hat{\boldsymbol{P}}_2, z) = \frac{4}{z(1-z)} P_{gg}(z) \, (\hat{\boldsymbol{P}}_1 \cdot \hat{\boldsymbol{P}}_2) \, \delta^{i\bar{i}}, \qquad (5.3)$$

where

$$P_{gg}(z) = N_c \left[\frac{z}{1-z} + \frac{1-z}{z} + z(1-z) \right],$$

is the leading-order Altarelli-Parisi splitting function [37].

Next we consider the 3-point function $\tilde{S}^{(3)}(t_2, t_1)$, which is calculated in appendix B.2. In the harmonic approximation it reads (cf. eq. (B.28))

$$(\boldsymbol{p}_2, \bar{\boldsymbol{q}}_2 - \boldsymbol{p}_2; \bar{\boldsymbol{q}}_2 | \tilde{S}^{(3)}(t_2, t_1) | \boldsymbol{p}_1, \boldsymbol{q}_1 - \boldsymbol{p}_1; \boldsymbol{q}_1) =$$

$$= \frac{8\pi[1 + z^2 + (1-z)^2]}{3\hat{q}\Delta t} \exp \left\{ -\frac{2[1 + z^2 + (1-z)^2](\boldsymbol{q}_1 - \bar{\boldsymbol{q}}_2)^2}{3\hat{q}\Delta t} \right\}$$

$$\times \frac{2\pi(1+i)}{k_{\mathrm{br}}^2 \sinh(\Omega\Delta t)} \exp \left\{ -(1+i)\frac{(\hat{\boldsymbol{P}}_1 + \hat{\boldsymbol{P}}_2)^2}{4k_{\mathrm{br}}^2 \coth(\Omega\Delta t/2)} - (1+i)\frac{(\hat{\boldsymbol{P}}_1 - \hat{\boldsymbol{P}}_2)^2}{4k_{\mathrm{br}}^2 \tanh(\Omega\Delta t/2)} \right\},$$

$$\tag{5.4}$$

with $\Delta t = t_2 - t_1$, and

$$\Omega \equiv \frac{1+i}{2\tau_{\mathrm{br}}}, \quad \tau_{\mathrm{br}} \equiv \sqrt{\frac{z(1-z)p_0^+}{\hat{q}_{\mathrm{eff}}}}, \quad k_{\mathrm{br}}^2 \equiv \hat{q}_{\mathrm{eff}} \, \tau_{\mathrm{br}} = \sqrt{z(1-z)p_0^+ \hat{q}_{\mathrm{eff}}}, \qquad (5.5)$$

where $\hat{q}_{\mathrm{eff}}$ denotes an average, z-dependent, version of the jet quenching parameter:

$$\hat{q}_{\mathrm{eff}} \equiv \frac{1}{2}\hat{q} \left[z^2 + (1-z)^2 + 1 \right]. \qquad (5.6)$$

In writing the expression above for the 3-point function, we have used the delta-function $\delta^{(2)}(\boldsymbol{p}_2 - \boldsymbol{q}_2)$ in eq. (5.1) in order to replace $\boldsymbol{q}_2$ by $\boldsymbol{p}_2$. This allowed us in particular to express $\tilde{S}^{(3)}(t_2, t_1)$ in terms of $\hat{\boldsymbol{P}}_2$. This expression (5.4) of $S^{(3)}(t_2, t_1)$ makes it clear that

the extent of region II is limited: indeed, since $1/\sinh(|\Omega|\Delta t) \propto \exp\{-\Delta t/\sqrt{2}\tau_{\mathrm{br}}\}$ for large Δt, the time separation $\Delta t = t_2 - t_1$ needs to be kept smaller that τ_{br} in order to avoid exponential suppression. Thus, as anticipated via simple considerations in section 2, and in the qualitative discussion of section 3.4, one sees that the time scale of the branching process is indeed determined by τ_{br}. Recall that this is also (approximately) the same time scale that controls the exponential damping of the non factorizable part of the 4-point function (see section 4 and appendix B.2, eq. (B.51)).

In order to proceed further, we shall exploit the fact that region II has limited extent and neglect in the factors $\mathcal{P}$ the fraction of momenta that can be attributed to momentum broadening within region II. Since this region is of extent τ_{br}, this fraction is typically of order τ_{br}/L as compared to the momentum acquired through propagation before and after the splitting (this is in fact explicit for the dependence of $\tilde{S}^{(3)}$ on $\boldsymbol{q}_1 - \bar{\boldsymbol{q}}_2$ in eq. (5.4), where it can be seen that $(\boldsymbol{q}_1 - \bar{\boldsymbol{q}}_2)^2$ is at most of order $\hat{q}\tau_{\mathrm{br}}$). Thus we shall replace in eq. (5.1) $\mathcal{P}(\boldsymbol{k}_b - \bar{\boldsymbol{q}}_2 + \boldsymbol{q}_2, t_L - t_2)$ by $\mathcal{P}(\boldsymbol{k}_b - \boldsymbol{q}_1 + \boldsymbol{q}_2, t_L - t_2)$ (ignoring the small difference $\boldsymbol{q}_1 - \bar{\boldsymbol{q}}_2$), and use as independent variables $\boldsymbol{q}_1, \hat{\boldsymbol{P}}_1, \hat{\boldsymbol{P}}_2, \boldsymbol{q}_1 - \bar{\boldsymbol{q}}_2$ in place of $\boldsymbol{q}_1, \boldsymbol{p}_1, \bar{\boldsymbol{q}}_2, \boldsymbol{q}_2$. Since the factors $\mathcal{P}$ do not depend on $\hat{\boldsymbol{P}}_1$ nor $\boldsymbol{q}_1 - \bar{\boldsymbol{q}}_2$, the integration over these variables in eq. (5.1) leaves these $\mathcal{P}$ factors intact. This allows us to define a kernel as follows

$$\mathcal{K}(\hat{\boldsymbol{P}}_2, t_2 - t_1, z) \equiv \frac{P_{gg}(z)}{[z(1-z)p_0^+]^2} \Re e \int_{\boldsymbol{q}_1 - \bar{\boldsymbol{q}}_2, \hat{\boldsymbol{P}}_1} (\hat{\boldsymbol{P}}_1 \cdot \hat{\boldsymbol{P}}_2) \, \tilde{S}^{(3)}(\Delta t, \hat{\boldsymbol{P}}_1, \hat{\boldsymbol{P}}_2, \boldsymbol{q}_1 - \bar{\boldsymbol{q}}_2), \quad (5.7)$$

where we have made explicit the independent momentum variables on which $\tilde{S}^{(3)}$ depends. A straightforward calculation of the gaussian integrals in eq. (5.7) yields

$$\mathcal{K}(\boldsymbol{p}, \Delta t, z) = P_{gg}(z) \frac{\hat{\boldsymbol{P}}_2^2}{2[z(1-z)p_0^+]^2} \Re e \left[\left(\frac{1}{\cosh^2(\Omega \Delta t)} \right) \exp \left\{ -\frac{i\hat{\boldsymbol{P}}_2^2}{2z(1-z)p^+\Omega} \tanh(\Omega \Delta t) \right\} \right]. \quad (5.8)$$

Using this definition for $\mathcal{K}$, one can rewrite eq. (5.1) as

$$\frac{\mathrm{d}^2\sigma}{\mathrm{d}\Omega_{k_a}\mathrm{d}\Omega_{k_b}} = 2g^2 z(1-z) \int_{t_0}^{t_L} \mathrm{d}t_2 \int_{t_0}^{t_2} \mathrm{d}t_1 \int_{\boldsymbol{p}_0, \hat{\boldsymbol{P}}_2, \boldsymbol{q}_1} \mathcal{P}(\boldsymbol{k}_a - \boldsymbol{q}_2, t_L - t_2) \mathcal{P}(\boldsymbol{k}_b - \boldsymbol{q}_1 + \boldsymbol{q}_2, t_L - t_2)$$

$$\times \, \mathcal{K}(\hat{\boldsymbol{P}}_2, \Delta t, z) \, \mathcal{P}(\boldsymbol{q}_1 - \boldsymbol{p}_0, t_1 - t_0) \frac{\mathrm{d}\sigma_{hard}}{\mathrm{d}\Omega_{p_0}}, \quad (5.9)$$

where $\mathrm{d}\sigma_{hard}/\mathrm{d}\Omega_{p_0} = |\boldsymbol{J}(p_0^+, \boldsymbol{p}_0)|^2$. Now, as already explained, the kernel $\mathcal{K}(t_2 - t_1)$ effectively restricts the time integrations in eq. (5.9) to $\Delta t \equiv t_2 - t_1 \lesssim \tau_{\mathrm{br}}$. This is a small time interval as compared to the typical values of t_1 and t_2, of order t_L, so, in line with our previous approximations, we integrate the kernel over Δt while neglecting the difference $t_2 - t_1$ in the various factors $\mathcal{P}$. We then redefine the kernel after integration over Δt:

(eq. (5.8), to be later restored)

$$\int_0^{t_2-t_0} \mathrm{d}\Delta t \, \frac{1}{2z(1-z)p_0^+} \left(\frac{\hat{\boldsymbol{P}}_2^2}{\cosh^2(\Omega\Delta t)} \right) \exp \left\{ -\frac{i\hat{\boldsymbol{P}}_2^2}{2z(1-z)p_0^+\Omega} \tanh(\Omega\Delta t) \right\}$$

$$= i \int_0^{t_2-t_0} \mathrm{d}\Delta t \, \frac{\mathrm{d}}{\mathrm{d}\Delta t} \exp \left\{ -\frac{i\hat{\boldsymbol{P}}_2^2}{2z(1-z)p_0^+\Omega} \tanh(\Omega\Delta t) \right\},$$

$$= i \left[\exp \left\{ -\frac{i\hat{\boldsymbol{P}}_2^2}{2z(1-z)p_0^+\Omega} \tanh(\Omega(t_2-t_0)) \right\} - 1 \right]. \tag{5.10}$$

To further simplify the kernel, and again in line with our approximations, we neglect the region of integration $t_2 \lesssim \tau_{\mathrm{br}} + t_0$. When $t_2 - t_0 \gg \tau_{\mathrm{br}}$, one can use $\tanh(\Omega(t_2 - t_0)) \approx 1$ and then the kernel becomes time-independent. After taking the real part in eq. (5.10) and restoring the proper factors from eq. (5.8), we finally obtain:

$$\mathcal{K}(\hat{\boldsymbol{P}}_2, z, p_0^+) \approx \frac{2}{z(1-z)p_0^+} P_{gg}(z) \, \sin \left[\frac{\hat{\boldsymbol{P}}_2^2}{2\boldsymbol{k}_{\mathrm{br}}^2} \right] \exp \left[-\frac{\hat{\boldsymbol{P}}_2^2}{2\boldsymbol{k}_{\mathrm{br}}^2} \right]. \tag{5.11}$$

This kernel generalizes the result obtained in [25] in the eikonal limit.

Putting everything together, and proceeding to various relabelings ($t_2 \to t$, $\hat{\boldsymbol{P}}_2 \to \boldsymbol{p} - z\boldsymbol{q}$, $\boldsymbol{q}_2 \to \boldsymbol{p}, \boldsymbol{q}_1 \to \boldsymbol{q}$), one recovers the expression for the cross-section for quasi-instantaneous medium-induced gluon branching given in eq. (2.21)

The kernel $\mathcal{K}(\boldsymbol{p} - z\boldsymbol{q}, z, p_0^+)$ describes the splitting of a gluon with longitudinal momentum p_0^+ and transverse momentum $\boldsymbol{q}$ into two gluons, one with longitudinal momentum fraction z and transverse momentum $\boldsymbol{p}$, the other with longitudinal momentum fraction $1-z$ and transverse momentum $\boldsymbol{q} - \boldsymbol{p}$. Note that $\mathcal{K}$ does not depend on $\boldsymbol{p}$ and $\boldsymbol{q}$ separately, but only on the combination $\boldsymbol{p} - z\boldsymbol{q}$, which may be understood as the relative momentum of the effective non relativistic two-dimensional motion of the gluons in the transverse plane (with $\boldsymbol{q}$ playing the role of the 'center of mass' momentum). We may also write $\boldsymbol{p} - z\boldsymbol{q} = p^+(\boldsymbol{v_p} - \boldsymbol{v_q}) = (p^+ - q^+)(\boldsymbol{v_{p-q}} - \boldsymbol{v_q})$, where $\boldsymbol{v_p} = \boldsymbol{p}/p^+$ etc. are transverse velocities. Interestingly, the quantity $|\boldsymbol{v_p} - \boldsymbol{v_q}|$ is a measure of the actual emission angle in three dimensions. To see that, let us introduce the three-dimensional velocities, $\vec{v}_{\boldsymbol{q}} = (v_{zq}, \boldsymbol{v_q})$ and $\vec{v}_{\boldsymbol{p}} = (v_{zp}, \boldsymbol{v_p})$, with $v_{zq}^2 + \boldsymbol{v_q}^2 = 1$, etc. Then, $(\boldsymbol{v_p} - \boldsymbol{v_q})^2 = 2(1 - \cos\theta_{\boldsymbol{p}}) \simeq \theta_{\boldsymbol{p}}^2$, and similarly for $|\boldsymbol{v_{q-p}} - \boldsymbol{v_q}|$. Since eq. (5.11) constrains the value of $\boldsymbol{p} - z\boldsymbol{q}$ to be of order k_{br} at most, emission angles are constrained as follows

$$|\theta_{\boldsymbol{p}}| \simeq |\boldsymbol{v_p} - \boldsymbol{v_q}| \lesssim \frac{k_{\mathrm{br}}}{zq^+}, \qquad |\theta_{\boldsymbol{q-p}}| \simeq |\boldsymbol{v_{q-p}} - \boldsymbol{v_q}| \lesssim \frac{k_{\mathrm{br}}}{(1-z)q^+}. \tag{5.12}$$

These formulæ make it clear that it is the softest offspring gluon which is emitted at the largest angle and hence that controls the geometry of the branching.

We may get more precise on the probabilistic interpretation of the kernel $\mathcal{K}$ by integrating the cross section over suitable elements of phase space. Consider the formula (2.21)

that we have just derived,

$$\frac{\mathrm{d}^2\sigma_1}{\mathrm{d}\Omega_{k_a}\mathrm{d}\Omega_{k_b}} = 2g^2 z(1-z) \int_{t_0}^{t_L} \mathrm{d}t \int_{\boldsymbol{p}_0,\boldsymbol{q},\boldsymbol{p}} \mathcal{P}(\boldsymbol{k}_a - \boldsymbol{p}, t_L - t)\, \mathcal{P}(\boldsymbol{k}_b - \boldsymbol{q} + \boldsymbol{p}, t_L - t)$$

$$\times \mathcal{K}(\boldsymbol{p} - z\boldsymbol{q}, z, p_0^+)\, \mathcal{P}(\boldsymbol{q} - \boldsymbol{p}_0, t - t_0) \frac{\mathrm{d}\sigma_{hard}}{\mathrm{d}\Omega_{p_0}}, \tag{5.13}$$

in which it is understood that $k_a^+ + k_b^+ = p_0^+$. From this we may calculate

$$\frac{\mathrm{d}\sigma_1}{\mathrm{d}z\mathrm{d}\Omega_0^+} = \frac{1}{2} \int \mathrm{d}^2\boldsymbol{k}_a \int \mathrm{d}^2\boldsymbol{k}_b \frac{\mathrm{d}\sigma_1}{\mathrm{d}\boldsymbol{k}_a\mathrm{d}\boldsymbol{k}_b\mathrm{d}z\mathrm{d}\Omega_0^+}. \tag{5.14}$$

This quantity represents the cross section for a gluon with initial $+$ momentum in the phase space element $\mathrm{d}\Omega_0^+ \equiv \mathrm{d}p_0^+/((2\pi)2p_0^+)$ to split into two gluons, one of which carries the fraction zp_0^+ of the initial $+$ momentum. The factor $1/2$ is a symmetry factor that accounts for the fact that each configuration of 2 identical gluons is counted twice in the integration over $\boldsymbol{k}_a$ and $\boldsymbol{k}_b$. The calculation is easily done and yields

$$\frac{\mathrm{d}\sigma_1}{\mathrm{d}z\mathrm{d}\Omega_0^+} = \frac{g^2}{4\pi} \int_{t_0}^{t_L} \mathrm{d}t \int_{\boldsymbol{p}-z\boldsymbol{q}} \mathcal{K}(\boldsymbol{p} - z\boldsymbol{q}, z, p_0^+) \frac{\mathrm{d}\sigma_{hard}}{\mathrm{d}\Omega_0^+}, \tag{5.15}$$

with

$$\frac{\mathrm{d}\sigma_{hard}}{\mathrm{d}\Omega_0^+} = \int \frac{\mathrm{d}\boldsymbol{p}_0}{(2\pi)^2} \frac{\mathrm{d}\sigma_{hard}}{\mathrm{d}\Omega_{\boldsymbol{p}_0}}. \tag{5.16}$$

From eq. (5.15), one reads the probability per unit time for a gluon with energy p_0^+ and transverse momentum $\boldsymbol{q}$ to produce a splitting with one of the produced gluon carrying a momentum fraction zp_0^+ and a transverse momentum $\boldsymbol{p}$:

$$\frac{\mathrm{d}P}{\mathrm{d}\boldsymbol{p}\,\mathrm{d}z\,\mathrm{d}t} = \frac{\alpha_s}{(2\pi)^2} \mathcal{K}(\boldsymbol{p} - z\boldsymbol{q}, z, p_0^+). \tag{5.17}$$

The integration over the transverse momentum yields

$$\mathcal{K}(z, p^+) \equiv \int \frac{\mathrm{d}^2\boldsymbol{q}}{(2\pi)^2} \mathcal{K}(\boldsymbol{q},\, z, p^+) = \frac{1}{2\pi} \frac{P_{gg}(z)}{\tau_{\mathrm{br}}(z, p^+)}. \tag{5.18}$$

Note that the gluon spectrum produced via a *single* medium-induced emission may be recovered from this formula, by integrating eq. (5.18) over time up to t_L and multiplying by a factor of $2z$:

$$z \frac{\mathrm{d}N}{\mathrm{d}z}\bigg|_{\text{one emission}} = \frac{\alpha_s}{\pi} z P_{gg}(z) t_L \sqrt{\frac{\hat{q}_{\mathrm{eff}}}{z(1-z)p^+}}. \tag{5.19}$$

This is recognized as the BDMPSZ spectrum, as expected [8–12].

The kernel in eq. (5.11) may turn negative for large value of the transverse momentum. This would not be a serious problem in practice since this occurs for momenta ($q \gtrsim \pi k_{\mathrm{br}}$) for which the gaussian in eq. (5.11) is very small, but it indicates a limitation of

the approximation that has been used to arrived at eq. (5.11). In fact, a large transverse momentum $q \gg k_{\rm br}$ cannot be acquired over a time scale $\sim \tau_{\rm br}$ as a result of soft multiple scattering. Rather it must be associated with some rare but hard collision, which can be more accurately treated in the single scattering approximation — that is, by keeping only the term linear in the dipole cross-section in the expansion of the 2-point function (2.14) —, but by keeping the logarithmic dependence upon r. When applied to the momentum broadening probability, this procedure yields for the Fourier transform in eq. (2.16), $\mathcal{P}(\Delta \boldsymbol{p}, \Delta t) \sim (\hat{q} \Delta t)/(\Delta \boldsymbol{p})^4$. We expect this procedure to lead to a similar behavior in $1/\boldsymbol{q}^4$ at large $\boldsymbol{q}$ for the kernel $\mathcal{K}(\boldsymbol{q}, z, p^+)$. We leave the detailed discussion of this particular point for a subsequent study.

6 Conclusions

In this paper, we have provided a complete calculation of medium-induced gluon branching in the regime where the gluons that take part in the branching undergo multiple soft scattering with the medium. The kernel that describes the branching has been calculated as a function of transverse momentum, beyond the eikonal approximation. An important conclusion of our study is that the offspring gluons lose color coherence with respect to each other on the same time scale as that of the branching process itself. Thus, as soon as they are produced, they propagate independently from each other, a picture that holds to within corrections of order $\tau_{\rm br}/L \ll 1$. Our explicit proof relies on a large–N_c approximation but we believe that our conclusions remain generally valid.

In the regime considered in this paper, where the energies of the emitted gluons are within the range $\omega_{\rm BH} \ll \omega \ll \omega_c$, a regime dominated by multiple scattering, subsequent emissions by these gluons do not interfere with each other. Indeed, the typical duration $\tau_{\rm br}(\omega)$ of a branching process is much smaller than the longitudinal extent L of the medium. Since the interference effects between the offspring gluons are possible only during this branching time $\tau_{\rm br}$, whereas independent emissions by these gluons can occur anywhere along the size L of the medium, the longitudinal phase-space for interference phenomena is suppressed compared to the corresponding phase-space for independent emissions by a factor $\tau_{\rm br}(\omega)/L \ll 1$.

The suppression of interference effects is a key ingredient for having independent emissions. The other key ingredient is that successive emissions do not overlap with each other, a situation which, as recalled in the introduction, may occur for sufficiently soft gluons, that can be produced at a high rate. Whether a fully probabilistic description of successive branchings can be given depends therefore on how well one can control the emission of very soft gluons (beyond the apparent infrared divergences produced by the splitting functions, and that are easily seen to cancel in the calculation of physical processes). We leave this point for a subsequent study.

There are further limitations of the present calculation that need to be emphasized. The calculation that we have presented is valid in a regime where interactions with the medium are dominated by soft multiple scattering. While this is a legitimate assumption for the leading particle and the hardest component of its medium-induced radiation, this

may not be also the case for the very soft gluons at the end of a cascade, especially if their energies approach the Bethe-Heitler energy. A proper treatment of this particular region would require a more accurate treatment of the single scattering between a gluon and the medium, which implies in particular relaxing the eikonal approximation. Also, we have not included in our formalism the vacuum-like emissions, that is, the emissions by which the energetic gluon that enters the plasma loses its initial (potentially large) virtuality. Such emissions are controlled by the standard splitting functions for bremsstrahlung. These are generally hard emissions at small angles. In fact, all the emissions at angles much smaller than θ_c should proceed exactly as in the vacuum with usual destructive interferences leading to angular ordering. Hard emissions at larger angles $\theta \gg \theta_c$ are possible as well, and for them interference effects become negligible because of medium effects [21–25]. For hard emissions at intermediate angles $\theta \sim \theta_c$ the situation is more complicated [21, 23], so in order to better understand this and also to have a unified description of the in-medium jet evolution, it would be very useful to extend our formalism by including vacuum-like emissions.

Acknowledgments

## A Gluon dynamics in a background field

In this appendix, we review briefly properties of the gluon propagator in a background field $A^-(x^+, \boldsymbol{x})$ which is independent of x^-. To within an inessential term that can be ignored, this propagator can be entirely expressed in terms of a $2+1$ dimensional "scalar" propagator (independent of Lorentz indices), that describes non-relativistic propagation in the transverse plane, with x^+ playing the role of time. The dependence on Lorentz indices is factored out into coefficients that are used to define an effective three-gluon vertex. This vertex and the scalar propagator can be used to simplify perturbative calculations for the effective non relativistic gluo-dynamics in the transverse plane.

We work in the light cone gauge $A^+ = 0$, with covariant derivative $D_\mu = \partial_\mu - ig A_\mu$, and the only non-vanishing component of the background field is $A^-(x^+, \boldsymbol{x})$. In this gauge, the free propagator reads, in momentum space,

$$G_0^{\mu\nu}(p) = -G_0(p)\, d^{\mu\nu}(p) \qquad d^{\mu\nu}(p) \equiv \left[g^{\mu\nu} - \frac{p^\mu n^\nu + p^\nu n^\mu}{n \cdot p} \right], \qquad G_0(p) \equiv \frac{-1}{p^2}, \ \ (A.1)$$

with $n^\mu = (n^+, n^-, \boldsymbol{n}_\perp) = (0, 1, \boldsymbol{0})$, so that $n \cdot A = A^+ = 0$ and $n \cdot p = p^+$. Note that $G_0^{\mu\nu}$ is symmetric under the interchange of μ and ν, and it vanishes if either index is $+$. The non vanishing components are

$$G_0^{ij}(p) = G_0(p)\delta^{ij}, \qquad G_0^{-i}(p) = \frac{p^i}{p^+} G_0(p), \qquad G_0^{--}(p) = 2\frac{p^-}{p^+} G_0(p). \qquad (A.2)$$
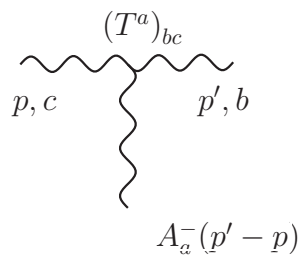
Figure 11. Representation of the vertex coupling the propagating gluon to the background field A_a^-. The matrix T^a is a matrix of the adjoint representation. The background field A_a^- is independent of x^-, so that there is no transfer of $+$ momentum at the vertex, that is, $p'^+ = p^+$.

In the presence of the background field, the propagator is modified. In particular, it is no longer diagonal in momentum space (except for the $+$ component of the momentum). It is is also a non diagonal matrix in color space. It may be written quite generally as $G_{ba}^{\mu\nu}(p', p)$, with the convention that p is incoming and p' is outgoing (and similarly for the color indices). That is, one may regard $G_{ba}^{\mu\nu}(p', p)$ as the matrix element $(p'\, b|G^{\mu\nu}|p\, a)$, which we shall also write $(p'|G_{ba}^{\mu\nu}|p)$ when convenient. To determine the structure of $G^{\mu\nu}$, we write

$$(p'\, b|G^{\mu\nu}|p\, a) = (p'|p)\delta_{ab}\, G_0^{\mu\nu}(p) + G_0^{\mu\mu'}(p')\, (p'\, b|\mathcal{T}_{\mu'\nu'}|p\, a)\, G_0^{\nu'\nu}(p), \tag{A.3}$$

with $(p'|p) = (2\pi)^4 \delta^{(4)}(p - p')$, and expand $\mathcal{T}^{\mu\nu}$ in powers of the background field. We get

$$\begin{aligned}
(p'|\mathcal{T}_{ba}^{\nu\mu}|p) = &-i(p'|V_{bca}^{\nu+\mu}|p)\, A_c^-(p' - p) \\
&- (p'|V_{bed}^{\mu+\mu'}|p'')\, A_e^-(p' - p'')\, G_{0,\mu'\nu'}(p'')\, (p''|V_{dca}^{\nu'+\nu}|p)\, A_c^-(p'' - p) + \cdots
\end{aligned} \tag{A.4}$$

Here, $(p'|V_{bca}^{\nu+\mu}|p)$ stands for $V_{bca}^{\nu+\mu}(p', p - p', -p)$, where V is the usual three-gluon vertex, defined generally as (with all momenta chosen outgoing), see figure 11,

$$V_{abc}^{\mu\nu\rho}(k, p, q) = -gf^{abc}\left[g^{\mu\nu}(k - p)^\rho + g^{\nu\rho}(p - q)^\mu + g^{\rho\mu}(q - k)^\nu\right]. \tag{A.5}$$

The fact that in eq. (A.4), or in eq. (A.3), $\mathcal{V}^{\nu+\mu}(p', p)$ is contracted with G_0 propagators, puts constraints on the values of the indices μ and ν (see eqs. (A.2)). A simple analysis reveals that the only relevant components of the vertex are

$$V_{bca}^{j+i}(p', p - p', -p) = gf^{bca}\, g^{ji}(p + p')^+ = -2igp^+\, (T^c)_{ba}\, g^{ji}, \tag{A.6}$$

where we have used $p'^+ = p^+$. It follows that $\mathcal{T}_{\mu'\nu'}(p', p)$ vanishes unless the indices μ and ν are spatial indices, and furthermore $\mathcal{T}^{ij}$ is diagonal. We shall set

$$\mathcal{T}_{ij}(p', p) = -\delta_{ij}\mathcal{T}(p', p). \tag{A.7}$$

Taking this property of $\mathcal{T}^{\mu\nu}$ into account, one can rewrite eq. (A.3) as

$$(p'|G_{ba}^{\nu\mu}|p) = (p'|p)\delta_{ab}\, G_0^{\nu\mu}(p) - G_0^{\nu i}(p')\, (p'|\mathcal{T}_{ba}|p)\, G_0^{i\mu}(p), \tag{A.8}$$

and, using (A.1), as

$$(p'|G_{ba}^{\nu\mu}|p) = -(p'|p)\delta_{ba}\, G_0(p)d^{\nu\mu} - d^{\nu i}d^{i\mu}\, G_0(p')\, (p'|\mathcal{T}_{ba}|p))\, G_0(p). \tag{A.9}$$

At this point, we define a 'scalar propagator' $(p'|G_{ba}|p)$

$$(p'|G_{ba}|p) = (p'|p)\delta_{ba}\, G_0(p) - G_0(p')\, (p'|\mathcal{T}_{ba}|p)\, G_0(p), \tag{A.10}$$

and substitute this into eq. (A.9) to obtain

$$G_{ba}^{\mu\nu}(p',p) = (p'|p)\delta_{ba}\, G_0(p)\left[-d^{\mu\nu}(p) - d^{\mu i}(p)d^{i\nu}(p)\right] + d^{\mu i}(p')d^{i\nu}(p)G_{ba}(p',p). \tag{A.11}$$

A direct calculation, using the explicit expression of $d^{\mu\nu}$ given in eq. (A.1) reveals that

$$(p'|p)\, G_0(p)\left[-d^{\mu\nu}(p) - d^{\mu i}(p)d^{i\nu}(p)\right] = -\delta^{\mu-}\delta^{\nu-}(p'|p)\,\frac{1}{(p^+)^2}. \tag{A.12}$$

We recognize the instantaneous contribution to the gluon propagator in light-cone perturbation theory. This contact term can be ignored in the present calculation. Thus we are left with

$$(p'|G_{ba}^{\nu\mu}|p) = d^{\nu i}(p')(p'|G_{ba}|p)d^{i\mu}(p), \tag{A.13}$$

which expresses the gluon propagator as the scalar propagator multiplied by factors that carry all information about Lorentz indices.

The Fourier transform of the scalar propagator, $(x|G|y) = G(x,y)$, is the solution of the equation

$$\left[\Box_x - 2ig(A^- \cdot T)\partial^+\right] G(x,y) = \delta(x-y), \tag{A.14}$$

an equation that naturally arises when solving the Yang-Mills equations for a fluctuating gauge field in the presence of the A^- background [36, 38]. This is easily seen by writing this equation as $G_0^{-1} + \Sigma = 1$, with Σ the self-energy, and then identifying $\mathcal{T} = \Sigma - \Sigma G_0 \Sigma + \cdots$. Eq. (A.14) can also be written as

$$\left[2\partial_x^+ \mathcal{D}_x^- - \nabla_\perp^2\right]_{ac} G_{cb}(x,y) = \delta(x-y)\delta_{ab}, \tag{A.15}$$

where $\mathcal{D}^- = \partial^- - igA^- \cdot T$, and we used the fact that $\partial^+ A^- = 0$. Since the background field A^- does not depend on x^-, the propagator $G(x,y)$ depends on x^- and y^- only through the difference $x^- - y^-$. It is then convenient to introduce a new Green's function

$$(x|G^{ab}|y) \equiv \int \frac{\mathrm{d}k^+}{2\pi}\, \mathrm{e}^{-ik^+(x^- - y^-)}\,\frac{i}{2k^+}(\boldsymbol{x}|\,\mathcal{G}^{ab}(x^+, y^+; k^+)\,|\boldsymbol{y}). \tag{A.16}$$

A simple calculation reveals that $\mathcal{G}$ satisfies the following equation

$$\left[i\mathcal{D}^- + \frac{\nabla_\perp^2}{2k^+}\right]_{ac}(\boldsymbol{x}|\,\mathcal{G}^{cb}(x^+, y^+; k^+)\,|\boldsymbol{y}) = i\delta_{ab}\delta(x^+ - y^+)\delta(\boldsymbol{x} - \boldsymbol{y}), \tag{A.17}$$

with $i\mathcal{D}^- = i\partial^- + gA^-$. Thus, $\mathcal{G}(x^+, y^+; k^+)$ is the propagator of a Schrödinger equation for a non relativistic particle of mass k^+ moving in a time dependent potential $A^-(x^+, \boldsymbol{x})$, with x^+ playing the role of the time. It can be written as a path integral

$$(\boldsymbol{x}|\,\mathcal{G}(x^+, y^+; k^+)\,|\boldsymbol{y}) = \int \mathcal{D}\boldsymbol{r} \, \mathrm{e}^{i\frac{k^+}{2}\int_{y^+}^{x^+} \mathrm{d}t\, \dot{\boldsymbol{r}}^2} \, \tilde{U}(x^+, y^+; \boldsymbol{r}), \qquad (A.18)$$

with $\boldsymbol{r}(y^+) = \boldsymbol{y}$, $\boldsymbol{r}(x^+) = \boldsymbol{x}$, and $\tilde{U}$ is a Wilson line evaluated along the path $\boldsymbol{r}(t)$

$$\tilde{U}(x^+, y^+; \boldsymbol{r}) = \mathrm{T}\exp\left\{ig\int_{y^+}^{x^+} \mathrm{d}t\, A_a^-(t, \boldsymbol{r}(t))\, T^a\right\}. \qquad (A.19)$$

From this relation, one easily deduces the following composition property (using the matrix notation)

$$\mathcal{G}(x^+, y^+; k^+) = \mathcal{G}(x^+, z^+; k^+)\,\mathcal{G}(z^+, y^+; k^+). \qquad (A.20)$$

Consider now the vertex that describes the splitting of a gluon of momentum q into a gluon of momentum p and a gluon of momentum $q - p$. This is given by the general expression (A.5), in which the momentum q is chosen incoming while the other two momenta are outgoing:

$$V_{abc}^{\mu\nu\lambda}(q, p, q - p) = g f^{abc}\left[g^{\mu\nu}(q + p)^\lambda + g^{\nu\lambda}(q - 2p)^\mu - g^{\lambda\mu}(2q - p)^\nu\right]. \qquad (A.21)$$

A modified vertex is obtained by combining $V_{abc}^{\mu\nu\lambda}$ with the factors $d^{\mu i}$ contained in the propagators attached to the vertex. Thus we define

$$\Gamma_{abc}^{ijl} = d^{i\mu}(q)d^{j\nu}(p)d^{l\nu}(q - p)V_{\mu\nu\lambda}^{abc}(q, p). \qquad (A.22)$$

Note that the indices on Γ are all transverse. Taking into account that the only non vanishing contributions of $d^{\mu i}$ are either of the form d^{ij} or d^{i-}, one obtains easily

$$\Gamma_{abc}^{ijl}(\boldsymbol{p} - z\boldsymbol{q}; z) = -2g f_{abc}\left\{-\frac{1}{1-z}(\boldsymbol{p} - z\boldsymbol{q})^l \delta^{ij} + (\boldsymbol{p} - z\boldsymbol{q})^i \delta^{jl} - \frac{1}{z}(\boldsymbol{p} - z\boldsymbol{q})^j \delta^{il}\right\}, \qquad (A.23)$$

where $z \equiv p^+/q^+$, and we have made explicit the dependence on the single momentum $\boldsymbol{p} - z\boldsymbol{q}$. This momentum has a simple physical interpretation in the effective non relativistic dynamics. It can indeed be written as $zq^+(\boldsymbol{v_p} - \boldsymbol{v_q})$, where $\boldsymbol{v_p} = \boldsymbol{p}/p^+$ and $\boldsymbol{v_q} = \boldsymbol{q}/q^+$. That is, $\boldsymbol{p} - z\boldsymbol{q}$ is proportional to the (transverse) velocity of one of the produced gluon relative to that of the parent gluon.

It is convenient also to consider $\Gamma_{abc}^{ijl}(\boldsymbol{p} - z\boldsymbol{q}; z)$ as a matrix connecting single gluon states to two gluon states. We set

$$(\boldsymbol{p}, b, j; \boldsymbol{k}, c, l|\,\Gamma(z)\,|\boldsymbol{q}, a, i) = (\boldsymbol{k}|\boldsymbol{q} - \boldsymbol{p})\Gamma_{abc}^{ijl}(\boldsymbol{p} - z\boldsymbol{q}; z), \qquad (A.24)$$

where it is understood that $p^+ = zq^+$, $k^+ = (1 - z)q^+$. Often, we also write $\Gamma_{abc}^{ijl}(\boldsymbol{p} - z\boldsymbol{q}; z) = g f^{abc}\, \Gamma^{ijl}(\boldsymbol{p} - z\boldsymbol{q}, z)$, isolating the coupling constant and the color factor from the momentum dependent piece.

In summary, the dynamics of gluons in the light cone gauge $A^+ = 0$, and in the presence of a background field that does not depend on x^-, are essentially those of a two dimensional non-relativistic field theory. Usual perturbative calculations can be simplified by using the propagator $\mathcal{G}$ and the vertex $gf^{abc}\,\Gamma^{ijl}(\boldsymbol{p}-z\boldsymbol{q},z)$ that we have discussed in this section. Note that the factor $1/2p^+$ which accompanies the propagator $\mathcal{G}$ (see eq. (A.16)) is not to be included on the external lines.

B Explicit calculations of n-point functions

In this section we calculate explicitly the n-point functions that are used in the main text. These n-point functions are products of propagators in the amplitude and its complex conjugate, i.e. products of $\mathcal{G}$'s and $\mathcal{G}^{\dagger}$', taken between the same initial time x^+ and the same final time y^+. At these times, the transverse coordinates in the various propagators may take different values. We shall denote generically by $\boldsymbol{X}$ the set of transverse coordinates in the various propagators at time x^+, and by $\boldsymbol{Y}$ the set of the corresponding coordinates at time y^+. Often, we shall include x^+ and y^+ in the sets X and Y, respectively, that is, we shall set $X = (x^+, \boldsymbol{X})$, $Y = (y^+, \boldsymbol{Y})$. In case of a single propagator, the same notation will be used, with $X = (x^+, \boldsymbol{x})$ and $Y = (y^+, \boldsymbol{y})$. Further details on the notation will be given as we proceed.

Let us recall that the free propagator reads (we set $\mathcal{G}_0^{ba}(Y, X) \equiv \delta^{ba}\mathcal{G}_0(Y, X)$)

$$\mathcal{G}_0(Y, X) = \left(\frac{\omega}{2\pi i \Delta t}\right) e^{i\frac{\omega(\boldsymbol{x}-\boldsymbol{y})^2}{2\Delta t}}, \qquad \Delta t \equiv y^+ - x^+, \tag{B.1}$$

where we have called ω the $+$ component of the momentum, a notation that will be used throughout this appendix. We also write $\mathcal{G}_0(Y, X)$ as the matrix element $(\boldsymbol{y}|\mathcal{G}_0(y^+, x^-)|\boldsymbol{x}) = (\boldsymbol{y}|\mathcal{G}_0(\Delta t)|\boldsymbol{x})$. The Fourier transform is

$$(\boldsymbol{q}|\mathcal{G}_0(\Delta t)|\boldsymbol{p}) = \int d\boldsymbol{y}\, d\boldsymbol{x}\, e^{-i\boldsymbol{q}\cdot\boldsymbol{y}}\, e^{i\boldsymbol{p}\cdot\boldsymbol{x}}\, (\boldsymbol{y}|\mathcal{G}_0(\Delta t)|\boldsymbol{x})$$

$$= (2\pi)^2 \delta(\boldsymbol{p} - \boldsymbol{q})\, e^{-i\frac{\boldsymbol{p}^2}{2\omega}\Delta t}. \tag{B.2}$$

B.1 The 2-point function

The scalar 2-point function $S^{(2)}(Y, X|\omega)$ is defined by

$$\delta^{b\bar{b}}\langle \mathcal{G}^{\dagger\bar{a}\bar{b}}(\bar{X}, \bar{Y}|\omega)\mathcal{G}^{ba}(Y, X|\omega)\rangle = \delta^{a\bar{a}}S^{(2)}(Y, X|\omega). \tag{B.3}$$

Note that, in order to avoid the proliferation of arguments in the functions that we discuss, we are using the same symbols to denote different variables, depending on the 'context', that is, depending on the object where these variables appear. Thus, in the propagators $\mathcal{G}(Y, X)$, $X = (x^+, \boldsymbol{x})$, $Y = (y^+, \boldsymbol{y})$, in $\mathcal{G}^{\dagger}(\bar{X}, \bar{Y})$, $\bar{X} = (x^+, \bar{\boldsymbol{x}})$, $\bar{Y} = (y^+, \bar{\boldsymbol{y}})$, while in the 2-point function $S^{(2)}(Y, X|\omega)$, $X = (x^+, \boldsymbol{x}, \bar{\boldsymbol{x}})$ and $Y = (y^+, \boldsymbol{y}, \bar{\boldsymbol{y}})$. We shall use later a similar 'contextual notation' for the 3 and 4-point functions, where X and Y will represent collectively larger sets of coordinates (figures, such as figure 12 will help to fix any ambiguity
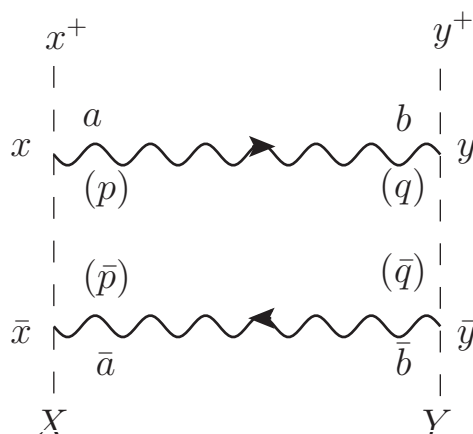
Figure 12. Graphical illustration for the 2-point function $S^{(2)}(Y, X | \omega)$, where $X = (x^+, \boldsymbol{x}, \bar{\boldsymbol{x}})$ and $Y = (y^+, \boldsymbol{y}, \bar{\boldsymbol{y}})$. In parenthesis are given the momenta conjugate to the respective coordinates in the (mixed) Fourier representation; the + component of the momenta is denoted here by ω and is the same in the amplitude and its complex conjugate. In the present study, a 2-point function appears typically as the product of a propagator $\mathcal{G}$ in an amplitude and a propagator $\mathcal{G}^\dagger$ in the complex conjugate amplitude. These propagators are represented here by oriented lines, with the arrow pointing to the right for $\mathcal{G}$ and to the left for $\mathcal{G}^\dagger$.

that may arise). To further simplify the notation, we shall most often omit to indicate explicitly the dependence on ω. Finally, whenever needed, we shall use a matrix notation, keeping separate the dependence on time arguments. Thus we shall occasionally write $S^{(2)}(Y, X)$ as the matrix element $(\boldsymbol{Y} | S^{(2)}(y^+, x^+) | \boldsymbol{X})$ with $\boldsymbol{X} = (\boldsymbol{x}, \bar{\boldsymbol{x}})$ and $\boldsymbol{Y} = (\boldsymbol{y}, \bar{\boldsymbol{y}})$, with boldface letters referring to transverse coordinates only.

By using the path integral representation of the propagators $\mathcal{G}$ and $\mathcal{G}^\dagger$ one gets, after doing the medium average,

$$
S^{(2)}(Y, X | \omega) = \int \mathcal{D} \boldsymbol{r} \mathcal{D} \bar{\boldsymbol{r}} \exp \left\{ \frac{i \omega}{2} \int_{x^+}^{y^+} \mathrm{d}t \left(\dot{\boldsymbol{r}}^2 - \dot{\bar{\boldsymbol{r}}}^2 \right) - \frac{N_c \, n}{2} \int_{x^+}^{y^+} \mathrm{d}t \, \sigma(\boldsymbol{r} - \bar{\boldsymbol{r}}) \right\},
$$

(B.4)

with paths $\boldsymbol{r}(t)$, $\bar{\boldsymbol{r}}(t)$ going from $\boldsymbol{r} = \boldsymbol{x}, \bar{\boldsymbol{r}} = \bar{\boldsymbol{x}}$ at time x^+ to $\boldsymbol{r} = \boldsymbol{y}, \bar{\boldsymbol{r}} = \bar{\boldsymbol{y}}$ at time y^+, respectively. The change of variables

$$
\boldsymbol{u} = \boldsymbol{r} - \bar{\boldsymbol{r}}, \qquad \boldsymbol{v} = \frac{1}{2}(\boldsymbol{r} + \bar{\boldsymbol{r}}),
$$

(B.5)

allows us to rewrite the path integral as

$$
S^{(2)}(Y, X | \omega) = \int \mathcal{D} \boldsymbol{u} \mathcal{D} \boldsymbol{v} \, \exp \left\{ i \omega \int_{x^+}^{y^+} \mathrm{d}t \, \dot{\boldsymbol{u}} \cdot \dot{\boldsymbol{v}} - \frac{N_c \, n}{2} \int_{x^+}^{y^+} \mathrm{d}t \, \sigma(\boldsymbol{u}) \right\}.
$$

(B.6)

To evaluate this path integral, we first factorize the dependence on the end points, entirely contained in the value of the action for the classical paths. It is easily verified that Euler-Lagrange equation for $\boldsymbol{u}(t)$, $\ddot{\boldsymbol{u}} = 0$, is not modified by the interaction (even though the

individual classical trajectories are no longer straight lines, as in the free case, the difference $\boldsymbol{u}(t) = \boldsymbol{r}(t) - \bar{\boldsymbol{r}}(t)$ remains a linear function of t). This is enough to calculate the classical action. We have, in particular,

$$\int_{x^+}^{y^+} \mathrm{d}t \, \dot{\boldsymbol{u}} \cdot \dot{\boldsymbol{v}} = \frac{1}{2\Delta t} \left[\boldsymbol{y} - \bar{\boldsymbol{y}} - (\boldsymbol{x} - \bar{\boldsymbol{x}}) \right] \cdot \left[\boldsymbol{y} + \bar{\boldsymbol{y}} - (\boldsymbol{x} + \bar{\boldsymbol{x}}) \right], \tag{B.7}$$

where we have used that $\dot{\boldsymbol{u}}$ is independent of time and set

$$\Delta t \equiv y^+ - x^+. \tag{B.8}$$

A standard calculation of the remaining quadratic path integral then yields

$$S^{(2)}(Y, X|\omega) = \left(\frac{\omega}{2\pi\Delta t} \right)^2 \exp\left\{ \frac{i\omega}{2\Delta t} \left[(\boldsymbol{y} - \boldsymbol{x})^2 - (\bar{\boldsymbol{y}} - \bar{\boldsymbol{x}})^2 \right] - \frac{N_c\, n}{2} \int_{x^+}^{y^+} \mathrm{d}t \, \sigma(\boldsymbol{u}(t)) \right\}$$

$$= \mathcal{G}_0(Y, X) \mathcal{G}_0^\dagger(\bar{X}, \bar{Y}) \exp\left\{ -\frac{N_c\, n}{2} \int_{x^+}^{y^+} \mathrm{d}t \, \sigma(\boldsymbol{u}(t)) \right\}, \tag{B.9}$$

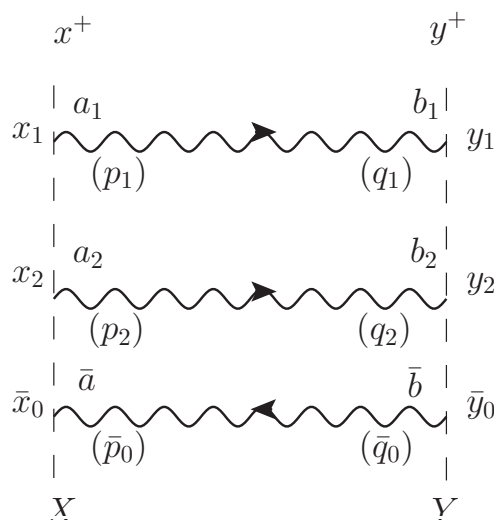where $\sigma(\boldsymbol{u}(t))$ is evaluated along the classical path.

By performing the Fourier transform with respect to the transverse coordinates only, we obtain the "mixed representation" of the 2-point function, $S^{(2)}(Q, P|\omega)$ where $Q = (y^+, \boldsymbol{q}, \bar{\boldsymbol{q}})$, $P = (x^+, \boldsymbol{p}, \bar{\boldsymbol{p}})$. That is, the 'momentum' variables denoted by capital letters contains the conjugate to the transverse coordinates, but also the light-cone time. One may also write $S^{(2)}(Q, P|\omega)$ as the matrix element $(\boldsymbol{Q}|S^{(2)}(y^+, x^+)|\boldsymbol{P})$, with $\boldsymbol{P} = (\boldsymbol{p}, \bar{\boldsymbol{p}})$, $\boldsymbol{Q} = (\boldsymbol{q}, \bar{\boldsymbol{q}})$. We have

$$S^{(2)}(Q, P|\omega) = \int \mathrm{d}\boldsymbol{x}\, \mathrm{d}\bar{\boldsymbol{x}}\, \mathrm{d}\boldsymbol{y}\, \mathrm{d}\bar{\boldsymbol{y}}\, \mathrm{e}^{-i\boldsymbol{q}\cdot\boldsymbol{y}}\, \mathrm{e}^{i\boldsymbol{p}\cdot\boldsymbol{x}}\, \mathrm{e}^{-i\bar{\boldsymbol{p}}\cdot\bar{\boldsymbol{x}}}\, \mathrm{e}^{i\bar{\boldsymbol{q}}\cdot\bar{\boldsymbol{y}}}\, S^{(2)}(Y, X|\omega), \tag{B.10}$$

where the signs in the various phase factors follow from our convention for the propagators $\mathcal{G}$ and $\mathcal{G}^\dagger$ that make up $S^{(2)}$. Translational invariance of $S^{(2)}(Y, X|\omega)$ (obvious on eq. (B.9)) allows us to perform the integral over the sum of coordinates, leading to a factor $(2\pi)^2\delta(\boldsymbol{p} - \bar{\boldsymbol{p}} - \boldsymbol{q} + \bar{\boldsymbol{q}})$. To proceed further, it is convenient to change to relative coordinates. In analogy with eq. (B.5) we define $\boldsymbol{u}_x = \boldsymbol{x} - \bar{\boldsymbol{x}}$, $\boldsymbol{v}_x = (\boldsymbol{x} + \bar{\boldsymbol{x}})/2$, and similarly for $\boldsymbol{y}, \bar{\boldsymbol{y}}$. The variable conjugate to $\boldsymbol{q} - \bar{\boldsymbol{q}}$ is $\boldsymbol{v}_y - \boldsymbol{v}_x$. We are interested in the particular Fourier component for which the momenta at y^+ are the same in the amplitude and in the complex conjugate amplitude, that is $\boldsymbol{q} = \bar{\boldsymbol{q}}$. In this case, the variable $\boldsymbol{v}_y - \boldsymbol{v}_x$ drops from the phase factors in eq. (B.10), and appears only in $S^{(2)}(Y, X|\omega)$, where $\left[(\boldsymbol{y} - \boldsymbol{x})^2 - (\bar{\boldsymbol{y}} - \bar{\boldsymbol{x}})^2 \right]/2 = (\boldsymbol{v}_y - \boldsymbol{v}_x)(\boldsymbol{u}_y - \boldsymbol{u}_x)$. The integration over $(\boldsymbol{v}_y - \boldsymbol{v}_x)$ then produces a factor $(2\pi\Delta t/\omega)^2\delta(\boldsymbol{u}_y - \boldsymbol{u}_x)$, which in turn implies that $\boldsymbol{u}(t)$ is independent of time, and also that the 2-point function depends only on the difference $\boldsymbol{p} - \boldsymbol{q}$ ($\boldsymbol{p} + \boldsymbol{q}$ being conjugate to $\boldsymbol{u}_x - \boldsymbol{u}_y$), and not on $\boldsymbol{p}$ and $\boldsymbol{q}$ separately. One finally gets

$$S^{(2)}(Q, P|\omega) = (2\pi)^2\delta^{(2)}(\boldsymbol{p} - \bar{\boldsymbol{p}}) \int \mathrm{d}\boldsymbol{u}_x \, \exp\left[i\boldsymbol{u}_x \cdot (\boldsymbol{p} - \boldsymbol{q}) - \frac{N_c\, n}{2} \sigma(\boldsymbol{u}_x)\Delta t \right],$$

$$\equiv (2\pi)^2\delta^{(2)}(\boldsymbol{p} - \bar{\boldsymbol{p}}) \, \mathcal{P}(\boldsymbol{p} - \boldsymbol{q}, \Delta t), \tag{B.11}$$

Figure 13. Graphical illustration for the 3-point function $S^{(3)}(Y, X|\boldsymbol{\omega})$, with $X = (x^+, \boldsymbol{x}_1, \boldsymbol{x}_2, \bar{\boldsymbol{x}}_0)$, $Y = (y^+, \boldsymbol{y}_1, \boldsymbol{y}_2, \bar{\boldsymbol{y}}_0)$ and $\boldsymbol{\omega} = (\omega_1, \omega_2, \omega_0)$. The typical 3-point function we deal with in this paper is the product of two $\mathcal{G}$ (right arrows) and one $\mathcal{G}^\dagger$ (left arrow). Also, the gluons 1 and 2 are issued from gluon 0, so that conservation of the + momentum implies $\omega_0 = \omega_1 + \omega_2$.

where the δ-function expresses momentum conservation after taking into account the condition $\boldsymbol{q} = \bar{\boldsymbol{q}}$. It is interesting to observe that the requirement $\boldsymbol{q} = \bar{\boldsymbol{q}}$ has cancelled completely the "free" contribution to $S^{(2)}(Q, P|\omega)$ (except for the momentum conserving δ-function), leaving only in (B.11) the Fourier transform of the interaction part of $S^{(2)}(Y, X|\omega)$ (the last term in the second line of eq. (B.9)). This cancellation results in the property of $S^{(2)}(Q, P|\omega)$ of being a function only of the difference of momenta $\boldsymbol{p} - \boldsymbol{q}$. In the absence of interaction, $\mathcal{P}(\boldsymbol{p} - \boldsymbol{q}, \Delta t)$ goes over to $(2\pi)^2 \delta(\boldsymbol{p} - \boldsymbol{q})$ and the dependence on Δt drops out.

The quantity

$$\mathcal{P}(\Delta \boldsymbol{p}, \Delta t) = \int d\boldsymbol{u} \ \exp\left[i\boldsymbol{u} \cdot \Delta \boldsymbol{p} - \frac{N_c \, n}{2} \, \sigma(\boldsymbol{u}) \, \Delta t\right]. \tag{B.12}$$

can be interpreted as the probability that a gluon acquires a transverse momentum $\Delta \boldsymbol{p}$ while traversing the medium during a time Δt.

B.2 The 3-point function

The 3-point function $S^{(3)}(Y, X|\boldsymbol{\omega})$ that we need is of the form

$$f^{b_1 b_2 \bar{b}_0} S^{(3)}(Y, X|\boldsymbol{\omega}) = f^{a_1 a_2 \bar{a}_0} \langle \mathcal{G}^{b_1 a_1}(Y, X|\omega_1) \mathcal{G}^{b_2 a_2}(Y, X|\omega_2) \mathcal{G}^{\dagger \, \bar{a}_0 \bar{b}_0}(\bar{X}, \bar{Y}|\omega_0) \rangle \tag{B.13}$$

where we use the contextual notation introduced earlier, with the variables X and Y having different meanings in $S^{(3)}$ and in $\mathcal{G}$ or in $\mathcal{G}^\dagger$ (see the caption of figure (13)). By expressing the individual propagators in terms of path integrals, and performing the medium average

of the Wilson lines, one gets

$$S^{(3)}(Y, X|\boldsymbol{\omega}) = \int \mathcal{D}\boldsymbol{r}_2 \mathcal{D}\boldsymbol{r}_1 \mathcal{D}\boldsymbol{r}_0 \exp\left\{\frac{i}{2}\int_{x^+}^{y^+} dt \left(\omega_1 \dot{\boldsymbol{r}}_1^2 + \omega_2 \dot{\boldsymbol{r}}_2^2 - \omega_0 \dot{\boldsymbol{r}}_0^2\right)\right\}$$
$$\times \exp\left\{-\frac{N_c\, n}{4}\int_{x^+}^{y^+} dt \left[\sigma(\boldsymbol{r}_1 - \boldsymbol{r}_0) + \sigma(\boldsymbol{r}_2 - \boldsymbol{r}_0) + \sigma(\boldsymbol{r}_2 - \boldsymbol{r}_1)\right]\right\}.$$
(B.14)

The integral runs over paths with endpoints $\boldsymbol{r}_i(x^+) \equiv \boldsymbol{x}_i$ and $\boldsymbol{r}_i(y^+) \equiv \boldsymbol{y}_i$ ($i = 0, 1, 2$), and the three dipole cross sections correspond to the three possible dipoles that can be formed with the three gluons.

We perform the following change of variables ($\boldsymbol{v}$ can be interpreted as the distance between gluon 0 and the "center of mass" of gluons 1 and 2)

$$\boldsymbol{u} = \boldsymbol{r}_1 - \boldsymbol{r}_2, \qquad \boldsymbol{v} = z\boldsymbol{r}_1 + (1-z)\boldsymbol{r}_2 - \boldsymbol{r}_0, \qquad \omega_1 = z\omega_0, \qquad \omega_2 = (1-z)\omega_0,$$
(B.15)

so that $\boldsymbol{r}_1 - \boldsymbol{r}_0 = \boldsymbol{v} + (1-z)\boldsymbol{u}$ and $\boldsymbol{r}_2 - \boldsymbol{r}_0 = \boldsymbol{v} - z\boldsymbol{u}$. For the endpoints, we set $\boldsymbol{u}_x = \boldsymbol{x}_1 - \boldsymbol{x}_2$, $\boldsymbol{v}_x = z\boldsymbol{x}_1 + (1-z)\boldsymbol{x}_2 - \bar{\boldsymbol{x}}_0$, and similarly for the $\boldsymbol{y}$ variables. In the variables (B.15), the 3-point function reads

$$S^{(3)}(Y, X|\boldsymbol{\omega}) = \int \mathcal{D}\boldsymbol{u} \mathcal{D}\boldsymbol{v} \mathcal{D}\boldsymbol{r}_0 \exp\left\{\frac{i\omega_0}{2}\int_{x^+}^{y^+} dt \left[\dot{\boldsymbol{v}}^2 + 2\dot{\boldsymbol{v}} \cdot \dot{\boldsymbol{r}}_0 + z(1-z)\dot{\boldsymbol{u}}^2\right]\right\}$$
$$\times \exp\left\{-\frac{N_c\, n}{4}\int_{x^+}^{y^+} dt \left[\sigma(\boldsymbol{u}) + \sigma(\boldsymbol{v} - z\boldsymbol{u}) + \sigma(\boldsymbol{v} + (1-z)\boldsymbol{u})\right]\right\}.$$
(B.16)

The calculation of the path integrals over $\boldsymbol{r}_0$ and $\boldsymbol{v}$ proceeds as for the 2-point function. One identifies easily that the classical path $\boldsymbol{v}(t)$ is a straight line, that is, the center of mass of gluons 1 and 2 move with respect to gluon 0 at constant velocity. This allows us to calculate the kinetic part of the action corresponding to the variables $\boldsymbol{r}_0$ and $\boldsymbol{v}$, and to perform the remaining quadratic path integrals over $\boldsymbol{r}_0$ and $\boldsymbol{v}$. One gets

$$S^{(3)}(Y, X|\boldsymbol{\omega}) \equiv \left(\frac{\omega_0}{2\pi\Delta t}\right)^2 \exp\left[\frac{i\omega_0}{2}\frac{\Delta\boldsymbol{v}}{\Delta t} \cdot (\Delta\boldsymbol{v} + 2\Delta\boldsymbol{r}_0)\right]$$
$$\times \int \mathcal{D}\boldsymbol{u} \exp\left\{\frac{i\hat{\omega}_0}{2}\int_{x^+}^{y^+} dt\, \dot{\boldsymbol{u}}^2 - \frac{N_c\, n}{4}\int_{x^+}^{y^+} dt \left[\sigma(\boldsymbol{u}) + \sigma(\boldsymbol{v} - z\boldsymbol{u}) + \sigma(\boldsymbol{v} + (1-z)\boldsymbol{u})\right]\right\}.$$
(B.17)

where, in the integral, $\boldsymbol{v}$ is to be taken as the classical path $\boldsymbol{v}(t)$, and we have set

$$\Delta\boldsymbol{v} \equiv \boldsymbol{v}_y - \boldsymbol{v}_x, \qquad \Delta\boldsymbol{r}_0 \equiv \bar{\boldsymbol{y}}_0 - \bar{\boldsymbol{x}}_0, \qquad \hat{\omega}_0 \equiv z(1-z)\omega_0,$$
(B.18)

with $\hat{\omega}_0$ the reduced mass for the relative motion of gluons 1 and 2. Note that in the absence of interaction with the medium, $S^{(3)}(Y, X|\boldsymbol{\omega})$ reduces to the product of three free

propagators, as it should. We have indeed

$$
\begin{aligned}
S_0^{(3)}(Y,X|\boldsymbol{\omega}) &= \left(\frac{\omega_0}{2\pi\Delta t}\right)^2 \mathrm{e}^{\frac{i\omega_0}{2}\frac{\Delta\boldsymbol{v}}{\Delta t}\cdot(\Delta\boldsymbol{v}+2\Delta\boldsymbol{r}_0)} \times \frac{\hat{\omega}_0}{2\pi i\Delta t} \, \mathrm{e}^{i\frac{\hat{\omega}_0}{2\Delta t}\Delta\boldsymbol{u}^2} \\
&= \frac{\omega_0\omega_1\omega_2}{(2\pi)^3 i\Delta t^3} \, \mathrm{e}^{\frac{i}{2\Delta t}\left(\omega_1\Delta\boldsymbol{r}_1^2+\omega_2\Delta\boldsymbol{r}_2^2-\omega_0\Delta\boldsymbol{r}_0^2\right)},
\end{aligned}
\tag{B.19}
$$

with $\Delta\boldsymbol{u} \equiv \Delta\boldsymbol{r}_1 - \Delta\boldsymbol{r}_2$, and $\Delta\boldsymbol{r}_i \equiv \boldsymbol{y}_i - \boldsymbol{x}_i$. The effect of the interaction is, as in the 2 gluon case discussed above, to produce a damping whenever the size of the dipoles exceed $1/(\hat{q}\Delta t)$. To analyze these effects further, it is convenient to perform a Fourier transform with respect to the transverse coordinates.

The Fourier transform (in the mixed representation) reads

$$
S^{(3)}(Q,P|\boldsymbol{\omega}) = \int_{\boldsymbol{x}_1\,\boldsymbol{x}_2\,\bar{\boldsymbol{x}}_0\,\boldsymbol{y}_1\,\boldsymbol{y}_2\,\bar{\boldsymbol{y}}_0} \mathrm{e}^{-i\boldsymbol{q}_1\cdot\boldsymbol{y}_1}\,\mathrm{e}^{-i\boldsymbol{q}_2\cdot\boldsymbol{y}_2}\,\mathrm{e}^{-i\bar{\boldsymbol{p}}_0\cdot\bar{\boldsymbol{x}}_0}\,\mathrm{e}^{i\boldsymbol{p}_1\cdot\boldsymbol{x}_1}\,\mathrm{e}^{i\boldsymbol{p}_2\cdot\boldsymbol{x}_2}\,\mathrm{e}^{i\bar{\boldsymbol{q}}_0\cdot\bar{\boldsymbol{y}}_0}\,S^{(3)}(Y,X|\boldsymbol{\omega}),
\tag{B.20}
$$

where translation invariance implies $\boldsymbol{p}_1 + \boldsymbol{p}_2 - \boldsymbol{q}_1 - \boldsymbol{q}_2 = \bar{\boldsymbol{p}}_0 - \bar{\boldsymbol{q}}_0$. It is convenient to introduce the following change of variables (with unit Jacobian)

$$
\boldsymbol{x}_1 = (1-z)\boldsymbol{u}_x + \boldsymbol{v}_x + \bar{\boldsymbol{x}}_0, \qquad \boldsymbol{x}_2 = -z\boldsymbol{u}_x + \boldsymbol{v}_x + \bar{\boldsymbol{x}}_0, \qquad \bar{\boldsymbol{x}}_0 = \bar{\boldsymbol{x}}_0,
\tag{B.21}
$$

and similarly for the variables $\boldsymbol{y}_1, \boldsymbol{y}_2, \bar{\boldsymbol{y}}_0$. The phase factor in eq. (B.20) becomes then $\mathrm{e}^{i\phi}$ with

$$
\phi = \bar{\boldsymbol{x}}_0(\boldsymbol{p}_1 + \boldsymbol{p}_2 - \bar{\boldsymbol{p}}_0) + \boldsymbol{u}_x[(1-z)\boldsymbol{p}_1 - z\boldsymbol{p}_2] + \boldsymbol{v}_x(\boldsymbol{p}_1 + \boldsymbol{p}_2)
\tag{B.22}
$$

$$
- \bar{\boldsymbol{y}}_0(\boldsymbol{q}_1 + \boldsymbol{q}_2 - \bar{\boldsymbol{q}}_0) - \boldsymbol{u}_y[(1-z)\boldsymbol{q}_1 - z\boldsymbol{q}_2] - \boldsymbol{v}_y(\boldsymbol{q}_1 + \boldsymbol{q}_2).
\tag{B.23}
$$

As obvious from its explicit expression (B.16), the 3-point function $S^{(3)}(Y,X|\boldsymbol{\omega})$ depends on $\bar{\boldsymbol{x}}_0$ and $\bar{\boldsymbol{y}}_0$ only through the difference $\bar{\boldsymbol{x}}_0 - \bar{\boldsymbol{y}}_0$, which is conjugate to the variable $[\boldsymbol{p}_1 + \boldsymbol{p}_2 - \bar{\boldsymbol{p}}_0 + \boldsymbol{q}_1 + \boldsymbol{q}_2 - \bar{\boldsymbol{q}}_0]/2 = \boldsymbol{q}_1 + \boldsymbol{q}_2 - \bar{\boldsymbol{q}}_0$. For the particular Fourier component which we are interested in, that for which $\boldsymbol{q}_1 + \boldsymbol{q}_2 = \bar{\boldsymbol{q}}_0$, this variable $\bar{\boldsymbol{x}}_0 - \bar{\boldsymbol{y}}_0$ drops from the phase factors in eq. (B.20). One can then perform the corresponding integration, which yields a factor $(2\pi\Delta t/\omega_0)^2\delta(\Delta\boldsymbol{v})$. The δ-function $\delta(\Delta\boldsymbol{v}) = \delta(\boldsymbol{v}_x - \boldsymbol{v}_y)$ implies that $\boldsymbol{v}(t)$ is independent of time. It also implies that, besides the momentum conserving δ-function, $S^{(3)}(Q,P|\boldsymbol{\omega})$ depends only on the difference $\bar{\boldsymbol{p}}_0 - \bar{\boldsymbol{q}}_0$ rather than on $\bar{\boldsymbol{p}}_0$ and $\bar{\boldsymbol{q}}_0$ separately. We are then left with

$$
\begin{aligned}
S^{(3)}(Q,P|\boldsymbol{\omega}) = (2\pi)^2\delta^{(2)}(\boldsymbol{p}_1+\boldsymbol{p}_2-\bar{\boldsymbol{p}}_0)\int \mathrm{d}\boldsymbol{u}_x \mathrm{d}\boldsymbol{u}_y \mathrm{d}\boldsymbol{v}_x \, \mathrm{e}^{i\boldsymbol{u}_x\cdot(\boldsymbol{p}_1-z\bar{\boldsymbol{p}}_0)-i\boldsymbol{u}_y\cdot(\boldsymbol{q}_1-z\bar{\boldsymbol{q}}_0)+i\boldsymbol{v}_x\cdot(\bar{\boldsymbol{p}}_0-\bar{\boldsymbol{q}}_0)} \\
\int \mathcal{D}\boldsymbol{u} \exp\left\{\frac{i\hat{\omega}_0}{2}\int \mathrm{d}t \, \dot{\boldsymbol{u}}^2 - \frac{N_c\,n}{4}\int \mathrm{d}t \, [\sigma(\boldsymbol{u})+\sigma(\boldsymbol{v}-z\boldsymbol{u})+\sigma(\boldsymbol{v}+(1-z)\boldsymbol{u})]\right\},
\end{aligned}
\tag{B.24}
$$

where the δ-function is that of momentum conservation, after taking into account that $\boldsymbol{q}_1 + \boldsymbol{q}_2 = \bar{\boldsymbol{q}}_0$.

– 42 –

To proceed further, we evaluate eq. (B.24) in the harmonic approximation, eq. (2.17). Then the path integral in the second line of eq. (B.24) reads simply

$$
\mathrm{e}^{-3\boldsymbol{v}_x^2 \hat{q}\Delta t/8[1+z^2+(1-z)^2]} \int \mathcal{D}\boldsymbol{u}\, \exp\left\{ i\hat{\omega}_0 \int_{x^+}^{y^+} \mathrm{d}t \, \left(\frac{\dot{\boldsymbol{u}}^2}{2} + i\omega_{\mathrm{br}}^2 \boldsymbol{u}^2 \right) \right\}, \qquad \text{(B.25)}
$$

where we have set

$$
\tau_{\mathrm{br}} \equiv \sqrt{\frac{\hat{\omega}_0}{\hat{q}_{\mathrm{eff}}}}, \qquad \omega_{\mathrm{br}}^2 \equiv \frac{1}{4\tau_{\mathrm{br}}^2}, \qquad \hat{q}_{\mathrm{eff}} \equiv \frac{1}{2}\hat{q}\left[(1-z)^2 + z^2 + 1\right].
$$

The calculation of the quadratic integral

$$
\mathcal{J}(\boldsymbol{u}_x, \boldsymbol{u}_y) = \int \mathcal{D}\boldsymbol{u}\, \exp\left\{ i\hat{\omega}_0 \int_{x^+}^{y^+} \mathrm{d}t \, \left(\frac{\dot{\boldsymbol{u}}^2}{2} + i\omega_{\mathrm{br}}^2 \boldsymbol{u}^2 \right) \right\}. \qquad \text{(B.26)}
$$

is standard, and yields

$$
\begin{aligned}
\mathcal{J}(\boldsymbol{u}_x, \boldsymbol{u}_y) &= \frac{k_{\mathrm{br}}^2 (1-i)}{4\pi \sinh\Omega\Delta t} \exp\left\{ \frac{(i-1)k_{\mathrm{br}}^2}{4\sinh\Omega\Delta t} \left[(\boldsymbol{u}_x^2 + \boldsymbol{u}_y^2)\cosh\Omega\Delta t - 2\boldsymbol{u}_x \cdot \boldsymbol{u}_y \right] \right\} \\
&= \frac{k_{\mathrm{br}}^2 (1-i)}{4\pi \sinh\Omega\Delta t} \exp\left\{ \frac{(i-1)k_{\mathrm{br}}^2}{2\sinh\Omega\Delta t} \left[\sinh^2\frac{\Omega\Delta t}{2}(\boldsymbol{u}_s + \boldsymbol{u}_y)^2 + \cosh^2\frac{\Omega\Delta t}{2}(\boldsymbol{u}_s - \boldsymbol{u}_y)^2 \right] \right\},
\end{aligned}
$$
$$\text{(B.27)}$$

with $\Omega \equiv (1+i)\omega_{\mathrm{br}}$ and $k_{\mathrm{br}}^2 \equiv \hat{q}_{\mathrm{eff}}\tau_{\mathrm{br}}$.

The Fourier transform can then be completed. We get

$$
S^{(3)}(Q, P|\boldsymbol{\omega}) = (2\pi)^2 \delta^{(2)}(\boldsymbol{p}_1 + \boldsymbol{p}_2 - \bar{\boldsymbol{p}}_0) \frac{8\pi[1 + z^2 + (1-z)^2]}{3\hat{q}\Delta t} \mathrm{e}^{-\frac{2[1+z^2+(1-z)^2](\bar{\boldsymbol{p}}_0 - \bar{\boldsymbol{q}}_0)^2}{3\hat{q}\Delta t}}
$$
$$
\times \frac{2\pi(1+i)}{k_{\mathrm{br}}^2 \sinh(\Omega\Delta t)} \exp\left\{ -(1+i)\frac{(\hat{\boldsymbol{P}}_1 + \hat{\boldsymbol{Q}}_1)^2}{4k_{\mathrm{br}}^2 \coth(\Omega\Delta t/2)} - (1+i)\frac{(\hat{\boldsymbol{P}}_1 - \hat{\boldsymbol{Q}}_1)^2}{4k_{\mathrm{br}}^2 \tanh(\Omega\Delta t/2)} \right\},
$$
$$\text{(B.28)}$$

where we have set $\hat{\boldsymbol{P}}_1 \equiv \boldsymbol{p}_1 - z\bar{\boldsymbol{p}}_0$ and $\hat{\boldsymbol{Q}}_1 \equiv \boldsymbol{q}_1 - z\bar{\boldsymbol{q}}_0$. Setting $S^{(3)}(Q, P|\boldsymbol{\omega}) = (2\pi)^2 \delta^{(2)}(\boldsymbol{p}_1 + \boldsymbol{p}_2 - \bar{\boldsymbol{p}}_0) \tilde{S}^{(3)}(Q, P|\boldsymbol{\omega})$, we note that $\tilde{S}^{(3)}(Q, P|\boldsymbol{\omega})$ is a function of just three variables, $\bar{\boldsymbol{p}}_0 - \bar{\boldsymbol{q}}_0$, and the variables $\hat{\boldsymbol{P}}_1, \hat{\boldsymbol{Q}}_1$ just defined, and which may be interpreted as the relative momenta of the 2-dimensional motion at x^+ and y^+, with $\boldsymbol{p}_0$ and $\bar{\boldsymbol{q}}_0$ playing the role of respective 'center of mass' momenta.

B.3 The path integral needed in the evaluation of the 4-point function

In this appendix we evaluate the path integral entering the evaluation of the non-factorizable piece of the 4-point function (see eq. (4.18)), which in coordinate space takes
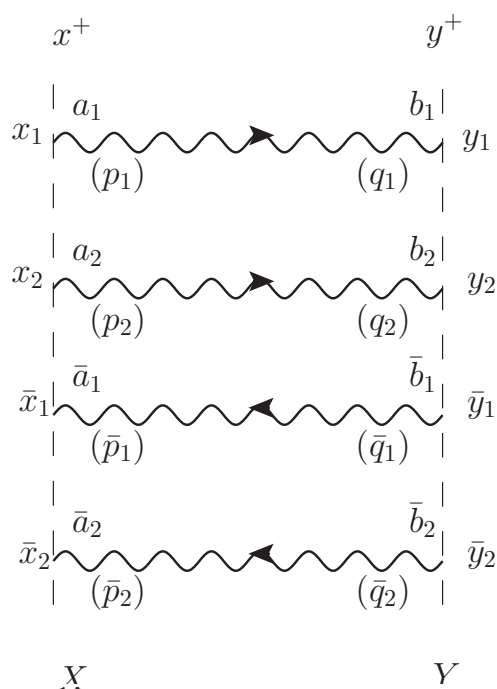
Figure 14. Graphical illustration for the path integral $\mathcal{I}(Y, X|\boldsymbol{\omega})$, with $X = (x^+, \boldsymbol{x}_1, \boldsymbol{x}_2, \bar{\boldsymbol{x}}_1, \bar{\boldsymbol{x}}_2)$, $Y = (y^+, \boldsymbol{y}_1, \boldsymbol{y}_2, \bar{\boldsymbol{y}}_1, \bar{\boldsymbol{y}}_2)$ and $\boldsymbol{\omega} = (\omega_1, \omega_2)$. The 4-point function is the product of two propagators $\mathcal{G}$ (for gluons 1 and 2, with + momenta ω_1 and ω_2), and two propagators $\mathcal{G}^\dagger$ corresponding to the same gluons in the complex conjugate amplitude. The notation is as in the previous two figures.

the form (see figure 14 for notation)

$$\mathcal{I}(Y, X|\boldsymbol{\omega}) = \int \mathcal{D}\boldsymbol{r}_1 \mathcal{D}\boldsymbol{r}_2 \mathcal{D}\bar{\boldsymbol{r}}_1 \mathcal{D}\bar{\boldsymbol{r}}_2 \exp\left\{ \frac{i}{2} \int_{x^+}^{y^+} \mathrm{d}t \left(\omega_1 \dot{\boldsymbol{r}}_1^2 + \omega_2 \dot{\boldsymbol{r}}_2^2 - \omega_1 \dot{\bar{\boldsymbol{r}}}_1^2 - \omega_2 \dot{\bar{\boldsymbol{r}}}_2^2 \right) \right\}$$

$$\times \exp\left\{ -\frac{C_F\, n}{2} \int_{x^+}^{y^+} \mathrm{d}t\ [\sigma(\boldsymbol{r}_1 - \bar{\boldsymbol{r}}_1) + \sigma(\boldsymbol{r}_2 - \bar{\boldsymbol{r}}_2) + \sigma(\boldsymbol{r}_1 - \boldsymbol{r}_2) + \sigma(\bar{\boldsymbol{r}}_1 - \bar{\boldsymbol{r}}_2)] \right\}.$$
(B.29)

The integral runs over paths with endpoints $\boldsymbol{r}_i(x^+) \equiv \boldsymbol{x}_i$ and $\boldsymbol{r}_i(y^+) \equiv \boldsymbol{y}_i$ ($i = 1, 2$), and similarly for $\bar{\boldsymbol{r}}_i$. The factor C_F in the second exponential of the formula above originates from the fact that the average of the Wilson lines that leads to this expression involves quark dipoles $C_q^{(2)}$ (see eq. (4.18)).

We perform the following change of variables (with unit Jacobian)

$$\boldsymbol{u} = \boldsymbol{r}_1 - \boldsymbol{r}_2, \quad \bar{\boldsymbol{u}} = \bar{\boldsymbol{r}}_1 - \bar{\boldsymbol{r}}_2, \quad \boldsymbol{v} = z(\boldsymbol{r}_1 - \bar{\boldsymbol{r}}_1) + (1 - z)(\boldsymbol{r}_2 - \bar{\boldsymbol{r}}_2),$$
$$\boldsymbol{w} = z\frac{\boldsymbol{r}_1 + \bar{\boldsymbol{r}}_1}{2} + (1 - z)\frac{\boldsymbol{r}_2 + \bar{\boldsymbol{r}}_2}{2}.$$
(B.30)

with as before $\omega_1 = z\omega_0$, $\omega_2 = (1 - z)\omega_0$, and $\hat{\omega}_0 = z(1 - z)\omega_0$. The inverse transformation

reads

$$r_1 = w + (1-z)u + \frac{v}{2}, \qquad r_2 = w - zu + \frac{v}{2},$$
$$\bar{r}_1 = w + (1-z)\bar{u} - \frac{v}{2}, \qquad \bar{r}_2 = w - z\bar{u} - \frac{v}{2}, \tag{B.31}$$

We also define

$$x_1 = w_x + (1-z)u_x + \frac{v_x}{2}, \qquad x_2 = w_x - zu_x + \frac{v_x}{2},$$
$$\bar{x}_1 = w_x + (1-z)\bar{u}_x - \frac{v_x}{2}, \qquad \bar{x}_2 = w_x - z\bar{u}_x - \frac{v_x}{2}, \tag{B.32}$$

and similarly for the y-variables. In the variables (B.30), the path integral reads

$$\mathcal{I}(Y, X|\boldsymbol{\omega}) = \int \mathcal{D}u\mathcal{D}\bar{u}\mathcal{D}v\mathcal{D}w \exp\left\{ \frac{i\hat{\omega}_0}{2} \int_{x^+}^{y^+} \mathrm{d}t \left[(\dot{u}^2 - \dot{\bar{u}}^2) + 2\dot{v}\cdot\dot{w} \right] \right\}$$
$$\times \, \mathrm{e}^{\left\{ -\frac{C_F\,n}{2} \int_{x^+}^{y^+} \mathrm{d}t\,[\sigma((1-z)(u-\bar{u})+v)+\sigma(-z(u-\bar{u})+v)+\sigma(u)+\sigma(\bar{u})] \right\}}. \tag{B.33}$$

The Euler Lagrange equation for w yields $\ddot{v} = 0$, that is, the classical path $v(t)$ is a linear function of time. This allows us to calculate the integral over v and w, and obtain

$$\mathcal{I}(Y, X|\boldsymbol{\omega}) = \left(\frac{\omega_0}{2\pi\Delta t} \right)^2 \mathrm{e}^{i\omega_0 \frac{\Delta v}{\Delta t}\Delta w} \int \mathcal{D}u\mathcal{D}\bar{u}\, \mathrm{e}^{\frac{i\hat{\omega}_0}{2} \int_{x^+}^{y^+} \mathrm{d}t\,(\dot{u}^2 - \dot{\bar{u}}^2)}$$
$$\times \, \mathrm{e}^{\left\{ -\frac{C_F\,n}{2} \int_{x^+}^{y^+} \mathrm{d}t\,[\sigma((1-z)(u-\bar{u})+v)+\sigma(-z(u-\bar{u})+v)+\sigma(u)+\sigma(\bar{u})] \right\}}, \tag{B.34}$$

where $\Delta w = w_y - w_x$, $\Delta v = v_y - v_x$ and $v(t) = v_x + (\Delta v/\Delta t)(t - x^+)$. Note that if one ignores the second line of eq. (B.34), one recovers $\mathcal{I}(Y, X|\boldsymbol{\omega})$ as a product of four free propagators, expressed in the variables (B.30).

At this point, it is convenient to go to the mixed representation, and take a Fourier transform with respect to the transverse coordinates. We get

$$\mathcal{I}(Q, P) = \int_{\{x,y\}} \mathrm{e}^{-iq_1\cdot y_1}\,\mathrm{e}^{-iq_2\cdot y_2}\,\mathrm{e}^{i\bar{q}_1\cdot\bar{y}_1}\,\mathrm{e}^{i\bar{q}_2\cdot\bar{y}_2}\,\mathrm{e}^{ip_1\cdot x_1}\,\mathrm{e}^{ip_2\cdot x_2}\,\mathrm{e}^{-i\bar{p}_1\cdot\bar{x}_1}\,\mathrm{e}^{-i\bar{p}_2\cdot\bar{x}_2}\,\mathcal{I}(Y, X), \tag{B.35}$$

where $\int_{\{x,y\}}$ denotes the integration over the 2×8 transverse coordinates, and the variables P, Q are those of the mixed representation, e.g., $P = (x^+, p_1, p_2, \bar{p}_1, \bar{p}_2)$. Translational invariance (one can easily verify that $\mathcal{I}(Y, X)$ is unchanged in a constant shift of all the coordinates) implies $p_1 + p_2 - \bar{p}_1 - \bar{p}_2 = q_1 + q_2 - \bar{q}_1 - \bar{q}_2$. After changing to the variables (B.32), and taking into account momentum conservation, one finds that $q_1 + q_2 - \bar{q}_1 - \bar{q}_2$ is conjugate to $w_x - w_y$. Now, we are interested in the particular Fourier component for which $q_1 + q_2 = \bar{q}_1 + \bar{q}_2$. For this component, the dependence of the phase factor in eq. (B.35) on $\Delta w = w_y - w_x$ drops out. The integration over Δw can then be

performed, leading to a factor $(2\pi\Delta t/\omega_0)^2\delta(\Delta v)$, while the integration over $\boldsymbol{w}_y + \boldsymbol{w}_x$ leaves a factor $(2\pi)^2\delta(\boldsymbol{p}_1 + \boldsymbol{p}_2 - \bar{\boldsymbol{p}}_1 - \bar{\boldsymbol{p}}_2)$. We are then left with

$$
\begin{aligned}
\tilde{\mathcal{I}}(Q,P) = \int_{\boldsymbol{v}_x u_x \boldsymbol{u}_y \bar{\boldsymbol{u}}_x \bar{\boldsymbol{u}}_y} & \mathrm{e}^{i\boldsymbol{v}_x \cdot (\boldsymbol{p}_1 + \boldsymbol{p}_2 - \boldsymbol{q}_1 - \boldsymbol{q}_2)} \\
\times\, & \mathrm{e}^{i\boldsymbol{u}_x \cdot ((1-z)\boldsymbol{p}_1 - z\boldsymbol{p}_2)} \, \mathrm{e}^{-i\boldsymbol{u}_y((1-z)\boldsymbol{q}_1 - z\boldsymbol{q}_2)} \, \mathrm{e}^{-i\bar{\boldsymbol{u}}_x \cdot ((1-z)\bar{\boldsymbol{p}}_1 - z\bar{\boldsymbol{p}}_2)} \, \mathrm{e}^{i\bar{\boldsymbol{u}}_y \cdot ((1-z)\bar{\boldsymbol{q}}_1 - z\bar{\boldsymbol{q}}_2)} \\
\times\, & \int \mathcal{D}\boldsymbol{u}\mathcal{D}\bar{\boldsymbol{u}} \;\, \mathrm{e}^{i\frac{\hat{\omega}_0}{2} \int_{x^+}^{y^+} \mathrm{d}t\,(\dot{\boldsymbol{u}}^2 - \dot{\bar{\boldsymbol{u}}}^2)} \\
\times\, & \mathrm{e}^{-\frac{C_F\,n}{2} \int_{x^+}^{y^+} \mathrm{d}t\,[\sigma((1-z)(\boldsymbol{u}-\bar{\boldsymbol{u}})+\boldsymbol{v})+\sigma(-z(\boldsymbol{u}-\bar{\boldsymbol{u}})+\boldsymbol{v})+\sigma(\boldsymbol{u})+\sigma(\bar{\boldsymbol{u}})]}.
\end{aligned}
\tag{B.36}
$$

In the path integral in the expression above, the endpoints of the paths are $\boldsymbol{u}_x, \boldsymbol{u}_y$ and $\bar{\boldsymbol{u}}_x, \bar{\boldsymbol{u}}_y$, respectively, and $\boldsymbol{v} = \boldsymbol{v}_x$ is a constant.

We shall evaluate the path integrals over $\boldsymbol{u}$ and $\bar{\boldsymbol{u}}$ in the harmonic approximation, i.e, set $N_c n\,\sigma(\boldsymbol{u}) \approx \hat{q}\,\boldsymbol{u}^2/2$. We write the path integral as

$$
\int \mathcal{D}\boldsymbol{u}\mathcal{D}\bar{\boldsymbol{u}} \;\, \mathrm{e}^{\int_{x^+}^{y^+} \mathrm{d}t\mathcal{L}(\boldsymbol{u},\bar{\boldsymbol{u}})}, \qquad \mathcal{L} = \mathcal{L}_0 + \mathcal{L}_1, \qquad \mathcal{L}_0 = i\frac{\hat{\omega}_0}{2}(\dot{\bar{\boldsymbol{u}}}^2 - \dot{\boldsymbol{u}}^2). \tag{B.37}
$$

In the harmonic approximation we get

$$
\mathcal{L}_1 \approx -\frac{C_F}{4N_c}\hat{q}\left\{A(\boldsymbol{u}^2 + \bar{\boldsymbol{u}}^2) - 2\,(A-1)\boldsymbol{u}\cdot\bar{\boldsymbol{u}} + 2B(\boldsymbol{u} - \bar{\boldsymbol{u}})\cdot\boldsymbol{v} + 2\,\boldsymbol{v}^2\right\}, \tag{B.38}
$$

with

$$
A = 1 + z^2 + (1-z)^2, \qquad B = 1 - 2z. \tag{B.39}
$$

The shift of variables

$$
\boldsymbol{u} \to \boldsymbol{u} - \frac{B}{2A-1}\,\boldsymbol{v} \qquad \bar{\boldsymbol{u}} \to \bar{\boldsymbol{u}} + \frac{B}{2A-1}\,\boldsymbol{v}, \tag{B.40}
$$

where $\boldsymbol{v}$ is a constant vector, leaves the measure of the path integral unchanged, as well as $\mathcal{L}_0$, and reduces $\mathcal{L}_1$ to

$$
\mathcal{L}_1 = -\frac{C_F}{4N_c}\hat{q}\left\{A(\boldsymbol{u}^2 + \bar{\boldsymbol{u}}^2) - 2\,(A-1)\boldsymbol{u}\cdot\bar{\boldsymbol{u}}\right\}. \tag{B.41}
$$

At this point, we perform a boost-like transformation,

$$
\begin{pmatrix} \boldsymbol{u} \\ \bar{\boldsymbol{u}} \end{pmatrix} = \gamma \begin{pmatrix} 1 & \beta \\ \beta & 1 \end{pmatrix} \begin{pmatrix} \boldsymbol{u}' \\ \bar{\boldsymbol{u}}' \end{pmatrix}, \qquad \gamma = \frac{1}{\sqrt{1-\beta^2}}, \tag{B.42}
$$

which again leaves $\mathcal{L}_0$ unchanged, that is, $\mathcal{L}_0(\boldsymbol{u}, \bar{\boldsymbol{u}}) = \mathcal{L}_0(\boldsymbol{u}', \bar{\boldsymbol{u}}')$. This leaves also the measure of the path integral unchanged. By choosing β as a solution of the equation

$$
\beta^2 + 1 - \frac{2A}{A-1}\beta = 0, \qquad \beta = \frac{A \pm \sqrt{2A-1}}{A-1}, \tag{B.43}
$$

one can write $\mathcal{L}_1$ in the factorized form

$$
\mathcal{L}_1 = -\frac{C_F}{4N_c}\hat{q}\gamma^2\left[A(1+\beta^2) - 2(A-1)\,\beta\right](\boldsymbol{u}'^2 + \bar{\boldsymbol{u}}'^2). \tag{B.44}
$$

Simple algebra yields

$$C(z) \equiv \frac{A(1+\beta^2) - 2(A-1)\beta}{1-\beta^2} = \pm\sqrt{2A-1} = \pm\sqrt{2z^2 + 2(1-z)^2 + 1}\,, \quad \text{(B.45)}$$

where the two signs correspond to the two possible solution of eq. (B.43). One can then write the path integral as

$$\int \mathcal{D}\boldsymbol{u}'\mathcal{D}\bar{\boldsymbol{u}}'\, \mathrm{e}^{i\frac{\hat{\omega}_0}{2}\int_{x^+}^{y^+}\mathrm{d}t(\dot{\boldsymbol{u}}'^2 - \dot{\bar{\boldsymbol{u}}}'^2)}\, \mathrm{e}^{-\frac{C_F}{4N_c}C(z)\int_{x^+}^{y^+}\mathrm{d}t\hat{q}(\boldsymbol{u}'^2 + \bar{\boldsymbol{u}}'^2)}\,, \quad \text{(B.46)}$$

and the convergence imposes the choice of the positive sign for $C(z)$. This is the product of two integrals of the type of eq. (B.26):

$$\mathcal{J}(\boldsymbol{u}'_x, \boldsymbol{u}'_y)\,\bar{\mathcal{J}}(\bar{\boldsymbol{u}}'_x, \bar{\boldsymbol{u}}'_y) \quad \text{(B.47)}$$

with here

$$\mathcal{J}(\boldsymbol{u}'_x, \boldsymbol{u}'_y) = \frac{\hat{\omega}_0\Omega}{2\pi i\sinh(\Omega\Delta t)}\,\exp\left\{i\frac{\hat{\omega}_0\Omega}{2\sinh(\Omega\Delta t)}\left[\cosh(\Omega\Delta t)(\boldsymbol{u}'^2_x + \boldsymbol{u}'^2_y) - 2\boldsymbol{u}'_x\cdot\boldsymbol{u}'_y\right]\right\}\,, \quad \text{(B.48)}$$

and similarly for $\bar{\mathcal{J}}$ with

$$\Omega = \frac{1+i}{2}\sqrt{\frac{\hat{q}\,C_F C(z)}{\hat{\omega}_0\,N_c}}\,, \qquad \bar{\Omega} = \frac{1-i}{2}\sqrt{\frac{\hat{q}\,C_F C(z)}{\hat{\omega}_0\,N_c}}\,, \quad \text{(B.49)}$$

and the values of $\boldsymbol{u}'_x$, $\boldsymbol{u}'_y$, $\bar{\boldsymbol{u}}'_x$, $\bar{\boldsymbol{u}}'_y$ can be obtained from the inverse transformation

$$\begin{pmatrix} \boldsymbol{u}' \\ \bar{\boldsymbol{u}}' \end{pmatrix} = \gamma \begin{pmatrix} 1 & -\beta \\ -\beta & 1 \end{pmatrix} \begin{pmatrix} \boldsymbol{u} + \frac{B}{2(A-1)}\boldsymbol{v} \\ \bar{\boldsymbol{u}} - \frac{B}{2(A-1)}\boldsymbol{v} \end{pmatrix}\,. \quad \text{(B.50)}$$

At this point, it is clear that the 4-point function that correlates gluons a and b is exponentially damped on a time scale comparable to that of the 3-point function, more specifically as

$$\Delta t \gtrsim \sqrt{\frac{\hat{\omega}_0}{\hat{q}\,C(z)}\frac{N_c}{C_F}} \approx \tau_{\mathrm{br}}\,.$$

C Color algebra

In this appendix we review the color algebra necessary to justify eq. (4.6) by replacing adjoint Wilson lines by fundamental ones. This manipulation can be made in several different ways, here we choose to first replace all adjoint Wilson lines by fundamental ones by means of the identity in eq. (4.5) and then remove all explicit color matrices t's and f's by using the Fierz identity $t^a_{ij}t^a_{kl} = \frac{1}{2}\delta_{il}\delta_{jk} - \frac{1}{2N_c}\delta_{ij}\delta_{kl}$ and the Lie algebra relation

$[t^a, t^b] = if^{abc}t^c$. In order to have shorter expressions we will use the shorthand notation $U_1 \equiv U(\boldsymbol{r}_1)$, $U(\bar{\boldsymbol{r}}_1) \equiv U_{\bar{1}}$ and similarly for the other coordinates and adjoint Wilson lines.

$$f^{mn\bar{e}}f^{\bar{c}\bar{d}\bar{e}}\tilde{U}_{1am}\tilde{U}_{2bn}\tilde{U}^{\dagger}_{\bar{1}\bar{c}a}\tilde{U}^{\dagger}_{\bar{2}\bar{d}b}$$
$$= 16f^{mn\bar{e}}f^{\bar{c}\bar{d}\bar{e}}\text{Tr}\left(U^{\dagger}_{\bar{1}}t^a U_1 t^m\right)\text{Tr}\left(U^{\dagger}_{\bar{2}}t^b U_2 t^n\right)\text{Tr}\left(U^{\dagger}_{\bar{1}}t^a U_{\bar{2}}t^{\bar{c}}\right)\text{Tr}\left(U^{\dagger}_{\bar{2}}t^b U_{\bar{2}}t^{\bar{d}}\right). \quad \text{(C.1)}$$

Here we can directly apply the Fierz identity to the pairs of matrices t^a and t^b. One can easily see that the second term of the identity would remove one of the color matrices form the traces, in which case the Wilson lines cancel out and one is left with a trace of a fundamental color matrix, which is zero. One therefore obtains

$$4f^{mn\bar{e}}f^{\bar{c}\bar{d}\bar{e}}\text{Tr}\left[U^{\dagger}_1 U_{\bar{1}}t^{\bar{c}}U^{\dagger}_{\bar{1}}U_1 t^m\right]\text{Tr}\left[U^{\dagger}_2 U_{\bar{2}}t^{\bar{d}}U^{\dagger}_{\bar{2}}U_2 t^n\right]. \quad \text{(C.2)}$$

Now all t matrices have different color indices. In order to proceed we need to get rid of the f symbols, arriving at

$$4\text{Tr}\left(U^{\dagger}_1 U_{\bar{1}}\left[t^{\bar{d}}, t^{\bar{e}}\right]U^{\dagger}_{\bar{1}}U_1 t^m\right)\text{Tr}\left(U^{\dagger}_2 U_{\bar{2}}t^{\bar{d}}U^{\dagger}_{\bar{2}}U_2 \left[t^m, t^{\bar{e}}\right]\right). \quad \text{(C.3)}$$

Now we have three pairs of t matrices with the same color index and therefore we can make use of the Fierz identity three more times. Notice that the contribution from the second term of the Fierz identity is always zero since it would eliminate one of the matrices inside a commutator. By successively eliminating matrices with the indices $\bar{d}$, m, and $\bar{e}$, we arrive at

$$2\left[\text{Tr}\left(U^{\dagger}_1 U_{\bar{1}}U^{\dagger}_{\bar{2}}U_2 \left[t^m, t^{\bar{e}}\right]U^{\dagger}_2 U_{\bar{2}}t^{\bar{e}}U^{\dagger}_{\bar{1}}U_1 t^m\right) - \text{Tr}\left(U^{\dagger}_1 U_{\bar{1}}t^{\bar{e}}U^{\dagger}_{\bar{2}}U_2 \left[t^m, t^{\bar{e}}\right]U^{\dagger}_2 U_{\bar{2}}U^{\dagger}_{\bar{1}}U_1 t^m\right)\right]$$
$$= \text{Tr}\left(U^{\dagger}_1 U_{\bar{1}}U^{\dagger}_{\bar{2}}U_2\right)\text{Tr}\left(t^{\bar{e}}U^{\dagger}_2 U_{\bar{2}}t^{\bar{e}}U^{\dagger}_{\bar{1}}U_1\right) - \text{Tr}\left(U^{\dagger}_1 U_{\bar{1}}U^{\dagger}_{\bar{2}}U_2 t^{\bar{e}}\right)\text{Tr}\left(U^{\dagger}_2 U_{\bar{2}}t^{\bar{e}}U^{\dagger}_{\bar{1}}U_1\right)$$
$$- \text{Tr}\left(U^{\dagger}_1 U_{\bar{1}}t^{\bar{e}}U^{\dagger}_{\bar{2}}U_2\right)\text{Tr}\left(t^{\bar{e}}U^{\dagger}_2 U_{\bar{2}}U^{\dagger}_{\bar{1}}U_1\right) + \text{Tr}\left(U^{\dagger}_1 U_{\bar{1}}t^{\bar{e}}U^{\dagger}_{\bar{2}}U_2 t^{\bar{e}}\right)\text{Tr}\left(U^{\dagger}_2 U_{\bar{2}}U^{\dagger}_{\bar{1}}U_1\right)$$
$$= \frac{1}{2}\left[\text{Tr}\left(U^{\dagger}_1 U_{\bar{1}}U^{\dagger}_{\bar{2}}U_2\right)\text{Tr}\left(U^{\dagger}_{\bar{1}}U_1\right)\text{Tr}\left(U^{\dagger}_2 U_{\bar{2}}\right) - \text{Tr}\left(U^{\dagger}_1 U_{\bar{1}}U^{\dagger}_{\bar{2}}U_2 U^{\dagger}_{\bar{1}}U_1 U^{\dagger}_2 U_{\bar{2}}\right)\right.$$
$$\left.- \text{Tr}\left(U^{\dagger}_1 U_{\bar{1}}U^{\dagger}_2 U_{\bar{2}}U^{\dagger}_{\bar{1}}U_1 U^{\dagger}_{\bar{2}}U_2\right) + \text{Tr}\left(U^{\dagger}_1 U_{\bar{1}}\right)\text{Tr}\left(U^{\dagger}_{\bar{2}}U_2\right)\text{Tr}\left(U^{\dagger}_2 U_{\bar{2}}U^{\dagger}_{\bar{1}}U_1\right)\right]. \quad \text{(C.4)}$$

The last line above is exactly the expression in (4.6).

Open Access. This article is distributed under the terms of the Creative Commons Attribution License which permits any use, distribution and reproduction in any medium, provided the original author(s) and source are credited.

References

[1] ALICE collaboration, K. Aamodt et al., *Suppression of Charged Particle Production at Large Transverse Momentum in Central Pb–Pb Collisions at $\sqrt{s_{NN}} = 2.76$ TeV*, *Phys. Lett.* **B 696** (2011) 30 [arXiv:1012.1004] [INSPIRE].

[2] ATLAS collaboration, *Observation of a Centrality-Dependent Dijet Asymmetry in Lead-Lead Collisions at $\sqrt{s_{NN}} = 2.77$ TeV with the ATLAS Detector at the LHC*, *Phys. Rev. Lett.* **105** (2010) 252303 [arXiv:1011.6182] [INSPIRE].

[3] CMS collaboration, *Observation and studies of jet quenching in PbPb collisions at nucleon-nucleon center-of-mass energy = 2.76 TeV*, *Phys. Rev.* **C 84** (2011) 024906 [arXiv:1102.1957] [INSPIRE].

[4] CMS collaboration, *Jet momentum dependence of jet quenching in PbPb collisions at $\sqrt{s_{NN}} = 2.76$ TeV*, *Phys. Lett.* **B 712** (2012) 176 [arXiv:1202.5022] [INSPIRE].

[5] STAR collaboration, J. Putschke, *First fragmentation function measurements from full jet reconstruction in heavy-ion collisions at $\sqrt{S_{\rm Nn}} = 200$ GeV by STAR*, *Eur. Phys. J.* **C 61** (2009) 629 [arXiv:0809.1419] [INSPIRE].

[6] STAR collaboration, S. Salur, *First Direct Measurement of Jets in $\sqrt{S_{Nn}} = 200$ GeV Heavy Ion Collisions by STAR*, *Eur. Phys. J.* **C 61** (2009) 761 [arXiv:0809.1609] [INSPIRE].

[7] PHENIX collaboration, Y.-S. Lai, *Probing medium-induced energy loss with direct jet reconstruction in p+p and Cu+Cu collisions at PHENIX*, *Nucl. Phys.* **A 830** (2009) 251C–254C [arXiv:0907.4725] [INSPIRE].

[8] R. Baier, Y.L. Dokshitzer, A.H. Mueller, S. Peigne and D. Schiff, *Radiative energy loss of high-energy quarks and gluons in a finite volume quark-gluon plasma*, *Nucl. Phys.* **B 483** (1997) 291 [hep-ph/9607355] [INSPIRE].

[9] R. Baier, Y.L. Dokshitzer, A.H. Mueller, S. Peigne and D. Schiff, *Radiative energy loss and p_T broadening of high-energy partons in nuclei*, *Nucl. Phys.* **B 484** (1997) 265 [hep-ph/9608322] [INSPIRE].

[10] R. Baier, Y.L. Dokshitzer, A.H. Mueller and D. Schiff, *Medium induced radiative energy loss: Equivalence between the BDMPS and Zakharov formalisms*, *Nucl. Phys.* **B 531** (1998) 403 [hep-ph/9804212] [INSPIRE].

[11] B. Zakharov, *Fully quantum treatment of the Landau-Pomeranchuk-Migdal effect in QED and QCD*, *JETP Lett.* **63** (1996) 952 [hep-ph/9607440] [INSPIRE].

[12] B. Zakharov, *Radiative energy loss of high-energy quarks in finite size nuclear matter and quark-gluon plasma*, *JETP Lett.* **65** (1997) 615 [hep-ph/9704255] [INSPIRE].

[13] U.A. Wiedemann and M. Gyulassy, *Transverse momentum dependence of the Landau-Pomeranchuk-Migdal effect*, *Nucl. Phys.* **B 560** (1999) 345 [hep-ph/9906257] [INSPIRE].

[14] U.A. Wiedemann, *Gluon radiation off hard quarks in a nuclear environment: Opacity expansion*, *Nucl. Phys.* **B 588** (2000) 303 [hep-ph/0005129] [INSPIRE].

[15] U.A. Wiedemann, *Jet quenching versus jet enhancement: A Quantitative study of the BDMPS-Z gluon radiation spectrum*, *Nucl. Phys.* **A 690** (2001) 731 [hep-ph/0008241] [INSPIRE].

[16] M. Gyulassy, P. Levai and I. Vitev, *NonAbelian energy loss at finite opacity*, *Phys. Rev. Lett.* **85** (2000) 5535 [nucl-th/0005032] [INSPIRE].

[17] M. Gyulassy, P. Levai and I. Vitev, *Reaction operator approach to nonAbelian energy loss*, *Nucl. Phys.* **B 594** (2001) 371 [nucl-th/0006010] [INSPIRE].

[18] P.B. Arnold, G.D. Moore and L.G. Yaffe, *Photon emission from ultrarelativistic plasmas*, *JHEP* **11** (2001) 057 [hep-ph/0109064] [INSPIRE].

[19] P.B. Arnold, G.D. Moore and L.G. Yaffe, *Photon emission from quark gluon plasma: Complete leading order results*, *JHEP* **12** (2001) 009 [hep-ph/0111107] [INSPIRE].

[20] P.B. Arnold, G.D. Moore and L.G. Yaffe, *Photon and gluon emission in relativistic plasmas*, *JHEP* **06** (2002) 030 [hep-ph/0204343] [INSPIRE].

[21] Y. Mehtar-Tani, C.A. Salgado and K. Tywoniuk, *Anti-angular ordering of gluon radiation in QCD media*, *Phys. Rev. Lett.* **106** (2011) 122002 [arXiv:1009.2965] [INSPIRE].

[22] Y. Mehtar-Tani, C. Salgado and K. Tywoniuk, *Jets in QCD Media: From Color Coherence to Decoherence*, *Phys. Lett.* **B 707** (2012) 156 [arXiv:1102.4317] [INSPIRE].

[23] J. Casalderrey-Solana and E. Iancu, *Interference effects in medium-induced gluon radiation*, *JHEP* **08** (2011) 015 [arXiv:1105.1760] [INSPIRE].

[24] Y. Mehtar-Tani, C.A. Salgado and K. Tywoniuk, *The radiation pattern of a QCD antenna in a dilute medium*, *JHEP* **04** (2012) 064 [arXiv:1112.5031] [INSPIRE].

[25] Y. Mehtar-Tani, C.A. Salgado and K. Tywoniuk, *The Radiation pattern of a QCD antenna in a dense medium*, *JHEP* **10** (2012) 197 [arXiv:1205.5739] [INSPIRE].

[26] A. Bassetto, M. Ciafaloni, G. Marchesini and A.H. Mueller, *Jet Multiplicity and Soft Gluon Factorization*, *Nucl. Phys.* **B 207** (1982) 189 [INSPIRE].

[27] A.H. Mueller, *On the Multiplicity of Hadrons in QCD Jets*, *Phys. Lett.* **B 104** (1981) 161 [INSPIRE].

[28] B. Ermolaev and V.S. Fadin, *Log - Log Asymptotic Form of Exclusive Cross-Sections in Quantum Chromodynamics*, *JETP Lett.* **33** (1981) 269 [INSPIRE].

[29] Y.L. Dokshitzer, V.A. Khoze, A.H. Mueller and S.I. Troian, *Basics of Perturbative QCD*, Ed. Frontieres, Gif-sur-Yvette, France (1991).

[30] R. Baier, A.H. Mueller, D. Schiff and D. Son, *'Bottom up' thermalization in heavy ion collisions*, *Phys. Lett.* **B 502** (2001) 51 [hep-ph/0009237] [INSPIRE].

[31] R. Baier, Y.L. Dokshitzer, A.H. Mueller and D. Schiff, *Quenching of hadron spectra in media*, *JHEP* **09** (2001) 033 [hep-ph/0106347] [INSPIRE].

[32] S. Jeon and G.D. Moore, *Energy loss of leading partons in a thermal QCD medium*, *Phys. Rev.* **C 71** (2005) 034901 [hep-ph/0309332] [INSPIRE].

[33] N. Armesto, L. Cunqueiro and C.A. Salgado, *Q-PYTHIA: A Medium-modified implementation of final state radiation*, *Eur. Phys. J.* **C 63** (2009) 679 [arXiv:0907.1014] [INSPIRE].

[34] B. Schenke, C. Gale and S. Jeon, *MARTINI: An Event generator for relativistic heavy-ion collisions*, *Phys. Rev.* **C 80** (2009) 054913 [arXiv:0909.2037] [INSPIRE].

[35] K.C. Zapp, J. Stachel and U.A. Wiedemann, *A local Monte Carlo framework for coherent QCD parton energy loss*, *JHEP* **07** (2011) 118 [arXiv:1103.6252] [INSPIRE].

[36] Y. Mehtar-Tani, *Relating the description of gluon production in pA collisions and parton energy loss in AA collisions*, *Phys. Rev.* **C 75** (2007) 034908 [hep-ph/0606236] [INSPIRE].

[37] G. Altarelli and G. Parisi, *Asymptotic Freedom in Parton Language*, *Nucl. Phys.* **B 126** (1977) 298 [INSPIRE].

[38] J.P. Blaizot, F. Gelis and R. Venugopalan, *High-energy pA collisions in the color glass condensate approach. 1. Gluon production and the Cronin effect*, *Nucl. Phys.* **A 743** (2004) 13 [hep-ph/0402256] [INSPIRE].